UC Berkeley
UC Berkeley Electronic Theses and Dissertations

Title

Mediators and markers of mammalian lifespan extension: Proteomic, proliferative and hormonal adaptations in mouse models of extended lifespan

Permalink

https://escholarship.org/uc/item/79b4q4wg

Author

Thompson, Airlia Camille Simone

Publication Date

2014

Peer reviewed|Thesis/dissertation

eScholarship.org Powered by the California Digital Library
University of California

Mediators and markers of mammalian lifespan extension: Proteomic, proliferative and hormonal adaptations in mouse models of extended lifespan

By

Airlia Camille Simone Thompson

A dissertation submitted in partial satisfaction

of the requirements for the degree of

Doctor of Philosophy

in

Metabolic Biology

in the

Graduate Division

of the

University of California, Berkeley

Committee in charge:

Professor Marc K. Hellerstein, Chair
Professor Joseph L. Napoli
Professor George A. Brooks

Spring 2014

Abstract

Mediators and markers of mammalian lifespan extension:
Proteomic, proliferative and hormonal adaptations
in mouse models of extended lifespan

by

Airlia Camille Simone Thompson

Doctor of Philosophy in Metabolic Biology

University of California, Berkeley

Professor Marc K. Hellerstein, Chair

Aging is broadly defined as the deterioration of bodily tissues over time. Excluding death due to infectious disease or accidents, aging is what ultimately places finite limits on lifespan and healthspan, the time in which in individual remains active and in good health. Although healthspan and lifespan are intimately linked, it is the extension of human healthspan that is a major goal of gerontological research. Such an achievement would have broad social and economic benefits and importantly would mitigate the dire consequences of the predicted future rise in the prevalence of age-related diseases due to the growing proportion of the population that is of advanced age (65yr and over). A broad understanding of the physiological, metabolic, hormonal, cellular and molecular factors that contribute to aging and lifespan determination will allow for the development of strategies to extend healthspan.

The work presented herein describes the use of three unique mouse models of extended healthspan and maximum lifespan, including calorie restricted (CR), Snell Dwarf and rapamycin-treated mice, to investigate several factors linked to healthspan and lifespan determination in mammals. These factors include reduced insulin-like growth factor-1 (IGF-1) expression, reduced cell proliferation, reduced protein synthesis and enhanced proteome stability. Using these three models the following conclusions have been drawn: 1) Physiological adaptations to CR previously suggested to confer the healthspan and lifespan benefits of CR in rodents cannot account for the global cell proliferation rate-lowering effect of CR; 2) Fibroblast growth factor 21 (FGF21) is not necessary for the reduction in IGF-1 or the reduction in global cell proliferation rates in response to moderate CR in adult mice; 3) A reduction in global cell proliferation rates is not a consistent predictor of maximum lifespan extension in mice; 4) A reduction in hepatic protein replacement rates is a sensitive and early predictor of maximum lifespan extension in mice and likely reflects a more stable and functional proteome.

Acknowledgments

Throughout graduate school I have been surrounded by an incredible support system. Many people mentored and supported me intellectually, others supported me emotionally and many did both.

When reviewing data, my PhD advisor, Dr. Marc K. Hellerstein, always encouraged me to develop, share and ultimately defend my own theories before sharing his own. This was instrumental in helping me to hone my critical thinking skills as a researcher. He also constantly pushed me to interpret the relevance of my data in the context of human health, a mindset that will benefit me in a wide range of future scientific endeavors.

I am incredibly indebted to Dr. Matthew D. Bruss, a previous graduate student in the Hellerstein lab. On the very first day that I stepped into the lab, Matt took me under his wing and started teaching me techniques. He then invited me to collaborate with him on several projects and then graciously encouraged me to make them my own, all the while continuously discussing with me the relevance and potential impact of the work we were doing. Matt is a gifted scientist and mentor and a true friend.

Marcy Dalidd and Lindsay Roberts are the most talented lab assistants I have ever had the pleasure to work with. Both contributed enormously to the feeding experiments and sample preparations that form the foundation of much of my dissertation work. Marcy and Lindsay were also a constant source of positive energy and laughter in the lab. The friendship that they share is truly an inspiration.

Several other current and previous graduate students in the Hellerstein lab, including Dr. Cyrus Khambatta, Candice Allister and Dr. DJ Roohk, taught me techniques, collaborated with me, made me laugh and listened to my woes. I am so lucky to have worked with such generous and fun lab mates.

Mark Fitch, our lab manager in the Hellerstein lab, is arguably one of the most selfless people I know. Mark was always available and willing to help with any question or problem that I had, big or small. He genuinely wants to help others and this is a rare and beautiful quality.

As undergrads, Ishita Aggarwal and Nitish Nag made significant contributions to my dissertation work and I am grateful for all their hard work.

While I technically did not work with Chelsea Bidlow, another lab assistant in the Hellerstein lab, she generously helped me with many weekend feedings and was all around an absolute joy to have in the lab.

Much of my dissertation work would not have been possible without the Emeryville-based company, KineMed. The proteomics techniques used in Chapter 3 were developed at KineMed with some assistance from members of the Hellerstein lab. Dr. JC Price graciously taught me the theory, practice and limitations of these LC-MS/MS-based proteomics techniques as well as offered me sage career advice. Dr. William Holmes, Dr. Thomas Angel and Dr. Kevin Li helped me analyze data and troubleshoot experiments. Dr. Marc Colangelo worked with me to develop several bioinformatics tools to analyze my large

proteomics datasets. Chancy Fessler and Joan Protasio injected and processed more proteomics samples of mine than I can count and I appreciate all of their assistance.

Throughout my years as a graduate student at UC Berkeley, Dr. Joseph Napoli and Dr. George Brooks have supported me in countless ways, including serving as thoughtful members on my oral qualifying exam and dissertation committees. In addition, Dr. Napoli provided me with many rich teaching opportunities while Dr. Brooks led several seminar courses that broadened my knowledge of metabolism and helped me hone my skills as a presenter. I am very grateful for all of their guidance and support.

Present and past NST administrative staff members, including Janna Conway-Hamilton, Nikki Milbrath and Olga O'connor all provided me with stellar and friendly support throughout the years.

I am indebted to several staff members at the Northwest Animal Facility. Bennie Mitchell submitted countless complicated and last-minute animal orders for me and went above and beyond to ensure that my animal experiments were successful. I could always count on him to be incredibly efficient, professional and friendly. Bob Williams and Brandin Alvarez were terrific animal technicians and I am grateful for all the care they took to ensure that my animal experiments were successful.

My time in Morgan Hall was enriched by early evening talks with the building custodian, Antonio Marino. Antonio and I found that we had a great deal in common and I cherish all the meaningful conversations that we shared.

I am so grateful for all my friends and all the happy hours, weekend trips, dinner parties and Game of Thrones nights that I looked forward to throughout graduate school and that I continue to look forward to.

My family members have been constant cheerleaders throughout my graduate career. This includes my father Stephen, my mother Tanya, my stepfather Barry and my sisters, Tatiana and Destinee. They are an incredible bunch and each of them has been there to share in my triumphs as well as to help me work through tough times. They have also been very understanding when I go "silent" for a week or two when I had a big exam or talk coming up. The most important thing is that they are always there for me…no question. It's so simple yet so profound.

And finally, Jose, my partner in life. He has listened to more of my practice talks and journal clubs than any one person should ever be subjected to and for that I am incredibly grateful. However, this pales in comparison to my gratitude for the amazing man that he is, the security that he provides me with and the beautiful life that we have built together.

Table of Contents

Introduction

Overview of the work described herein

The purpose of the work described herein is to i) contribute to the body of knowledge regarding the physiological, metabolic, hormonal, cellular and molecular factors that underlie mammalian aging and how perturbation of these factors may modulate healthspan and lifespan and ii) identify factors that predict healthspan and maximum lifespan outcomes in mammals that can serve as screening criteria for healthspan and maximum lifespan modulators.

Using three unique mouse models of healthspan and maximum lifespan extension, including calorie restricted (CR), Snell dwarf and rapamycin-treated mice, the three main chapters presented here address the following five central questions (**Fig 1**): **1)** Which if any of the well-characterized physiological adaptations to CR including reduced food intake, energy expenditure, body fat and/or body weight can account for its cell proliferation rate-lowering effect? **2)** Is fibroblast growth factor 21 (FGF21) necessary for the reduction in insulin-like growth factor-1 (IGF-1) and the reduction in global cell proliferation rates in response to CR? **3)** Is a reduction in global cell proliferation rates a common feature across all three models and, therefore, potentially a predictive marker of healthspan and maximum lifespan extension? **4)** What are the characteristic alterations in proteome dynamics in each of these three models? **5)** Are certain alterations in proteome dynamics predictive of healthspan and maximum lifespan extension across all three models?

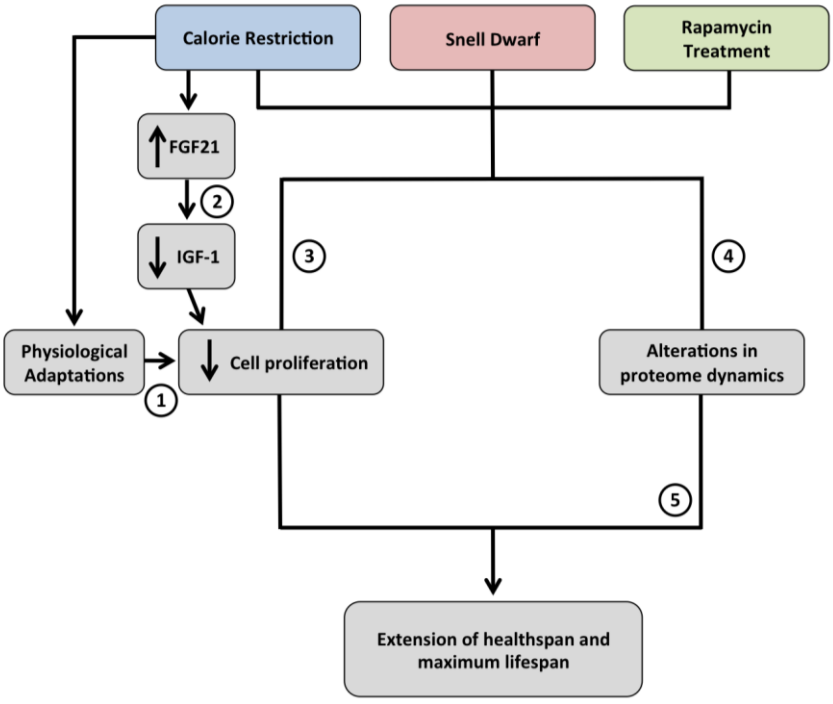

Figure 1: Overview of central questions addressed

Overview of mammalian aging

The natural lifecycle of most multicellular organisms, including mammals, is exquisitely similar. We are born, we develop, we typically reproduce, but we inevitably begin a slow but steady deterioration that ultimately results in death. It is this progressive deterioration that we call aging. More specifically, aging is characterized by the progressive deterioration of cellular, tissue, organ and organismal function due to the accumulation of damage, leading to an increased prevalence of disease and susceptibility to stress, thereby resulting in an increased risk of mortality[1,2].

Age-related diseases including heart disease, cancer, stroke, diabetes and neurodegenerative diseases like Alzheimer's disease, account for the majority of deaths and healthcare spending in the developed world[3–6]. In the US, the proportion of the population that is of advanced age (65yr and over) is projected to increase sharply in decades to come and cause a dramatic increase in the prevalence of age-related diseases[7]. Therefore, there is a tremendous amount of interest in fully elucidating the physiological, metabolic, hormonal, cellular and molecular alterations that underlie mammalian aging in order to attenuate the development of age-related diseases and thus extend healthspan, the time in which an organism remains active and in good health, as well as to potentially extend lifespan.

To this end, the approach our group and many other groups have taken is to study known models of maximum lifespan and healthspan extension in closely related organisms, like rodents, to determine what factors are predictive of and/or causally related to the slowing of the aging process in these models.

Because aging is defined as an increased risk of mortality, the gold-standard method for measuring the rate of aging, Gompertzian analysis, measures the age-specific mortality rate doubling time (MRDT, the time it takes for the mortality rate to double in a given population)[8]. Therefore, the models studied in the work presented here as well as any other model in which the population-level age-specific MRDT is increased, and thus maximum lifespan is increased, is deemed to exhibit a slowing of the aging process. Focusing on extension of maximum lifespan (hereto for referred to as lifespan in this introduction) is critical because aging increases the risk for numerous pathologies. Therefore, it is medically and fiscally advantageous to emphasize attenuating the underlying processes that are common to age-related diseases instead of individual age-related diseases. Indeed, *Olshansky et al* calculated that eliminating only cancer or ischemic heart disease in humans would increase life expectancy at birth by only 4.3% and 4.4%, respectively[9].

The very notion of slowing the aging process and thus extending healthspan and lifespan underscores the fact that there are finite limits to both, although the magnitude of these limits differs greatly depending on the organism. It was previously proposed that the rate of deterioration of organisms that ultimately results in mortality (senescence) and, therefore, limits lifespan, was programmed into organisms as a population control mechanism or as a means to promote regular turnover of populations to ensure adaptability to changing environments [10]. However, in the wild, most species do not die as a result of senescence but rather due to scarce resources, predation, cold exposure and

infectious disease[10]. Yet, when these factors are eliminated, organisms still undergo deterioration and age at discrete rates and thus only live for a finite period of time. This begs the question of "why do organisms age in the first place?" Answering this question requires an evolutionary perspective.

Germ-line mutations accumulate throughout an organism's life due to both exogenous and endogenous insults. As originally appreciated by Medawar[11], if a given germ-line mutation gives rise to a trait that manifests prior to and/or during an organism's reproductive period, it is subjected to intense selection. Any germ-line mutation that gives rise to a trait that reduces fitness during this period will be selected against and, therefore, titrated out of the population. However, if a given germ-line mutation gives rise to a trait that does not manifest until later in life, after an organism's reproductive period, it is not subjected to intense selection and, therefore, may persist in the population. Among many things, these late-manifesting traits may contribute to the deterioration of cellular, organ and, therefore, organismal function, resulting in the phenotype that we call aging. This concept of an accumulation of deleterious germ-line mutations that give rise to late-manifesting traits that contribute to senescence is called the "mutation accumulation" theory of aging[11,12].

Intriguingly, traits that enhance fitness due to early-life benefits may actually become deleterious later in life, a phenomenon known as antagonistic pleiotropy (originally proposed by Williams,[10,13]). Despite becoming deleterious later in life, such traits are maintained in a population because there is strong positive selection for traits that enhance fitness, but there is weak negative selection for traits that do not become deleterious until later in life. For example, in mammals, having high growth factor levels early in life improves fitness by conferring growth and reproductive advantages. These advantages, however, come at the expense of maintaining the integrity of somatic (and potentially gametic) cells. This is because high growth factor levels promote shunting of available resources towards growth and reproduction and away from somatic maintenance processes, including maintaining cellular defense systems to combat protein misfolding, endogenous and exogenous oxidants as well as toxins. It is not until later in life that the consequences of this imbalance between growth and reproduction and somatic maintenance manifest as premature stem cell exhaustion, an elevated frequency of tumor development and potentially a shortened lifespan[14]. It is, therefore, not surprising that a recurring theme in models of healthspan and lifespan extension is the exact opposite of this, wherein growth and reproduction are attenuated and somatic maintenance is enhanced.

Intertwined with this phenomenon of antagonistic pleiotropy is the "Disposable Soma" theory of aging, originally proposed by Thomas Kirkwood[15]. This theory states that there is a tradeoff between somatic maintenance and growth and reproduction given that metabolic resources are finite. Importantly, somatic maintenance, which promotes optimal cellular and, therefore, organismal health, is only necessary for as long as an organism has a reasonable chance for survival in the wild. Therefore, if an organism has only a small chance of living past a certain age, it is advantageous to allocate metabolic resources before this age, to processes that promote immediate survival and propagation of the species. For example, in the context of finite metabolic resources, it is evolutionarily advantageous for mice, which only live for approximately one year in the wild and are vulnerable to death by

cold exposure, to allocate these resources to thermogenesis, motility to gather food and reproduction, rather than to cellular processes that maintain somatic cells in optimal condition (e.g. antioxidant defenses and DNA repair mechanisms).

One prediction of the amalgamation of the above mentioned phenomena and theories on aging would be that if extrinsic causes of mortality like scarce resources, predation, cold exposure and infectious disease were reduced in a population, that over many generations the rate of aging of that population would be slowed and thus lifespan would be increased. This would be due to the fact that germ-line mutations that gave rise to late-manifesting deleterious traits would be under greater negative selection and thus more readily titrated out of the population while mutations that gave rise to traits that promote somatic maintenance later in life would be under greater positive selection and thus more likely to be maintained in the population. Another prediction would be that if reproduction in a population were delayed that this would slow the rate of aging and increase the lifespan of that population. Indeed, at least in flies, both reducing extrinsic mortality as well as delaying reproduction slows the rate of aging and extends lifespan[16–19]. While informative on the influences of extrinsic mortality and early reproduction on the rate of aging and lifespan determination, these studies fail to explain the core physiological, metabolic, hormonal, cellular and molecular factors that accompany and potentially govern the aging process.

The hormonal, molecular and cellular basis of aging

By comparing young and old organisms and by studying models of premature and attenuated aging, many of the factors that accompany and likely govern the aging process, including in mammals, at the hormonal, cellular and molecular level, have been coming into focus over the past ~80 years.

Lessons from comparative studies in young and old wild type (WT) organisms

To develop strategies to attenuate aging and the development of age-related diseases, it is essential to first characterize the hormonal, cellular and molecular alterations that accompany physiological decline as an organism advances in chronological age. Comparative studies between young and old WT organisms have shed much needed light on these alterations. In no particular order, these alterations include (but are not limited to): accumulation of oxidatively damaged proteins[20], lipids[21] and DNA[22]; telomere attrition; genomic instability (point mutations, chromosomal aneuploidies); mitochondrial dysfunction; altered growth hormone (GH), insulin/insulin-like growth factor-1 (IGF-1) and target of rapamycin (TOR) signaling; reduced protein synthesis; reduced proteasome activity; reduced protein turnover; accumulation of protein aggregates; reduced proliferative capacity; stem cell exhaustion and the accumulation of senescent cells[2,20,23–25].

A wealth of knowledge on what factors regulate these alterations as well as how these alterations contribute to physiological decline have been gleaned from genetic, dietary and pharmacological models of premature and/or attenuated aging.

Lessons from yeast and invertebrates

In yeast, worms and flies, hundreds of genes that modulate the aging process and lifespan have been identified and a large number of these genes are associated with nutrient sensing pathways, namely the interconnected pathways of insulin or IGF-1 signaling (IIS) and TOR signaling. For example, homologs of the mammalian genes encoding the IGF-1 receptor (IGF-1R), insulin receptor substrate (IRS), phosphoinositide 3-kinase (PI3K), protein kinase B (Akt-1), TOR and S6 kinase (S6K), all of which positively regulate nutrient signaling, extend lifespan in one or more invertebrate model when their expression is attenuated[26–30]. Conversely, elevated expression of homologs of mammalian genes that negatively regulate nutrient signaling including Forkhead box O (FOXO) transcription factors, adenosine monophosphate (AMP)-activated protein kinase (AMPK), tuberous sclerosis complex (TSC) and 4E-BP, extend lifespan in one or more invertebrate model[29,31–34].

Consistent with extended lifespan in mutants with reduced IIS and TOR signaling, lifespan extension has been reported in response to reduced expression of a growing number of genes involved in protein synthesis (which is positively regulated by IIS and TOR signaling). This includes genes encoding translation initiation factors, ribosomal proteins and ribsosomal RNA (rRNA) processing proteins[29,35,36].

Intriguingly, many of the genes that extend lifespan in invertebrates (and vertebrates) also increase resistance to stress, including stress induced by heat, UV light and oxidants, likely through the upregulation of cellular defense systems, including detoxification enzymes and chaperones[37–40]. Similarly, lifespan extension in rodents appears to be strongly associated with a general upregulation in stress resistance pathways[41]. Consistent with this, mild stressors, which stimulate stress responses, have beneficial effects (hormetic effects) in worms and flies (and mammals), including lifespan extension and resistance to other stresses[42].

A mild stressor that robustly slows the aging process and extends lifespan in invertebrates (and vertebrates) is calorie restriction (CR), defined as a reduction in caloric intake below *ad libitum* (AL) levels without malnutrition. Similar to genetic models of lifespan extension, CR reduces IIS and TOR signaling and enhances stress resistance[43].

Several examples of pharmacological extension of lifespan have been reported in invertebrates. These include treatment with the TOR inhibitor, rapamycin, the AMPK activator, metformin, as well as treatment with antioxidants. Additionally, treatment with resveratrol, a molecule that activates Sir2, an NAD+-dependent protein deacetylase, extends lifespan in worms[44].

Importantly, many of the above mentioned factors that regulate aging and lifespan determination in invertebrate models also regulate mammalian aging and lifespan determination.

Lessons from mammalian models of premature aging

<u>Growth hormone transgenic mice</u>

The lifespans of transgenic mice overexpressing bovine or human growth hormone (GH-Tg) are reduced by as much as 50%. GH-Tg mice, also known as “giant mice” owing to

their drastically increased body size, exhibit features of premature aging (although severe glomerulonephritis appears to be a major cause of early death in these mice)[45]. These features of premature aging include early onset of glomerulosclerosis and mammary tumorogenesis and a premature decline in the replicative potential of cells as well as shortened reproductive lifespan. Owing to their pro-mitotic effects, elevated circulating levels of GH, IGF-1 and insulin are likely contributing factors to the increased incidence of tumors and the premature decline in the replicative potential of cells in GH-Tg mice. Energy budget analyses in GH-Tg mice provide evidence that rapid and excessive growth in these mice occurs at the expense of reproduction and repair processes[46]. Consistent with this, studies assessing antioxidant enzymes in young and middle-aged mice have shown that GH-Tg mice have reduced renal Cu-Zn superoxide dismutase and renal and hepatic glutathione peroxidase activities[47]. These findings suggest that GH-Tg mice are at an increased risk of free radical-induced damage to these tissues, which can potentially explain the premature deterioration of these tissues in GH-Tg mice.

klotho-deficient mice

Mice deficient for the *klotho (also known as alpha-klotho)* gene are short-lived (mean lifespan of ~60 days) and exhibit characteristics of premature aging, including premature skin atrophy, thymus atrophy, osteoporosis, vascular calcification and atherosclerosis as well as pulmonary emphysema[48]. At the time of the discovery that *klotho* deficiency shortens lifespan and results in features of premature aging in mice, its biological function was unknown. It was later determined that *klotho* is a single-pass transmembrane protein expressed in the kidney, parathyroid hormone, brain, pancreas, heart, gonads, placenta and pituitary glands and acts as a cofactor for the interaction of the endocrine fibroblast growth factor (FGF) family member, FGF23, with its FGF receptors (FGFR), thus regulating the action and tissue-specificity of FGF23[49–51]. FGF23 itself, suppressed phosphate reabsorption and vitamin D synthesis in the kidney[52]. Importantly, two isoforms of *klotho* exist due to alternative transcriptional termination, giving rise to either a membrane bound form (m*klotho*) or a secreted soluble form (s*klotho*)[53]. This humoral quality of *klotho* explains why *klotho* deficiency (and overexpression) has such widespread effects in the body.

Hutchinson-Gilford progeria syndrome

Hutchinson-Gilford progeria syndrome (HGPS) is a human progeriod syndrome. Progeriod syndromes are a cluster of genetic disorders that result in premature physiological aging. HGPS is an autosomal dominant condition caused by a mutation in the lamin A/C (LMNA) gene that results in an aberrantly spliced lamin A isoform, called progerin, that is permanently farnesylated[30]. From a very young age, patients with HGPS are afflicted with numerous health problems associated with aging, including alopecia, joint abnormalities, loss of subcutaneous fat, atherosclerosis and typically do not live past ~13yr. Much has been learned about the cellular and molecular basis of premature aging in HGPS from studies in fibroblasts from HGPS patients as well as from numerous mouse models genetically engineered to accumulate progerin and thus mimic many of the premature aging phenotypes of HGPS[54].

Lamins are intermediate filaments that comprise the nuclear lamina along with several lamin-associated proteins. In addition to their structural roles in the nucleus, A-type lamins also coordinate the activity of many transcription factors and regulate epigenetic silencing of heterchromatin and thus influence a variety of cellular processes. Mutations in the LMNA gene that give rise to HGPS result in abnormal nuclear morphology, enhanced DNA damage, defective DNA repair, enhanced genomic instability, enhanced telomere attrition, premature decline in replicative potential of cells (including stem cells), all of which are cellular and/or molecular characteristics of aging[30].

Werner Syndrome

The progeriod syndrome, Werner syndrome (WS), is an autosomal recessive condition caused by a mutation in the gene encoding a member of the RecQ family of proteins called Werner syndrome ATP-dependent helicase (WRN). WRN possess 3' to 5' helicase and exonuclease activity and is involved in the repair of double strand DNA breaks and as a member of the RecQ family of helicases is considered a "guardian of the genome"[55]. Patients with WS begin to exhibit health problems associated with aging starting around the age of 10-20yr, including cataracts, graying of the hair, loss of hair, osteoporosis, atherosclerosis and neoplasms (although not the neoplasms that typically occur during normal aging) and live only to a median age of 54yr. Much has been learned about the cellular and molecular basis of premature aging in WS from studies in fibroblasts from WS patients as well as from mouse models of WS. WRN-mutant cells exhibit elevated DNA damage, defective DNA repair, accelerated telomere attrition, elevated genomic instability, increased cell death, increased cellular senescence and a premature decline in the replicative potential of cells, all of which are cellular and/or molecular characteristics of aging[30,56,57].

Other models that recapitulate progeria phenotypes

Several other human diseases recapitulate a subset of progeria phenotypes including cachexia, kyphosis, retinal degeneration, deafness, neurodevelopmental delays and/or shortened lifespan. These progeria-associated syndromes include Cockayne syndrome, trichothiodystrophy and ataxia telangiectasia and are all linked to defects in DNA repair[30].

Lessons from mammalian models of attenuated aging

Genetic models

The recurring themes of reduced IIS and TOR signaling in invertebrate models of attenuated aging and extended lifespan are echoed in mammals. For example, a number of pituitary dwarf mouse strains with blunted signaling through the somatotropic axis (GH/IGF-1 axis) exhibit profound extensions in lifespan (16-68% depending on strain and gender) as well as characteristics of attenuated aging. This includes the "*little*' mouse which lacks the GH releasing hormone receptor (GHRHR), the Laron mouse which lacks the GH receptor/binding protein (GHR/BP), the Ames Dwarf mouse which lacks the transcription factor prophet of pituitary transcription factor 1 (Pit-1) (Prop-1) which is required for transcriptional activation of the Pit-1 gene which is required for normal

anterior pituitary gland development[58]. The body weights of mice from these strains are 30-70% lower than the body weights of their WT counterparts and all exhibit drastically reduced levels of circulating IGF-1 levels[58–61].

Another pituitary dwarf strain, the Snell dwarf mouse, is homozygous for a loss-of-function point mutation in the Pit1 gene. This mutation in the Pit1 gene prevents DNA-binding of its gene product, Pit1. The Pit1 gene product is a transacting POU domain protein and as previously mentioned is involved in anterior pituitary gland development as it drives differentiation of pituitary lactotrophs, thyrotrophs and somatotrophs. Therefore, mice homozygous for this mutation are prolactin, thyroid stimulating hormone, GH and consequentially, IGF-1 deficient[62,63]. Snell heterozygotes (Het, $Pit1^{dw/+}$) are phenotypically indistinguishable from Snell WT mice (WT, $Pit1^{+/+}$) while Snell dwarf mice ($Pit1^{dw/dw}$) are approximately one third the size of and exhibit a ~26-40% extension in lifespan relative to Het and WT mice[64,65]. In addition, Snell dwarf mice exhibit characteristics of delayed aging, including attenuated development of osteoarthritis, splenomegaly, splenic T-cell proliferation dysfunction, collagen cross-linking and immune system dysfunction as measured by the pool size and function of age-sensitive T-cell subsets[64,66–68]. Snell dwarf mice also exhibit a reduced incidence of neoplastic diseases and similar to long-lived invertebrates with reduced IIS and TOR signaling, exhibit heightened resistant to numerous forms of stress. This includes resistance of tail skin-derived fibroblasts to UV light, paraquat, hydrogen peroxide (H_2O_2), heat and cadmium[69].

Other long-lived mouse strains mimic the hormonal deficiencies associated with pituitary dwarfism. For example, mice overexpressing FGF21, which has been implicated as a negative regulator of GH and IGF-1 signaling, exhibit a 16% extension in lifespan as well as reduced circulating IGF-1 levels[70–74].

In contrast to short-lived *klotho*-deficient mice, mice overexpressing *klotho* exhibit a ~20-30% extension in lifespan[75]. The widespread premature aging phenotypes of *klotho*-deficient mice and the somewhat restricted tissue expression of this gene suggested that *kloth* may function as an endocrine factor. And indeed, two isoforms of *klotho* exist due to alternative transcriptional termination giving rise to either a membrane bound form (m*klotho*) or a secreted soluble form (s*klotho*)[53]. The s*klotho* form regulates the function of cell surface glycoproteins through its sialidase activity[76]. Importantly, s*klotho* inhibits insulin and IGF-1 signaling, suggesting that lifespan extension in *klotho*-Tg mice may be mediated through reduced IIS signaling. It has been proposed that s*klotho* may regulate insulin receptor and IGF-1 receptor activity or abundance at the plasma membrane by modifying glycans on these receptors[77]. *klotho* also reduces oxidative damage, enhances resistance to oxidative stress and protects against ER stress[75,78].

Other long-lived mouse strains, while not reported to have reduced circulating IGF-1 levels, have reduced signaling downstream of the IGF-1 receptor. For example, mice carrying two copies of a hypomorphic mTOR allele ($mTOR^{\Delta/\Delta}$) exhibit a ~10-20% extension in lifespan and attenuated development of a variety of age-related markers including expression of senescence-associated $p16^{INK4A}$, accumulation of nitrotyrosine (a marker of oxidative damage), accumulation of polyubiquitinated proteins, decline in spatial learning and memory, decline in balance and coordination and decline in grip strength[79]. Similar to $mTOR^{\Delta/\Delta}$ mice, mice lacking S6 kinase 1 (S6K1 -/-), which is a positive regulator

of protein synthesis and is activated via phosphorylation by mammalian TOR complex 1 (mTORC1), exhibit a ~10% extension in lifespan, although this effect was only observed in females[80].

Mice with attenuated insulin signaling also exhibit lifespan extension. This includes mice overexpressing phosphatase and tensin homolog (PTEN-Tg), mice expressing one WT and one hypomorphic PI3K allele as well as mice in which the insulin receptor has been knocked out in adipose tissue[81–83].

In addition to reduced IIS and TOR signaling, overexpression of the NAD+-dependent deacetylase, Sir2, extends lifespan in invertebrates[30]. Interestingly, overexpression of SIRT1, the mammalian homolog of Sir2, has no effect on lifespan in mice, although importantly, SIRT1-Tg mice exhibit attenuated age-related increases in senescence-associated $p16^{INK4A}$ expression, DNA damage and cancer incidence[84]. However, overexpression of another member of the sirtuin family extends lifespan in mice. Male mice overexpressing SIRT6 exhibit a ~15% extension in lifespan (no lifespan extension observed in females). Consistent with the gender-specific effect on lifespan, male but not female SIRT6-Tg mice exhibit reduced levels of circulating IGF-1 and IGF-1 signaling in white adipose tissue. Notably, there were no differences between WT and long-lived SIRT6-Tg males in the frequency of the age-related pathologies that were assessed, including femoral osteoporosis, basal ganglia calcification and adrenal cortical hyperplasia[85]. SIRT6 is an NAD+-dependent protein deacetylase expressed throughout the body that functions as a histone H3 lysine 9 (H3K9) deacetylase that regulates telomere maintenance and is required for stable association of WRN (the RecQ helicase mutated in the human progeriod disease Werner Syndrome) with DNA and when knocked out leads to premature cellular senescence[86]. Therefore, lifespan extension in male SIRT6-Tg mice may be linked to enhanced genomic stability.

Other mouse models of extended lifespan characterized by enhanced genomic stability or enhanced protection against oxidative stress have been reported. This includes mice overexpressing BubR1, a component of the mitotic checkpoint that ensures proper segregation of sister chromatids, mice overexpressing catalase targeted to mitochondria[87,88] and mice lacking p66Sch, a mitochondrial redox signaling protein that through a variety of mechanisms increases reactive oxygen species (ROS) production and promotes apoptosis[89,90].

Dietary models

Calorie restriction (CR) is the reduction of caloric intake below *ad libitum* (AL) levels without malnutrition. To date, CR, is the most robust non-genetic intervention shown to attenuate aging and extend lifespan across phyla, including in yeast[91], flies[92], worms[93] and rodents[94,95].

In rodent research, the caloric intake of animals on CR regimens is typically reduced by 20-40% relative to the caloric intake of AL-fed controls with the degree of CR having a dose-dependent effect on lifespan extension[96]. In rodents, CR attenuates the development of a wide range of diseases and characteristics associated with aging, including insulin resistance[23,97], neurodegeneration[98], exhaustion of the replicative capacity of cells[99,100], stem cell exhaustion/dysfunction[101,102] and cancer[103]. CR enhances resistance to various

forms of stress, including heat and various toxic drugs[8], although fibroblasts from CR mice are no more resistant to a variety of cytotoxic and DNA-damaging agents than those derived from AL mice[104].

One of the prevailing theories of aging is the Free Radical Theory of Aging (FRTA), originally proposed by Harman in 1956[105]. In its initial form, this theory posited that aging is a consequence of the accumulation of oxidative damage to macromolecules in the cell due to the generation of free radicals by mitochondria and that increased metabolic rate is linked to increased free radical production. Subsequent work over the decades by various groups provided evidence that free radical production is in fact not linked to metabolic rate and that reactive species other that oxygen-derived free radicals are important contributors to oxidative damage, necessitating revisions to the original FRTA[106]. Nevertheless, the FRTA has been proposed to explain, at least in part, CR-induced lifespan extension because CR reduces free radical leak from mitochondria and attenuates the age-related accumulation of oxidatively damaged macromolecules in rodents[107–109].

Similar to the recurring themes of reduced IIS and TOR signaling in genetic models of attenuated aging and lifespan extension, CR reduces signaling through the somatotropic axis (GH/IGF-1). Indeed, CR rodents exhibit reduced circulating IGF-1 levels and reduced mTORC1 signaling, although GH secretory dynamics are preserved in old CR rats[23,110]. Other endocrine alterations in response to CR in rodents include elevated glucocorticoid levels, consistent with CR being a mild stressor, and reduced thyroxine (T4) levels[94,111]. Data regarding the status of circulating FGF21 levels remain ambiguous with some reports that it is unchanged[112] and some reports that it is elevated[70,113] in CR mice. Data described in Chapter 2 of the present body of work are consistent with diurnal fluctuations in FGF21 expression in adult mice on both AL and CR feeding regimens.

It is important to note that CR is not a universal lifespan-extending intervention in mice as evidenced by the fact that 40% CR actually shortened mean lifespan more often than it extended mean lifespan when tested in 41 different inbred strains of mice[114]. Specifically, 40% CR extended mean lifespan in male mice in 5% of the strains tested (mean lifespan extended by ~48-64%) while 40% CR extended mean lifespan in female mice in 21% of the strains tested (mean lifespan extended by ~8-100%). 40% CR shortened mean lifespan in male mice in 27% of the strains tested (mean lifespan shortened by ~10-79%) while 40% CR shortened mean lifespan in female mice in 26% of the strains tested (mean lifespan shortened by ~38-69%)[114]. The effects of a more modest degree of CR on mean lifespan in these strains of mice remains to be determined.

While data are conflicting as to whether or not CR extends lifespan in nonhuman primates, long-term CR in these animals improves healthspan by reducing the incidence of many age-related pathologies, including obesity, type 2 diabetes, cardiovascular disease, cancer, neurodegeneration and sarcopenia[115–118]. Whether or not CR will extend lifespan in humans is currently unknown but several studies have reported beneficial health effects of CR in humans. These health benefits include reduced incidence of age-related pathologies like obesity, type 2 diabetes and inflammation, reduced risk factors for cardiovascular disease and cancer as well as rejuvenated transcriptional profiles in muscle[117–119]. Consistent with enhanced resistance to oxidative stress in CR rodents, serum from CR humans promotes resistance to oxidative stress in cultured cells[120].

In addition to restricting total caloric intake, as is the practice in CR, reducing the amount of a specific nutrient without reducing total calories, a practice termed dietary restriction (DR), attenuates aging and extends lifespan in some cases. For example, protein restriction (PR) has a robust effect on lifespan, with 10 out of 11 studies in various mice and rat strains reporting an extension in lifespan in response to 40-85% PR. Comparisons of these studies to CR studies in rodents suggest that ~50% of the lifespan-extending effects of CR can be attributed to PR. Comparisons between CR and PR rodents also demonstrate that PR mimics many of the beneficial effects of CR, including reduced mitochondrial free radical leakage, tumor formation, glomerulosclerosis, nephropathy and cardiomyopathy[121].

In rodents, 65-80% restriction of the amino acid methionine extends lifespan[122–124]. Furthermore, in mice, 65% methionine restriction delays the age-related development of cataracts and decline in immune system function as measured by the levels of age-sensitive T-cell subsets[124]. Methionine-restricted mice also have reduced circulating levels of insulin, IGF-1, glucose and T4. Similar to CR mice, methionine-restricted mice are resistant to oxidative damage induced by an intraperitoneal dose of acetaminophen. Consistent with enhanced resistance to oxidative stress, methionine-restricted rats exhibit elevated blood levels of the antioxidant glutathioine (GSH), although GSH levels were reduced in the livers of these same animals[123].

Pharmacological models

At a workshop sponsored by the National Institute on Aging (NIA) in 2000, the Interventions Testing Program (ITP) was conceived[125]. The goal of this program is "to evaluate agents that are considered plausible candidates for delaying aging or preventing multiple forms of late-life disease in laboratory mice"[126]. By testing candidate agents at three independent sites, the ITP is designed to identify only those agents that have a robust effect on aging and lifespan parameters. Furthermore, by testing all candidate agents in genetically heterogeneous male and female mice, the ITP is designed to reduce the likelihood that any observed effects on health and lifespan outcomes are strain- or sex-specific. As of February 2014, a total of 26 agents had entered the ITP testing pipeline. Of the agents for which lifespan studies had been completed, only 2 extended lifespan in both male and female mice. These 2 agents are rapamycin and acarbose.

Rapamycin (also known as Sirolimus) is a macrolide originally isolated from the bacterium *Streptomyces hygroscopicus* in a soil sample from Easter Island (known as Rapa Nui)[127]. Rapamycin inhibits mTORC1 through its intracellular receptor FK506 binding protein (FKBP12), which when bound to rapamycin, binds to and inhibits mTORC1[128–131]. Rapamyin is an immunosuppressant that inhibits the proliferation of a number of cell types, including T-cells[132–138] and is FDA approved to prevent host-rejection in kidney transplant and for use in drug eluting stents[130]. Rapamycin is also used off-label for the treatment of a number of cancers[139].

In ITP studies, rapamycin treatment at 14ppm in the diet started at 9 months of age extended lifespan by 8-16% in males and 11-13% in females[140,141]. Strikingly, rapamycin treatment at this same dose but started at 20 months of age extends lifespan by 9% in males and 14% in females[142]. Results from follow-up studies using three different doses of

rapamcyin (4.7ppm, 14ppm or 42ppm in the diet), show that rapamycin extends lifespan in a dose-dependent manner[141].

Given rapamycin's anti-proliferative effects, it is possible that its lifespan-extending effects are merely due to reduced neoplastic diseases rather than a slowing of the rate of aging and thus an attenuation of a variety of age-related pathologies. An analysis of a wide range of age-dependent changes provided convincing evidence that this is not the case. In fact, rapamycin treatment attenuates the age-related development of liver degeneration, atypical nuclei in cardiomyocytes, endometrial cystic hyperplasia, adrenal tumors and tendon stiffening as well as attenuates the age-related decline in spontaneous activity[143]. In studies by other groups, rapamycin treatment suppresses pathological features in mouse models of neurodegenerative diseases, including, Alzheimer's, Parkinson's and Huntington's disease as well as in primary fibroblasts from HGPS patients[144]. Rapamycin, however, is not a panacea as evidenced by a higher incidence of testicular degeneration, cataracts and insulin resistance in rapamycin-treated mice[143,145].

The other agent that extended lifespan in both male and female mice in the ITP studies is acarbose. Acarbose treatment at 1000ppm in the diet started at 4 months of age extends lifespan by 11% in males and 9% in females. Acarbose inhibits alpha-glucosidases in the intestine thereby slowing glucose liberation from disaccharides and starches, thus preventing postprandial hyperglycemia. Despite reports that acarbose treatment increases food intake, chronic acarbose treatment in mice results in reduced body weight and body fat. These effects are similar to those observed in CR mice as is the reduction in circulating levels of IGF-1 and the attenuated age-related glucoregulatory dysfunction observed in acarbose-treated mice[141].

In studies that did not follow the same rigorous experimental design as the ITP, the biguanide, metformin, widely used for the treatment of type 2 diabetes and thought to exert its effects through both AMPK-dependent and -independent mechanisms, has also shown promise as a modulator of aging and lifespan in mice. In female SHR mice, metformin treatment at 100 mg/kg in drinking water starting at 3 months of age extends lifespan by ~3.3-20%[146–148]. Subsequent studies in male C57BL/6 mice demonstrated that metformin treatment also attenuates the age-related development of inflammation, cataracts and accumulation of oxidative damage[149].

Lessons from other studies

While having no effect on lifespan (maximum lifespan) and thus no effect on the rate of aging, as reported for the preceding examples, there are many interventions in rodents that extended mean lifespan (the age at which 50% of animals in a given population remain alive). Like maximum lifespan extension, an extension in mean lifespan represents an extension of healthspan, the time in which an organism remains active and in good health. While healthspan extension in the context of mean lifespan extension may be due to the attenuated development of only one age-related pathology, and thus has no bearing on general aging mechanisms, interventions that extend mean lifespan nevertheless contribute to our understanding of aging and by virtue of their ability to extend healthspan, have significant potential for translation into humans. Examples of interventions that extend mean lifespan in rodents include exercise, aspirin treatment and nordihydroguaiaretic acid (NDGA) treatment[150,151].

Insight into common factors associated with aging across a wide-range of genetic backgrounds has come from work by the Jackson Aging Center. The Jackson Aging Center has characterized lifespan, IGF-1 levels, age of female sexual maturation as well as many other metrics in 31 genetically diverse inbred strains of mice. These studies have revealed that a delay in the age of female sexual maturation is correlated with an increase in lifespan. Longer lifespan was also correlated with lower levels of circulating IGF-1 at 6 months of age (although this correlation disappeared when tested at 12 and 18 months of age)[152,153]. These data provide additional evidence in support of the existence of genetic tradeoffs between reproduction, growth and lifespan.

Other characteristics associated with long-life have been revealed through comparisons of long-lived taxonomically diverse organisms. These comparisons have revealed that the unique composition of lipids, proteins and DNA in long-lived animals makes them intrinsically highly resistant to oxidative modification. This resistance is likely achieved in part through reduced fatty acid saturation, reduced methionine content in proteins and reduced AT content in mtDNA in long-lived animals. It has been proposed that this resistance of macromolecules to oxidative modification may be mechanistically linked to superior longevity[107].

More lessons from humans

The motivation to study aging and the development of age-related diseases in non-human organisms is at its core to gain insight into how the development of age-related diseases in humans can feasibly be attenuated. Given the practical and ethical roadblocks to performing robust aging studies in humans, researchers must turn to model organisms and assume that mechanisms of aging in these organisms are conserved in humans. Encouragingly, the sparse data available on genetic factors that influence human lifespan are consistent with the prevailing themes that have emerged from research in model organisms. This includes the themes of reduced insulin and GH/IGF-1 signaling.

For example, a population of Ecuadorians carrying GHR mutations that confer GHR deficiency have reduced circulating insulin and IGF-1 levels and are protected against the development of diabetes and cancer. Compared to serum from relatives who do not harbor mutations in GHR, human mammary epithelial cells (HMECs) treated with serum from individuals with these GHR mutations were more resistance to oxidative damage induced by hydrogen peroxide, an effect shown to be dependent on reduced IGF-1 levels[154].

Other studies have revealed the following: i) polymorphisms in the IGF-1 receptor (IGF-1R) that confer partial loss-of-function are overrepresented in Ashkenazi Jewish centenarians[155], ii) polymorphisms in the IGF-1R and PI3CKB genes associated with lower serum IGF-1 levels are present in increased proportions in long-lived individuals (>85 yr)[156] and iii) genetic variation in Foxo1A and Foxo3A genes (the products of which are components of the IIS pathway) and the *klotho* gene (the product of which regulates insulin receptor and IGF-1R activity) are associated with lifespan in certain human populations[157–160].

GH/IGF-1 axis and mammalian aging

As previously mentioned, a review of examples of attenuated aging and lifespan extension in mammals reveals reduced signaling through the GH/IGF-1 axis (somatotropic axis) as a recurring theme. Indeed, more than half of the genetic mouse models of attenuated aging and extended lifespan are characterized by deficiencies in this axis, including Snell Dwarf, Ames Dwarf, GHR/BP-KO (Laron), GHRHR-KO (Little) mice as well as many others[161]. In addition, a robust hormonal response in rodents to the lifespan-extending dietary intervention, CR, is a reduction in circulating IGF-1 levels[23]. Emerging data is also revealing links between aging and lifespan in humans and perturbations in this axis. The mechanisms linking reduced GH/IGF-1 signaling to attenuated aging and lifespan extension are not fully understood, however, a growing body of evidence suggests that reduced mTORC1 signaling, enhanced defense mechanisms and enhanced insulin sensitivity play key roles[41].

This axis begins in the brain where hypothalamic peptides regulate the synthesis and secretion of GH (also known as somatotropin) from specialized cells called somatotrophs in the anterior lobe of the pituitary gland. The stimulatory and inhibitory effects of the hypothalamic peptides, GH releasing hormone (GHRH) and somatotropin release inhibitory factor (SRIF or somatostatin), on GH secretion from the pituitary gland, respectively, account for the pulse-like nature of GH secretion into circulation[41]. Once in circulation, one of the functions of GH is to regulate the production of IGF-1.

The liver is the primary source of circulating IGF-1[162]. In this tissue, GH from the circulation binds simultaneously to two GH receptors (GHR) on hepatocytes dimerizing the receptors and stimulating their association with the intracellular kinase, janus kinase 2 (JAK2), which subsequently autophosphorylates and phosphorylates the GHRs creating binding sites for signal transducer and activator of transcription 5 (STAT5). Once bound to the GHRs, STAT5 is phosphorylated by JAK2, which stimulates STAT5 to dimerize and translocate to the nucleus where STAT5 activates the transcription of IGF-1 and the IGF-1 stabilizing factor, acid labile subunit (ALS)[163].

As its name implies, IGF-1 is a growth factor. Upon secretion from tissues, IGF-1 circulates in the blood bound to ALS and IGF-1 binding proteins (IGFBP). Binding of IGF-1 to the IGF-1R activates intracellular signaling pathways, including MAPKinase and PI3K/AKT/mTOR pathways, resulting in the stimulation of cell growth, cell proliferation, protein synthesis as well as the inhibition of apoptosis[164–166]. IGF-1 is also produced locally in many tissues via GH-dependent as well as –independent mechanisms[41]. MAPKinase and PI3K/AKT/mTOR pathway signaling is also stimulated by GH via IGF-1-independent mechanisms[41].

Another important function of GH is to stimulate lipolysis in adipose tissue in the fasted state[167,168]. This function of GH is strikingly apparent in long-lived GH-deficient mice, which have increased adiposity relative to their WT counterparts[64,169,170].

Circulating levels of GH and IGF-1 decrease with age in both rodents and humans[23,41]. Reductions in these anabolic hormones are believed to contribute to various aspects of physiological deterioration associated with aging including increased adiposity, reduced muscle mass and cognitive decline. Moreover, repletion of these hormones in aged

rodents partially rescues many age-related phenotypes including the age-related decline in protein synthesis in skeletal muscle, immune function and memory[23,171–174]. Not surprisingly, these rejuvenating effects have generated a great deal of interest in GH/IGF-1 supplementation as an anti-aging treatment in humans[170]. However, despite any potential benefits of GH/IGF-1 supplementation in old age, there is a wealth of evidence to support a role for lifelong reductions in GH/IGF-1 signaling in the attenuation of the aging process, an effect believed to be conferred in part via a reduction in mTORC1 signaling.

mTORC1 and mammalian aging

Target of rapamycin (TOR) is a serine/threonine kinase belonging to the phosphatidylinositol 3-kinase-related kinase protein family conserved from yeast to humans that functions as a central integrator of a variety of cellular signals including those associated with nutrient availability, stress and growth[166]. In mammals, TOR (known as mammalian TOR or mTOR) interacts with two different repertoires of proteins to form two distinct complexes, mTOR complex 1 (mTORC1) and mTOR complex 2 (mTORC2). While both complexes include, mTOR, mLST8 (also known as GßL), tti1/tel2, and deptor, only mTORC1 contains raptor and pras40 whereas only mTORC2 contains rictor, mSin1 and protor1/2[175]. Owing to their unique constellation of proteins, these two complexes respond to different stimuli and regulate distinct processes in the cell.

mTORC2 is activated by growth factors and regulates cell survival, metabolism and cytoskeletal organization. mTORC1 responds to amino acids, stress, oxygen levels, energy levels and growth factors and when activated promotes cell growth, cell proliferation, ribosome biogenesis, protein synthesis and lipid biogenesis and inhibits autophagy. These two complexes also differ in their sensitivity to the macrolide rapamycin. While mTORC1 is highly sensitive to inhibition by rapamycin, mTORC2 is insensitive, except when rapamycin treatment is prolonged[176]. Importantly, rapamycin attenuates aging and extends lifespan in mice, whereas TOR deficiency has similar effects across a variety of organisms, including yeast, worms and flies[142,177]. The unique role of TOR, and specifically mTORC1 in mammals, as a central node linking nutrient sensing and growth, make it well poised to regulate the tradeoffs between growth and somatic maintenance believed to underlie rates of aging and lifespan determination as previously discussed. How might this be possible?

To begin, it is helpful to briefly revisit the disposable soma theory of aging, which posits that there is a tradeoff between somatic maintenance and growth and reproduction because metabolic resources are finite. Somatic maintenance involves maintaining cellular defense systems that combat protein misfolding, endogenous and exogenous oxidants as well as toxins and thus promotes optimal cellular and, therefore, organismal health. Evolutionarily, it is only necessary to maintain the soma for as long as an organism has a reasonable chance for survival in the wild. Therefore, if an organism has only a small chance of living past a certain age, it is advantageous to allocate metabolic resources before this age to processes that promote immediate survival (growth) and propagation of the species (reproduction)[10]. However, in times of highly limited resources, it would be advantageous to delay growth and reproduction and allocate resources to somatic maintenance until conditions become more amenable to successfully rearing offspring.

mTORC1 is activated when the cell has ample nutrients (particularly the amino acids leucine and arginine) and/or energy levels (low AMP:ATP ratio) as well as in response to growth factors signaling. One of the major functions of active mTORC1 is to promote protein synthesis. This is accomplished through a combination of mechanisms that ultimately promote cap-dependent mRNA translation. These mechanisms include: i) phosphorylation and activation of S6K1 which phosphorylates and activates ribosomal protein S6 ((RPS6) a component of the 40S ribosomal subunit) and eIF4B which activates the helicase activity of eIF4A which facilitates unwinding of the 5' untranslated region (UTR) of mRNAs (particularly those with highly structured 5'UTRs) thus facilitating scanning by the 40S ribosomal subunit for the initiation codon and ii) phosphorylation and inhibition of 4E-BP1 which when active binds to and inhibits eukaryotic initiation factor 4E (eIF4E) from forming a functional eIF4F cap-binding complex (composed of eIF4E, eIF4G and eIF4A)[178,179].

Inhibition of mTORC1 results in a reduction in cap-dependent mRNA translation and subsets of mRNAs with specific sequence motifs are particularly sensitive to mTORC1 inhibition. This includes mRNAs containing 5' terminal oligopyrimidine tract (TOP) motifs (defined as mRNAs with a cytidine immediately after the 5'-cap, followed by an uninterrupted stretch of 4–14 pyrimidines) and TOP-like motifs (defined as a stretch of at least five pyrimidines within four nucleotides of the most frequent transcriptional start site)[180]. Most TOP and TOP-like mRNAs encode protein biosynthesis factors including ribosomal proteins and translation factors, thus explaining the promotion of ribosomal biogenesis by active mTORC1[181,182].

Translation, including mTORC1-mediated translation, is inhibited by a variety of stresses. For example, nutrient deprivation, hypoxia and DNA damage all inhibit mTORC1[175]. Translation is also inhibited through inhibition of the eukaryotic initiation factor F2 (eIF2) in response to heme deprivation, oxidative stress, heat shock, ER stress, nutrient deprivation, proteasome inhibition, UV radiation and viral infection[183]. Importantly, while these stresses result in a general reduction in mRNA translation, the translation of a subset of mRNAs encoding proteins involved in stress responses is actually increased.

Differential mRNA translation and stress responses

Mammalian cells have a program that globally reduces mRNA translation in response to various stresses but upregulates translation of mRNAs that encode proteins that remediate cellular stress. This "integrated stress response" is mediated by phosphorylation of eIF2 by four kinases that respond to various stresses[184]. eIF2 forms the ternary complex (TC) along with GTP and aminoacylated initiator methionyl-tRNA (Met-$tRNA_i^{MET}$)[185]. The TC combines with the 40S ribosomal subunit to form the 43S pre-initiation complex, which scans for the start codon on mRNAs. When the start codon is recognized, eIF2-GTP is converted into eIF2-GDP. eIF2-GDP must be converted back to eIF2-GTP by its guanine nucleotide exchange factor (GEF), eIF2B, before it can form another functional TC. When the alpha subunit of eIF2 is phosphorylated at Ser51, eIF2B can no longer exchange GDP for GTP on eIF2 and, therefore, the number of functional TCs becomes limiting and global mRNA translation is suppressed[178].

Four kinases have been identified that phosphorylate eIF2alpha, including general control non-derepressible-2 (GCN2), protein kinase R (PKR), PKR-like ER kinase (PERK) and heme-regulated inhibitor (HRI). These kinases are activated in response to various stresses. For example, GCN2 is activated in response to nutritional deprivation, proteasome inhibition and UV radiation, PERK by ER stress, HRI by heme deprivation, oxidative stress and heat shock and PKR by viral infection[184]. eIF2alpha phosphorylation by these kinases results in a general suppression of mRNA translation but the translation of mRNAs encoding activating transcription factor 4 (ATF4) is actually increased. When functional TCs are limiting, scanning by the 40S subunit is pro-longed increasing the probability that it will reach the protein-coding initiation codon of ATF4 (which is downstream of several non-protein coding upstream open reading frames (uORFs) in its 5'UTR) and associate with a functional TC on the way[185]. ATF4 activation results in the transcriptional upregulation of genes encoding stress remediation proteins including proteins involved in amino acid import, maturation and degradation of proteins, glutathione synthesis and the control of redox, autophagy, mitochondrial function and control of apoptosis[186]. Similarly, stressors like ER stress, hypoxia and nutrient deprivation that reduce cap-dependent translation, also increase translation of mRNAs containing internal ribosome entry sites (IRES). Many of the mRNAs containing IRESs encode proteins involved in the protection of cells from stress and the control of apoptosis[187].

There is also precedence that globally reduced mRNA translation coupled with differential translational upregulation of subsets of mRNAs mediates lifespan extension in some organisms. For example, while DR in flies reduces global mRNA translation, DR-induced lifespan extension in flies is partially dependent on differential translational upregulation of mRNAs encoding mitochondrial proteins[33]. Compared to average 5'UTRs, the 5'UTRs of these mRNAs encoding mitochondrial proteins were shorter, had lower GC content and weaker secondary structures.

In worms, while eIF4G knockdown reduces global mRNA translation, translation of several mRNAs encoding stress response proteins was upregulated and in some cases required for lifespan extension in eIF4G-deficient worms[188]. These translationally upregulated mRNAs had average 3'UTR lengths and overall ORF lengths greater than translationally downregulated mRNAs (which were enriched for mRNAs encoding proteins involved in growth and reproduction).

It is clear that in response to an array of stresses, cells employ various strategies to suppress global mRNA translation (and thus growth) and through a variety of mechanisms increase the translation of mRNAs that encode proteins that can combat stress. The extent to which differential translational control of mRNAs encoding stress response proteins contributes to attenuating aging and extending lifespan in mammals is currently unknown. However, as described in previous sections, stress resistance is a recurring theme in mice with GH/IGF-1/mTORC1 level or signaling deficiencies and their enhanced ability to combat stress, prevent cellular damage and thus maintain their soma, likely contributes to the attenuation of aging and the lifespan extension observed in these mice[41,42]. It is important to note that these genetic (pituitary dwarfs and others), dietary (CR, methionine restriction and protein restriction) and pharmacological (rapamycin, acarbose, metformin) interventions all induce forms of chronic stress via growth factor deprivation, nutrient deprivation or suppression of nutrient signaling. This coupling of what amounts to

reduced growth signaling and enhanced resistance to stress across a variety of models of attenuated aging and lifespan extension provides strong support for the existence of tradeoffs between growth and somatic maintenance and that aging can be delayed when somatic maintenance is favored.

One key aspect of somatic maintenance is the maintenance of the proteome.

Proteome maintenance and aging

As organisms age, their ability to detect, repair and replace damaged proteins diminishes, and consequently, aging is associated with an accumulation of damaged proteins[25]. Damaged proteins are defined as proteins that are oxidized, misfolded and/or aggregation-prone. This impaired ability to maintain proteome stability (proteostasis) compromises cellular, tissue and ultimately organismal homeostasis. To understand how proteostasis diminishes with age, it is helpful to first review the processes that normally contribute to proteostasis, including processes that prevent against protein damage as well as processes that detect, repair and, if necessary, replace damaged proteins.

Proteostatic mechanisms

The proper folding of proteins into their functional (native) three-dimensional structure as well as defenses against oxidative damage are two critical processes that prevent against protein damage in the cell. Molecular chaperones in the cell facilitate the folding of proteins into their native conformations[189]. Molecular chaperones are proteins that aid other proteins in acquiring their native active conformation but are not part of the final protein structure[190]. Members of the heat shock protein (HSP) family of proteins including, the HSP70s, HSP90s and HSP60s, facilitate *de novo* protein folding via ATP- and cofactor-regulated binding and release cycles. These chaperones bind to exposed hydrophobic regions on non-native proteins, which prevents them from aggregating. These chaperones then release their client proteins in an ATP-dependent manner allowing folding to proceed[189].

In the ER, folding of secreted and membrane-bound proteins is facilitated by various molecular chaperones including protein disulfide isomerases (PDIs), classical chaperones in the HSP family like BiP (also known as glucose-regulated protein 78 (GRP78)) and carbohydrate-binding chaperones like calnexin and calreticulin, which recognize unique *N*-linked glycans attached to folding proteins[191]. PDIs facilitate folding of nascent polypeptide chains by catalyzing the formation and breakage of disulfide bonds as proteins fold into their native conformation. Like other members of the HSP70 family, BiP cyclically binds to and releases exposed hydrophobic regions of non-native proteins preventing their aggregation and facilitating their folding.

In the ER, nascent polypeptide chains are also modified by N-linked glycans on Asn residues by oligosaccharyltransferase (OST). These glycans serve several functions, including stabilizing hydrophobic regions on non-native proteins and serving as signals for retention in the ER. As nascent polypeptides are cotranslationally translocated into the lumen of the ER, OST transfers a preassembled carbohydrate comprised of three glucoses, nine mannoses, and two N-acetyl glucosamines ($Glc_3Man_9GlcNAc_2$) onto Asn residues in the

Asn-X-Ser/Thr sequence. As the polypeptide chain begins to fold, glucosidases remove terminal glucoses from this glycan moiety generating a monoglucosylated glycan that the carbohydrate-binding chaperones, calnexin and calreticulin, can bind. Calnexin and calreticulin then facilitate efficient folding of these non-native proteins by, among many things, preventing aggregation, facilitating the formation of disulfide bonds through their association with the oxidoreductase ERp57 and importantly, retaining non-native proteins in the ER for continued attempts at proper folding. When the final glucose is removed from the glycan moiety, calnexin and calreticulin can no longer bind to the glycated protein. If this freed protein is in its native conformation it can exit the ER. However, if the freed protein is still not folded properly, UDP-glucose: glycoprotein glucosyltransferase 1 (UGT1) reglycosylates its glycan moiety so that it can once again associate with calnexin and calreticulin to continue attempts at proper folding[191].

In general, proteins that fail to achieve their native conformation may not function properly, are prone to aggregation and are more susceptible to oxidative damage[192,193]. Likewise, oxidation of proteins can typically result in some degree of unfolding[194]. Therefore, preventing protein misfolding and oxidative damage to proteins is central to proteostasis.

Several defense systems exist in the cell to prevent against oxidative damage to proteins and other macromolecules by metabolizing and deactivating ROS. During aerobic respiration, leakage of electrons from the electron transport chain (ETC) leads to the univalent reduction of molecular oxygen producing the superoxide anion radical ($O_2^{\bullet -}$). The superoxide anion radical is also produced by enzymes in the cell including xanthine oxidase, lipoxygenase and several others[195]. This superoxide anion radical can react with transition metals within enzymes compromising the function of these enzymes and generating Fe^{2+} and Cu^{+} in the process (known as the Fenton reaction). The antioxidant enzyme superoxide dismutase (SOD) can convert the damaging superoxide anion radical to hydrogen peroxide (H_2O_2), which is a mild oxidant. However, hydrogen peroxide can react with Fe^{2+} and Cu^{+} to form the highly toxic hydroxyl radical ($OH^{\bullet}$). To limit the production of the hydroxyl radical, additional antioxidant enzymes, including glutathione peroxidases, peroxiredoxins and catalase convert hydrogen peroxide into water[194,196].

Nevertheless, some proteins will inevitably become damaged and/or unfolded and various stresses may increase the demand for protein recycling or lead to the accumulation of damaged and/or unfolded proteins. The cell, however, has several repair systems that function to reestablish proteostasis when it is perturbed.

Specialized repair enzymes can reverse some types of protein oxidative damage. For example, oxidative damage to the sulfur-containing amino acids, which are the amino acids most susceptible to oxidative damage, can be repaired via the glutaredoxin/glutathione/glutathione reductase (cysteine), thioredoxin/thioredoxin reductase (cysteine) or methyl-sulfoxide reductase (methionine) systems[197]. Other forms of protein damage are irreversible including the formation of carbonyls, cysteine sulfonic acid (SO3-), cleavage of the polypeptide chain as well as lipid peroxidation and glycoxidation adducts. To preserve proteostasis, these irreversibly damaged proteins must be degraded and replaced[197].

Basal levels of degradation of both normal and damaged proteins occur primarily via the proteasome[198]. The 26S proteasome is composed of a central 20S subunit and two 19S regulator caps, all of which can be found in both the cytoplasm and nucleus[199]. The cylindrical 20S subunit is composed of two inner beta rings and an alpha ring on either end, with each ring composed of 7 subunits. The proteolytic activity of the 20S (and 26S) proteasome resides in 3 subunits within the inner beta rings. The 20S proteasome preferentially binds to and degrades oxidized and/or unfolded proteins and is itself quite resistant to oxidative stress. Similar to classical chaperones, the alpha rings of the 20S proteasome are believed to recognize oxidized and unfolded proteins via their exposed hydrophobic patches. The Lon protease in mitochondria also preferentially degrades oxidized proteins[200]. The 26S proteasome on the other hand, restricts degradation to ubiquitylated proteins, appears to have no preference for oxidized versus normal proteins and is more sensitive to deactivation following oxidative stress[194].

In addition to the central 20S subunit, the 26S proteasome has two 19S regulators that cap the ends of the 20S subunit. These 19S regulators recognize polyubiquitylated proteins and feed them into the 20S core. Proteins are ubiquitylated on lysine residues via the sequential action of three enzymes, an E1 ubiquitin activating enzyme, an E2 ubquitin carrier enzyme and an E3 ubiquitin ligase. A polyubiquitin chain can then be generated on a protein via the sequential attachment of additional ubiquitin molecules to lysine residues on the ubiquitin protein itself[194].

In response to various stresses, including starvation and growth factor deprivation, cells can upregulate another degradation pathway mediated by the lysosome called autophagy. Through two ubiquitin-like conjugation reactions, a double membrane structure called a phagophore is formed that engulfs cytosolic components, including proteins and organelles, and then closes to form an autophagosome. Autophagosomes then fuse with the lysosome and lysosomal hydrolases degrade the contents of the resulting autophagolysosomes. The resulting molecules can then be returned to the cytosol for reuse[201]. Autophagy is regulated by a variety of factors. Negative regulators of autophagy include growth factors and mTORC1, whereas amino acid deprivation, AMPK and ROS are positive regulators[202,203].

In the ER, newly synthesized proteins that do not achieve their native conformation are ultimately degraded via a processed termed ER-associated degradation (ERAD). This pathway involves the recognition of unfolded proteins by chaperones, dislocation of these proteins from the ER lumen across the ER membrane into the cytosol and ultimately their ubiquitination and degradation via the 26S proteasome[204]. However, if the concentration of unfolded proteins exceeds the folding capacity of the ER, a remediation pathway known as the unfolded protein response (UPR) will be induced.

The UPR^{ER} reestablishes proteostasis by suppressing global protein synthesis, hastening the degradation of misfolded proteins and increasing the folding capacity of the ER by upregulating the expression of chaperones and expanding the size of the ER. All of these processes are triggered by the accumulation of unfolded proteins in the ER, which results in the titration of the chaperone BiP away from three ER transmembrane proteins (ATF6, IRE1 and PERK), which results in their activation. Titration of BiP away from ATF6 leads to trafficking of ATF6 from the ER to the golgi where it is proteolytically cleaved.

Cleaved ATF6 can then enter the nucleus and bind to ER-stress response elements (ERSEs) and induce the expression of genes, like BiP and XBP1. Titration of BiP away from the kinase IRE1 results in homodimerization, autophosphorylation and activation of IRE1. Active IRE1 possesses endoribonuclease activity and selectively processes XBP1 mRNA to generate a spliced XBP1 mRNA (XBP1s) that encodes an XBP1s protein capable of binding to UPR elements (UPREs) and inducing the transcription of genes encoding proteins involved in ERAD, lipid biosynthesis as well as disulphide bond formation and glycosylation. Titration of BiP away from the kinase PERK results in its autophosphorylation and activation. Active PERK phosphorylates the alpha subunit of eIF2 (eIF2alpha) inhibiting the formation of the ternary complex (composed of eIF2, GTP and aminoacylated initiator methionyl-tRNA) and thus suppressing global mRNA translation. Importantly, mRNAs containing upstream open reading frames (uORFs), like those encoding ATF4, escape translational suppression. Once translated, ATF4 translocates to the nucleus where it binds UPREs and induces the expression of BiP and other UPR target genes[205].

UPRs that are distinct from the UPR^{ER} can also be triggered in the cytosol as well as in mitochondria. The cytosolic version of the UPR is termed the heat shock response. Under normal conditions, the transcription factor heat shock transcription factor 1 (HSF1) is sequestered in the cytoplasm via interactions with the chaperones, HSP70 and HSP90. Because HSP70 and HSP90 preferentially interact with unfolded proteins, when unfolded proteins accumulate in the cytosol, HSP70 and HSP90 are titrated away from HSF1 freeing it to translocate to the nucleus where it binds to heat shock elements (HSEs) and induces the expression of HSP70 and HSP90[206]. In response to perturbations in protein folding in mitochondria, the expression of mitochondrial chaperones, including HSP60 and mtHSP70, is induced[207].

Regardless of the type or cause of damage to proteins and regardless of the cellular mechanisms employed to handle protein damage, the preservation of proteostasis requires that irreversibly damaged proteins not only be detected and degraded, but that they also be resynthesized to replenish protein pools.

Proteostasis and aging

Loss of proteostasis is associated with several age-related pathologies in mammals, including cataracts, sarcopenia and neurodegenerative diseases, and is widely appreciated as a hallmark of aging[2,25,208]. Indeed, aging is associated with impairments in protein repair enzymes, reduced chaperone capacity, defects in autophagy, reduced proteasome activity (due to reduced proteasome biosynthesis and reduced expression and function of proteasome subunits with age), reduced protein synthesis and a concomitant accumulation of damaged proteins[25,194,197,209].

Importantly, experimental perturbations that impair proteostasis have been shown to exacerbate features of aging while experimental perturbations that preserve proteostasis have been shown to delay features of aging[2]. For example, deficiency in the ubiquitin ligase/cochaperone carboxyl terminus of Hsp70-interacting protein (CHIP), which targets chaperone substrates for proteasomal degradation results in reduced proteasome activity, increased oxidative damage, premature replicative senescence and shortened lifespan in mice[210]. Conversely, preventing the age-related decline in chaperone-

mediate autophagy in the liver results in lower intracellular accumulation of damaged proteins, an enhanced ability to handle protein damage and improved organ function in mice[211]. In addition, reduced IGF-1R signaling in a mouse model of Alzheimer's disease has been show to result in tightly packed amyloid-beta aggregates and protection from behavioral impairment, neuroinflammation, and neuronal loss[212]. Overall, these data show that the capacity to detect, repair or replace damaged proteins is tightly linked to cellular homeostasis, and when compromised, contributes to the aging process.

In addition to maintenance of homeostasis at the proteome and cellular level, maintenance of tissue homeostasis is also of utmost importance for the preservation of organismal health. A fundamental cellular process linked to tissue homeostasis is cell proliferation.

Cell proliferation, cell proliferative capacity, cellular senescence and aging

Mammalian aging is characterized by a progressive decline in the regenerative capacity of tissues, which in turn compromises the ability of an organism to respond to endogenous and exogenous insults requiring a proliferative response. This decline in the regenerative capacity of tissues may be due to the decline in the proliferative capacity of stem cells, which in turn has been suggested to be a result of telomere shortening and/or the accumulation of cellular damage leading to a senescent state[213–215]. Therefore, preserving the proliferative capacity of stem cells may ultimately extend lifespan by preserving the regenerative and functional capacity of organs.

Evidence that a limit to cell proliferative capacity exists was first described by *Hayflick* in 1965[216]. In this seminal paper, *Hayflick* demonstrated in three independent human fetal fibroblast cell lines that *in vitro* cell division ceased after ~51 divisions. Consistent with *in vitro* data, others have shown that *in vivo* cell proliferative capacity is not infinite. For example, *Harrison et al*. showed in mice that the ability of marrow cells to repopulate a depleted niche declines after transplantation regardless of whether the transplantation was by injection or parabiosis following lethal irradition or recovery from sublethal irradiation without transplantation[217]. In addition, genetic models of accelerated aging exhibit premature exhaustion of cell proliferative capacity. "Giant" mice over-expressing bovine GH have a 50% reduction in maximum lifespan relative to age-matched controls and exhibit early-life hyperproliferation of their fibroblasts and epithelial cells followed by significant reductions in the proliferative capacity of these cells at later stages in life[14]. Similarly, fibroblasts derived from individuals with the human progeroid disease, Hutchinson-Gilford progeria syndrome, exhibit an initial phase of hyperproliferation followed by the premature accumulation of apoptotic cells, while fibroblasts derived from individuals with another human progeroid disease, Werner's Syndrome, display severely reduced replicative potential[56,218]. In contrast, CR in mice has been shown to attenuate the age-related decline in both the *in vitro* and *in vivo* proliferative capacity of a variety of cells of both nonhematopoetic and hematopoetic origin[99,100]. Together these data from *in vitro* and *in vivo* studies provide convincing evidence that mammalian aging is associated with a decline in cellular proliferative capacity and that attenuating this decline may confer lifespan benefits. However, to preserve cell proliferative capacity, we first must

understand what factors lead to irreversible cell proliferation arrest, a phenomenon known as cellular senescence[219].

Cellular senescence is governed by at least two tumor suppressor pathways including the p53/p21 pathway and the $p16^{INK4a}$/pRB pathway[220]. These pathways are activated in response to a variety of stresses and play important roles in suppressing tumorigenesis. However, their repressive effects on cell proliferation also compromise the regenerative capacity of tissues. What stresses then activate these pathways?

Genomic damage that cannot be readily resolved leads to a persistent DNA damage response and p53-mediated transcriptional upregulation of the cell cycle inhibitor p21 and subsequent cell cycle arrest[221]. A persistent DNA damage response, as well as other forms of stress like oxidative stress, may also lead to $p16^{INK4a}$-mediated activation of pRB which silences the expression of certain proliferative genes via heterochromatinization leading to cell cycle arrest[222]. A well-documented inducer of senescence is telomeric damage. This type of DNA damage arises from telomere shortening, which is a consequence of the absence in many cells of telomerase, the enzyme that maintains telomere length during DNA replication[223]. Furthermore, both the p53/p21 and $p16^{INK4a}$/pRB tumor suppressor pathways can be activated by persistent mitogenic signaling[220]. Therefore, in addition to preventing or efficiently repairing DNA damage, reducing cell proliferation, and potentially the telomere shortening that accompanies it, by suppressing mitogenic signals may provide a legitimate way to combat cellular senescence.

Intriguingly, one of the most robust cellular responses to CR is a reduction in the rate of cell proliferation. The cell proliferation rate-lowering effect of CR was originally characterized by Bullough et al. in 1945 in epidermal cells in mice[224]. Others, including our lab, have subsequently extended this originally finding that CR reduces the rate of cell proliferation to cells of the liver, kidney, mammary gland, pancreas, urinary bladder, dermis, esophagus, spleen and the crypts of the colo-rectum, jejunum and duodenum[99,225–228]. Therefore, CR reduces the rate of cell proliferation in a global manner. Our lab (unpublished observations) and other labs have also shown that like its lifespan-extending effects, this global cell proliferation rate-lowering effect of CR is dose-dependent[96,226].

If indeed there exists a limit to cellular proliferative capacity, this reduction in basal rates of global cell proliferation in response to CR may function to chronologically extend the proliferative capacity of cells by delaying cellular senescence and additionally it may create a non-permissive environment for cancer development by inhibiting the promotional phase of carcinogenesis.

The mechanism(s) by which CR leads to a reduction in global rates of cell proliferation is unknown. There is, however, evidence to suggest a causal role for reduced circulating IGF-1 in the attenuation of cell proliferation and cancer promotion in rodents on a CR regimen. For example, in rats, the CR-induced reduction in the proliferation of transplanted mononuclear cell leukemia is attenuated by repletion of circulating IGF-1 back to AL levels[229]. Similarly, in p53 heterozygous mice treated with the bladder carcinogen, p-cresidine, the CR-induced reduction in the proliferation of cells in hyperplastic foci is attenuated by repletion of circulating IGF-1 back to AL levels[230]. In a non-cancer model in rats, the CR-induced reductions in thymus and splenic T-cell number are attenuated by repletion of circulating IGF-1 back to AL levels[231].

These data, combined with the knowledge that chronic mitotic signaling can induce cellular senescence, provide evidence that a reduction in mitogenic signaling via reduced circulating IGF-1 levels or through other mechanisms, may delay age-related loss of tissue function.

The seemingly ubiquitous nature of reduced IGF-1 signaling across various models of attenuated aging and extended lifespan and IGF-1's role in fundamental cellular processes like protein synthesis and cell proliferation that are tightly linked to organimsal aging, has sparked great interest in fine-tuning our understanding of how the levels of this hormone are regulated, particularly in the context of CR.

FGF21 and the GH/IGF-1 axis in CR

As previously reviewed, circulating IGF-1 is primarily produced in the liver in response to GH signaling[162]. Total energy intake, protein intake, insulin and thyroid hormone also contribute to IGF-1 protein expression underscoring the pivotal role of nutritional status in the regulation of IGF-1 expression[232]. The amount of bioavailable IGF-1 in circulation also depends on the stability of IGF-1 in circulation which is enhanced by forming a ternary complex with acid-labile subunit (ALS) and one of the IGF-1 binding proteins (IGFBPs), IGFBP-3, both of which are also transcriptionally upregulated by GH signaling[233,234]. IGF-1 signaling via its cell surface receptor, IGF-1R, is regulated by IGF-1R expression as well as by multiple proteases and IGFBPs that influence local IGF-1 action[235]. One of these IGFBPs, IGFBP-1, which is upregulated in response to fasting and CR, reduces IGF-1 bioavailability[232,236].

The exact mechanism(s) by which circulating IGF-1 levels are reduced in response to CR is not fully understood and is likely the result of a variety of contributing factors that could include changes in circulating GH, insulin, thyroid hormone and IGFBP levels, GHR levels and intracellular GHR signaling. In food-restricted humans, GH levels are actually increased, ruling out reduced GH secretion as the cause of reduced circulating IGF-1 in this context[237]. However, in CR rats, GH levels are reduced and, therefore, may contribute to the CR-induced reduction in circulating IGF-1 levels in this species[229,238]. Interestingly, while GH levels are reduced in young CR rats relative to age-matched AL controls, GH levels are higher in old CR rats compared to age-matched AL controls[239]. The role that changes in GH levels may play in the CR-induced reduction in IGF-1 levels in mice has not been directly assessed. However, a study in 2008 demonstrated that fibroblast growth factor 21 (FGF21), which is induced in response to fasting, is a novel negative regulator of IGF-1 expression in mice, likely acting through a mechanism that involves GH-resistance[71]. This finding, led our group as well as others to test the hypothesis that FGF21 is necessary for the reduction in circulating IGF-1 levels in response to CR in mice.

FGF21 is a novel member of the superfamily of fibroblast growth factor (FGF) genes which are primarily involved in developmental processes, including cell proliferation, differentiation and growth[240,241]. Unlike canonical FGFs, which are secreted from cells and function in an autocrine/paracrine fashion through interactions with both heparan sulfate proteoglycans (HSPGs) and FGF receptors (FGFRs), endocrine-like FGFs including FGF15/19, 21 and 23, have low affinities for HSPGs enabling them to enter circulation and function in an endocrine fashion[242]. Also, in contrast to canonical FGFs, FGF21 signaling

through the FGFR (primarily FGFRs 1c, 2c and 3c) involves the transmembrane co-factor β-klotho[49,243–245]. Binding of FGF21 to FGFR and β-klotho stimulates canonical FGFR signaling through FRS-2, MAPK, SHP-2 and Akt[246,247]. FGF21 is primary produced by the liver, adipose tissue and pancreas and its target tissue specificity is determined by β-klotho expression, which is restricted to the adipose tissue, liver, gall bladder, colon, pancreas and testis[248]. Interestingly, while its name implies that it is a growth factor, FGF21 is not mitogenic, unlike the majority of FGFs[245,249,250].

FGF21 was originally identified via homology-based PCR due to its sequence similarity to FGF19 and was subsequently identified in a screen of secreted factors as a stimulator of glucose uptake into 3T3-L1 adipocytes[249,251]. Expanding its potential therapeutic utility, subsequent studies suggested a role for FGF21 in regulating IGF-1 production in the fasted state[71]. In these studies, FGF21-transgenic (FGF21-Tg) mice that express FGF21 under the control of the ApoE promoter exhibited reduced hepatic IGF-1 and ALS and increased IGFBP-1 mRNA expression, all changes that reduce the bioavailability of IGF-1. Not surprisingly, these mice were smaller and had significantly reduced circulating IGF-1 levels. Interestingly, while these mice had increased circulating GH levels and increased hepatic levels of the phosphorylated/active form of JAK2, they had significantly reduced hepatic levels of the phosphorylated/active form of STAT5 suggesting GH-resistance in these mice. In addition, hepatic mRNA expression of suppressor of cytokine signaling 2 (SOCS2), which inhibits the GH-signaling cascade, was reduced in these mice[252]. Given that STAT5 is a transcription factor that regulates the expression of IGF-1 and ALS, these data suggest that during fasting, FGF21 inhibits GH-mediated IGF-1 production by inhibiting STAT5 phosphorylation, possibly through upregulation of SOCS2. These findings, along with reports that FGF21-Tg mice live longer than WT controls, prompted investigations into potential roles for FGF21 in CR, including a role in the CR-induced reduction in circulating IGF-1 levels and reduction in global cell proliferation rates[74].

Data regarding changes in FGF21 expression in response to CR in mice are conflicting with some studies reporting an increase[70,113] and others reporting no change relative to AL controls[74,112]. In studies using whole-body FGF21-knock out (FGF21-KO) mice, FGF21 proved to be necessary for the full undernutrition-related reduction in hepatic mRNA and circulating levels of IGF-1[70].

Biomarkers of aging and lifespan extension

The motivation to assess FGF21's role in CR is the same motivation that prompts most gerontological research: the identification of factors that govern the aging processes. The ultimate goal is to then use this knowledge to develop interventions that delay the development of age-related pathologies that normally limit human healthspan. To be implemented, such an intervention would have to be proven to robustly attenuate aging. Testing candidate interventions in humans, however, is not feasible for ethical and practical reasons. Therefore, to test if an intervention attenuates aging, researchers must conduct long-term healthspan and lifespan studies in physiologically relevant model organisms, like rodents. Unfortunately, these studies still take years to complete and require large numbers of animals at considerable cost.

The identification of biomarkers of lifespan extension would provide an alternate initial route for candidate intervention testing if these biomarkers manifested and were predictive of healthspan and lifespan outcomes relatively soon after the initiation of an intervention. Such a panel of biomarkers could function as a coarse filter for inclusion or exclusion of candidate interventions into more in-depth studies, including long-term healthspan and lifespan studies in rodents and would greatly enhance the search for interventions that attenuate aging and extend human healthspan by increasing the rate at which candidate interventions can be tested. In addition, biomarkers of lifespan extension identified in rodents may be translatable into humans, thus allowing for the relatively rapid testing of the therapeutic potential of candidate interventions in humans directly. Accordingly, considerable effort over the past several decades has been put into identifying biomarkers.

Initial efforts were focused on identifying what are termed "biomarkers of aging", which have been defined as having the following criteria[253]:

A biomarker of aging:

1. Should predict the outcome of a wide range of age-sensitive tests in multiple physiological and behavioral domains, in an age-coherent way, and do so better than chronological age.
2. Should predict remaining longevity at an age at which 90% of the population is still alive, and do so for most of the specific illnesses that afflict the species under study.
3. Should not alter life expectancy or the outcome of subsequent tests of other age-sensitive tests, as a consequence of measuring it.

In 1988 the NIA and the National Center for Toxicological Research (NCTR) initiated a massive effort to identify biomarkers of aging called the "Biomarkers of Aging Program". This program spanned 10 years and 18 different research labs. The goal of this program was to "identify and validate a panel of biomarkers of aging in rodents in order to rapidly test the efficacy and safety of interventions designed to slow aging"[254]. To avoid only identifying strain-specific aging phenotypes, they used four mouse and three rat strains for a total of 60,000 animals which were fed AL or CR because at the time, CR was the only known intervention to reliably extend maximum lifespan[255]. Unfortunately, this 10-year and extremely expensive program was ultimately a failure. Richard Sprott, who was one of the original designers of the program even said, "While these studies resulted in a great many publications related to biomarker research, a panel of biomarkers that could be used for intervention testing was not obtained"[256]. In hindsight, this program had three major limitations. Firstly, it focused on what are termed "lesion" biomarkers (e.g. pancreatic exocrine atrophy) that accompany aging and, therefore, can only be assessed late in life, thereby necessitating long-term studies, rather than on markers that can be assessed early on after the initiation of an intervention[257]. Secondly, the program only assessed one lifespan-extending intervention, CR. While CR is a powerful tool for studying aging and possibly identifying biomarkers of aging, a strategy that employs multiple unique lifespan-extending interventions is more likely to uncover biomarkers that represent conserved healthspan/lifespan assurance pathways or processes that are fundamental to the biology

of aging. And finally, the metrics tested did not capture the activity of functionally interpretable processes that contribute etiologically to cellular homeostasis.

Since the Biomarkers of Aging Program, other biomarkers of aging have been proposed or suggested. This includes:

- Telomere attrition[258,259]
- $p16^{INK4A}$ expression[220]
- Exhaustion of cellular proliferative capacity[260]
- Decline in stem cell function[261]
- Alterations in T-cell subsets[262]
- Reduced protein synthesis[263]
- Reduced proteasomal activity[24]
- Accumulation of oxidative damage[264]
- Reduced circulating GH and IGF-1[23,265]

Unfortunately most of these candidate biomarkers of aging may only have limited utility in large-scale screens for interventions that attenuate aging. This is because most of these markers only manifest after a long period of time, again necessitating long-term studies. Therefore, these biomarkers of aging are not appropriate "to rapidly test the efficacy and safety of interventions designed to slow aging"[254].

Instead an emphasis should be placed on identifying biomarkers in which changes manifest soon after the initiation of an intervention and are predictive of healthspan and lifespan outcomes at early time point measurements. These biomarkers would be considered biomarkers of lifespan extension (or delayed aging). Importantly, a robust biomarker of lifespan extension should be predictive of healthspan and lifespan outcomes in response to diverse lifespan-extending interventions across a variety of genetic backgrounds.

The purpose of the research to be subsequently presented was to investigate several factors linked to healthspan and lifespan determination in mammals, including reduced insulin-like growth factor-1 (IGF-1) expression, reduced cell proliferation, reduced protein synthesis and enhanced proteome stability. The following three chapters describe in detail studies conducted employing three unique mouse models of healthspan and maximum lifespan extension, including CR, Snell dwarf and rapamycin-treated mice, to address the following five central questions (**Overview of the work described herein Fig 1**): In Chapter 1: Which if any of the well-characterized physiological adaptations to CR including reduced food intake, energy expenditure, body fat and/or body weight can account for its cell proliferation rate-lowering effect? In Chapter 2: Is FGF21 necessary for the reduction in IGF-1 and the reduction in global cell proliferation rates in response to CR? In Chapter 3: Is a reduction in global cell proliferation rates a common feature across all three models and, therefore, potentially a predictive marker of healthspan and maximum lifespan extension? What are the characteristic alterations in proteome dynamics in each of these three models? Are certain alterations in proteome dynamics predictive of healthspan and maximum lifespan extension across all three models?

Chapter 1: The effects of physiological adaptations to calorie restriction on global cell proliferation rates

Airlia C.S. Thompson*, Matthew D. Bruss*, Ishita Aggarwal, Cyrus F. Khambatta and Marc K. Hellerstein

*These authors contributed equally to this work

This chapter has been published in the American Journal of Physiology: Endocrinology and Metabolism. (Reference: Bruss, M. D., Thompson, A. C. S., Aggarwal, I., Khambatta, C. F. & Hellerstein, M. K. The effects of physiological adaptations to calorie restriction on global cell proliferation rates. *Am. J. Physiol. Endocrinol. Metab.* **300,** E735–745 (2011))

Introduction

Calorie restriction (CR), defined as a reduction in caloric intake without malnutrition, increases lifespan, delays the onset of age-related diseases and slows the functional decline of various organs[94]. While the mechanisms mediating these effects are unclear, one of the most rapid and robust effects of CR is a reduction in the rate of cell proliferation in mitotic tissues[225,227,266]. The turnover rates of keratinocytes, liver cells, mammary epithelial cells (MECs), splenic T-cells and prostate cells are decreased by 30-50% following several weeks of CR, and the effects persist throughout the intervention period[227]. It has been suggested that this reduction in cell proliferation could mediate many of the longevity and anti-cancer effects of CR by delaying replicative senescence and reducing the promotional phase of carcinogenesis[94,267]. Considering that the rate of cell proliferation is an integrated response that comprises many genetic and hormonal signals, and appears to be mechanistically linked to aging, this cellular process represents a potential target for monitoring therapeutic interventions aimed at delaying the onset of age-related diseases. Accordingly, identifying upstream physiological inputs or hormonal signals that may mediate reduced cell proliferation rates in response to CR could provide insights into mechanisms of aging and age-related diseases.

Reductions in food intake[268,269], energy expenditure[270], percent body fat[83,271,272] and body weight[95,273,274] have all been suggested to mediate the effects of CR. To date, however, it is still not clear which, if any, of these physiological adaptations are sufficient to increase longevity. In addition, the hormonal mediators translating these physiological adaptations to cellular responses have not been fully characterized. Progress in this field has been limited by the difficulty in dissociating the individual physiological effects of CR, as well as the time and resources required for classical longevity studies in mice, which take up to 3 years to complete[268].

Previous studies have established that changes in ambient housing temperature and voluntary wheel running can alter food intake, energy expenditure, percent body fat, and body weight[275,276]. We hypothesized that the use of these interventions might allow for the assessment of alterations in these physiological adaptations on cell proliferation rates, independent of classical CR. In addition, if cell proliferation rates can serve as a biomarker of interventions that increase lifespan, the application of this biomarker-based approach could provide an efficient method for investigating the effects of different factors on health and longevity. However, the effects of altering these physiological parameters through changes in ambient temperature or voluntary wheel running, on cell proliferation have not previously been established.

Therefore, the goal of this study was to mimic physiological adaptations to CR through changes in ambient housing temperature and voluntary wheel running in order to determine the effects of food intake, energy expenditure, percent body fat and body weight on "global" cell proliferation rates (keratinocyte, liver cell, MEC and splenic T-cell proliferation) in young C57BL/6 mice.

Methods

Mice and diets

12 week-old C57BL/6 mice (Charles River Breeding, Wilmington, MA, USA) were housed individually and maintained under temperature- and light-controlled conditions (12-h light/dark cycle, lights on at 0700 h and off at 1900 h). For all experiments mice were provided semi-purified AIN-93M diet (Bio-Serv, Frenchtown, NJ, USA) and free access to water. Mice on restricted diets were provided with food daily at approximately 1200h. Food intake was recorded for each individual mouse every other day. All protocols and procedures were approved by the University of California Berkeley Animal Use Committee.

Experiment 1 design:

After 1 week of adaptation to their environments and AIN-93M diet, female C57BL/6 mice were randomly assigned to one of three groups (n=3 to 5); *ad libitum*-fed and housed at 22°C in a temperature-controlled room (AL/22), *ad libitum*-fed and housed at 27°C in a temperature-controlled room (AL/27) or pair-fed to the AL/27 group but housed at 22°C in a temperature-controlled room (PF/22) (each mouse in the PF/22 group was provided food equal to the average food intake of the AL/27 group from the previous day). The groups were designed to modulate two of the physiological adaptations to CR, reduced food intake and reduced energy expenditure, independent of CR itself. Mice were maintained on the feeding regimen for 4 weeks and labeled with $^{2}H_2O$ for the final 3 weeks.

Experiment 2 design:

After 1 week of adaptation to their environments and AIN-93M diet, female C57BL/6 mice were assigned randomly to one of four groups (n=15); *ad libitum*-fed and sedentary (AL/SED), *ad libitum*-fed and provided 24h access to a voluntary running wheel (AL/EX), pair-fed to the AL/SED group and provided 24h access to a voluntary running wheel (PF/EX) or calorie restricted to body weight match the PF/EX group and sedentary (CR/SED). The groups were designed to modulate two of the physiological adaptations to CR, reduced percent body fat and reduced body weight, independent of CR itself. Mice were maintained on the feeding regimen for 5 weeks and labeled with $^{2}H_2O$ for the final 3 weeks.

Experiment 3 design:

The group design for Experiment 3 was identical to Experiment 2, except 12 week-old male C57BL/6 mice were used instead of female mice. Male C57BL/6 mice were used in this experiment as they have elsewhere been shown to compensate incompletely to voluntary exercise through *ad libitum* food intake and, therefore, weigh less than *ad libitum*-fed sedentary controls[277]. The groups were designed to modulate one of the physiological adaptations to CR, reduced body weight, independent of CR itself. Mice were maintained on the feeding regimen for 5 weeks and labeled with $^{2}H_2O$ for the final 3 weeks.

Voluntary exercise

AL/EX and PF/EX mice in Experiments 2 and 3 were provided 24hr access to a 24cm-running wheel (mini-Mitter) attached to a digital counter. Revolutions were recorded daily.

Body weight measurement, ^2H_2O labeling, and blood and tissue collection

The body weight of each mouse was measured one to three times per week. Mice were labeled with an intraperitoneal injection of 100% ^2H_2O (0.35ml/ 10g body weight) 3 weeks prior to the end of the study and were then provided 8% ^2H_2O as drinking water for the remainder of the study, as described previously[278]. Upon completion of each experiment, mice were anesthetized under 3% isoflurane and blood was collected via cardiac puncture, followed by cervical dislocation and tissue collection.

Keratinocyte isolation

After euthanasia, the back of each mouse was shaved followed by an application of Nair for complete hair removal (Carter Products, New York, NY, USA). A small piece of the dorsal skin was dissected, washed with phosphate buffered saline solution (PBS; Gibco, Grand Island, NY, USA), cut into three small sections, and placed in 5mL PBS with 10 units of dispase II (Roche, Indianapolis, IN, USA). Dorsal skins were incubated for 3.5 hour with shaking at 100rpm at 37°C. The epidermis was then peeled from the dermis and collected for DNA isolation.

Liver cell isolation

A section of the liver (~30mg) was dissected and homogenized and total DNA from all liver cells was isolated.

Mammary epithelial cell isolation

Mammary epithelial cells were isolated using a protocol adapted from Fata et al.[279]. Briefly, the 4L and 4R inguinal mammary glands were removed, placed in Dulbecco's Modified Eagle Medium (DMEM; Gibco, Grand Island, NY, USA) and minced. The minced tissue was incubated in 20mL collagenase/trypsin solution (0.2% Collagenase A (Worthington Biochemical, Lakewood, NJ, USA), 0.2% Trypsin, 5% fetal bovine serum in DMEM) for 20min, shaking at 100 rpm at 37°C. Following digestion, the tissue suspension was centrifuged at 1500 rpm for 10min and the collagenase/trypsin solution and upper fat layer were discarded and the pellet was resuspended in 10mL DMEM. The suspension was pelleted via centrifugation at 1500 rpm for 10min, resuspended in 4mL DMEM containing 5ul DNase (≥500U/mL; Sigma, St. Louis, MO, USA), shaken vigorously for 2min and then incubated at room temperature for 5min. 6mL of DMEM were added to the suspension, which was then pelleted via centrifugation at 1500 rpm for 10min. The pellet was resuspended in 10mL DMEM and the suspension was briefly centrifuged at 1500 rpm and the supernatant discarded. The pellet was subjected to a total of three rounds of this brief differential centrifugation at 1500 rpm. The resulting pellet containing the mammary epithelial cells was then collected for DNA isolation.

Splenic T-cell isolation

Upon dissection, the spleen was homogenized and passed through a 40μM nylon cell strainer. T-cells were isolated from the single cell suspension using mouse anti-CD90.2 microbeads and the MACS cell separation column following the manufacturer's instructions (Miltenyi Biotec, Auburn, CA, USA), pelleted and then collected for DNA isolation.

Bone marrow cell isolation

The femur was dissected for isolation of bone marrow cells. Bone marrow cells were flushed from the femur with 2mL of PBS and were then pelleted and collected for DNA isolation.

DNA isolation

DNA was extracted using DNeasy kits (Qiagen, Valencia, CA, USA). Briefly, isolated keratinocytes, liver, MECs, T-cells, and bone marrow cells were digested overnight at 37 °C in proteinase K solution followed by DNA isolation and elution into 200ul water.

DNA synthesis measurement

Determination of ^{2}H incorporation into purine deoxyribose (dR) of DNA was performed as described previously[278]. Briefly, isolated DNA was hydrolyzed overnight at 37 °C with nuclease S1 and potato acid phosphatase. Hydrolyzates were reacted with pentafluorobenzyl hydroxylamine and acetic acid, then acetylated with acetic anhydride and *1*-methylimidazole. Dichloromethane extracts were dried, resuspended in ethyl acetate, and analyzed by GC/MS on a DB-17 column with negative chemical ionization, using He as carrier and CH_4 as reagent gas. The fractional molar isotope abundances at m/z 435 (M_0 mass isotopomer) and 436 (M_1) of the pentafluorobenzyl triacetyl derivative of purine dR were quantified using ChemStation software. Excess fractional M_{+1} enrichment (EM_1) was calculated as:

$$EM1 = \frac{(\text{abundance m/z 436})_{\text{sample}}}{(\text{abundance m/z 435 + 436})_{\text{sample}}} - \frac{(\text{abundance m/z 436})_{\text{std}}}{(\text{abundance m/z 435 + 436})_{\text{std}}}$$

where sample and standard (std) refer to the analyzed sample and an unenriched pentafluorobenzyl triacetyl purine dR derivative standard, respectively. The fractional synthesis rate (f) of keratinocytes, liver, MECs and T-cells was calculated by a comparison to bone marrow cells in the same animal, which represents an essentially fully turned over population of cells.

Body composition analysis

Percent body fat was determined by chemical extraction[280]. Briefly, mouse carcasses where weighed before and after freeze drying to determine percent water. Dried carcasses were placed in a Soxhlet extraction apparatuses and extracted in ether for 7 days and in acetone for 5 days. The carcasses were then removed and placed in a fume hood for

3 days to allow complete solvent evaporation and then weighed to determine percent body fat.

Serum analyte measurements

On the day before the termination of each experiment, CR and PF mice were provided with food at approximately 1200h as described in the subsection, *Mice and diets*. All AL mice were given 24hr access to their food for the entirety of the experiments. On the termination day of each experiment, between 0900h and 1200h, mice were anesthetized under 3% isoflurane and blood was collected via cardiac puncture followed by cervical dislocation and tissue collection. Following centrifugation, serum was collected and stored at -20°C. Serum concentrations (ng/mL) of the following analytes were determined via ELISAs following the manufacture's instructions: insulin-like growth factor-1 (R&D Systems, Minneapolis,MN, USA) in triplicate (Ex 2) or duplicate (Ex 3) , insulin-like growth factor binding protein-3 (R&D Systems, Minneapolis,MN, USA) in duplicate, triiodothyronine (T_3) (Calbiotech,Spring Valley, CA, USA) in singlet and thyroxine (T_4) (Calbiotech,Spring Valley, CA, USA) in singlet. The intra-assay coefficient of variation for the reported assays was 3.85% for IGF-1 (Ex 2), 1.91% for IGF-1 (Ex-3), and 3.81% for IGFBP-3.

Statistical analyses

All results are presented as mean ± SEM. Repeated-measures ANOVA followed by Bonferroni *post hoc* test was used to analyze change in body weight over time. Following a significant result on repeated-measures ANOVA, single time point comparisons were made using one-way ANOVA followed by a Tukey *post hoc* test. For cell proliferation, differences between groups were analyzed by one-way ANOVA with Tukey *post hoc* test. For correlations between serum IGF-1 and cell proliferation rates, linear regression analyses were performed and coefficient of determination values (r^2) were determined. Data were analyzed by Prism Graphpad software (version 5.0a).

Results

Experiment 1: *The effect of mimicking physiological adaptations to CR via changes in housing temperature on cell proliferation rates*

To determine the effects of reduced food intake and energy expenditure on cell proliferation rates, independent of classical CR, female C57BL/6 mice were randomized into one of three groups: *ad libitum*-fed and housed at the standard 22°C (AL/22), *ad libitum*-fed and housed at 27°C (AL/27), or pair-fed to the AL/27 group and housed at the standard 22°C (PF/22). The rationale for the group design in Experiment 1 was based on two primary assumptions: i) AL/27 mice are closer to thermoneutrality than AL/22 mice and will, therefore, expend less energy to maintain body temperature, and ii) AL/27 mice will voluntarily decrease their food intake to maintain energy balance, due to decreased energy expenditure and will, therefore, have comparable body weights to AL/22 mice, despite reduced food intake.

The average daily food intake of both the AL/27 and PF/22 mice was significantly lower than that of AL/22 mice (AL/22: 3.3 ± 0.05, AL/27 2.6 ± 0.06, PF/22: 2.6 ± 0 g/day) (**Fig 1A**). There was no difference in average body weight between AL/22 and AL/27 mice while PF/22 mice weighed significantly less than both AL groups at the end of the experiment (AL/22: 22.0 ± 0.7, AL/27 22.5 ± 0.7, PF/22: 18.0 ± 0.3g) (**Fig 1B**). The maintenance of body weight in the face of decreased food intake in AL/27 mice relative to AL/22 mice was presumably due to a decrease in energy expenditure.

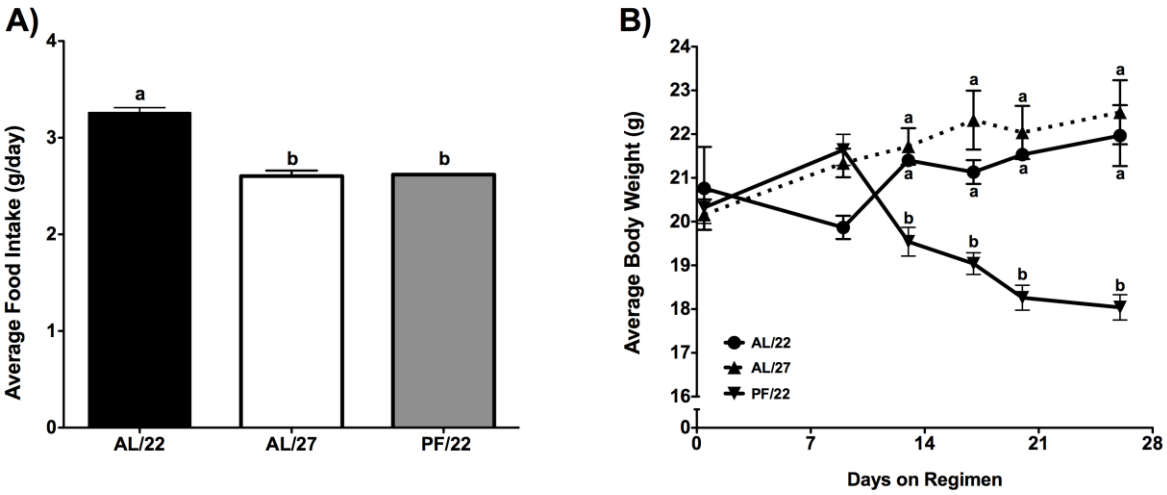

Figure 1: Effect of housing temperature on food intake and body weight (Ex 1)

Female mice were divided into 3 groups; *ad libitum*-fed and housed at 22°C (AL/22), *ad libitum*-fed and housed at 27°C (AL/27) and pair-fed to the AL/27 group and housed at 22°C (PF/22). Food was provided once daily at 1200 hours. (A) Food consumption was recorded every other day. Data represent the mean food intakes over the 4-week experiment. (B) Body weights were recorded once per week. Data represent the mean weekly body weights. All values are expressed as means ± SEM, n=3 to 5 for each group. One-way ANOVA with Tukey's post hoc test was used for all between–group analyses; means not sharing a common letter are significantly different ($p < 0.05$).

All mice remained on their regimens for a total of four weeks at which point they were euthanized and their tissues were collected for cell proliferation analysis. Cell proliferation rates were significantly lower in all cell types analyzed in PF/22 mice compared to AL/22 mice (24%, 71%, 51% and 32% lower in keratinocytes, liver, mammary epithelial and splenic T-cells, respectively) (**Fig 2A-D**). Interestingly, despite a significantly lower average daily food intake and energy expenditure compared to AL/22 mice, there were no differences in cell proliferation rates in any of the cell types analyzed in AL/27 mice compared to AL/22 mice (**Fig 2A-D**). These data indicate that reduced food intake and energy expenditure are not sufficient to account for the cell proliferation rate-lowering effects of CR.

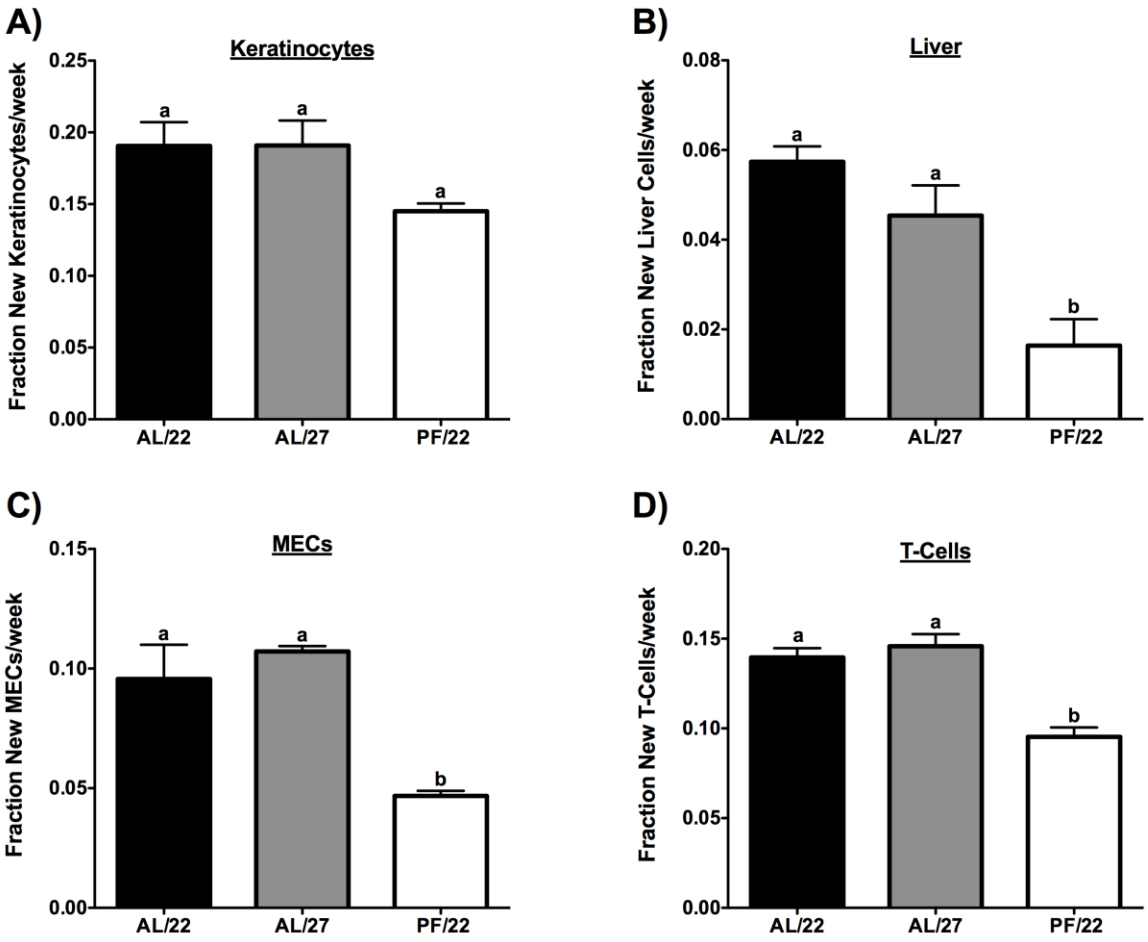

Figure 2: Effect of housing temperature on cell proliferation rates (Ex 1)

Cell proliferation rates in (A) keratinocytes, (B) liver, (C) mammary epithelial and (D) splenic T-cells. Values are expressed as means ± SEM, n=3 to 5 for each group. One-way ANOVA with Tukey's post hoc test was used for all between–group analyses; means not sharing a common letter are significantly different ($p < 0.05$).

Experiment 2: *The effect of mimicking physiological adaptations to CR via voluntary wheel running on cell proliferation rates (female mice)*

To determine the effects of reductions in percent body fat and body weight on cell proliferation rates, independent of classical CR, female C57BL/6 mice were randomized into one of four groups: *ad libitum*-fed and sedentary (AL/SED), *ad libitum*-fed with free access to a voluntary running wheel (AL/EX), pair-fed to the AL/SED group with free access to a voluntary running wheel (PF/EX) or calorie restricted to body weight match PF/EX mice and sedentary (CR/SED). The rationale for the group design in Experiment 2 was based on three primary assumptions: i) female AL/EX mice, while expending more energy than AL/SED mice, will voluntarily increase their food intake to compensate for an increase in energy expenditure and will, therefore, have comparable body weights to AL/SED mice, ii) PF/EX mice will lose body weight compared to AL/SED and iii) exercising mice in either dietary setting will have decreased percent body fat compared to AL/SED mice.

The average daily food intake of the AL/EX mice was significantly elevated compared to both AL/SED and PF/EX mice (AL/SED: 3.1 ± 0.02, AL/EX: 3.9 ± 0.05, PF/EX 3.0 ± 0.03, CR/SED 2.4 ± 0.01 g/day) (**Fig 3A**). There was no difference in average body weight between AL/SED and AL/EX mice at the end of the experiment. Similarly, there was no difference in average body weight between PF/EX and CR/SED mice, while mice in these two groups did have significantly lower body weights than both AL/SED and AL/EX mice (AL/SED: 23.0 ± 0.3, AL/EX: 22.9 ± 0.2, PF/EX 18.8 ± 0.3, CR/SED 18.0 ± 0.3 g) (**Fig 3B**). Body composition analyses confirmed that percent body fat was significantly reduced in AL/EX and PF/EX mice compared to AL/SED and CR/SED mice, which did not differ significantly from one another (AL/SED: 14.8 ± 1.0, AL/EX: 9.3 ± 0.5, PF/EX 7.6 ± 1.3, CR/SED 14.0 ± 1.2 g fat/g body weight) (**Fig 3C**).

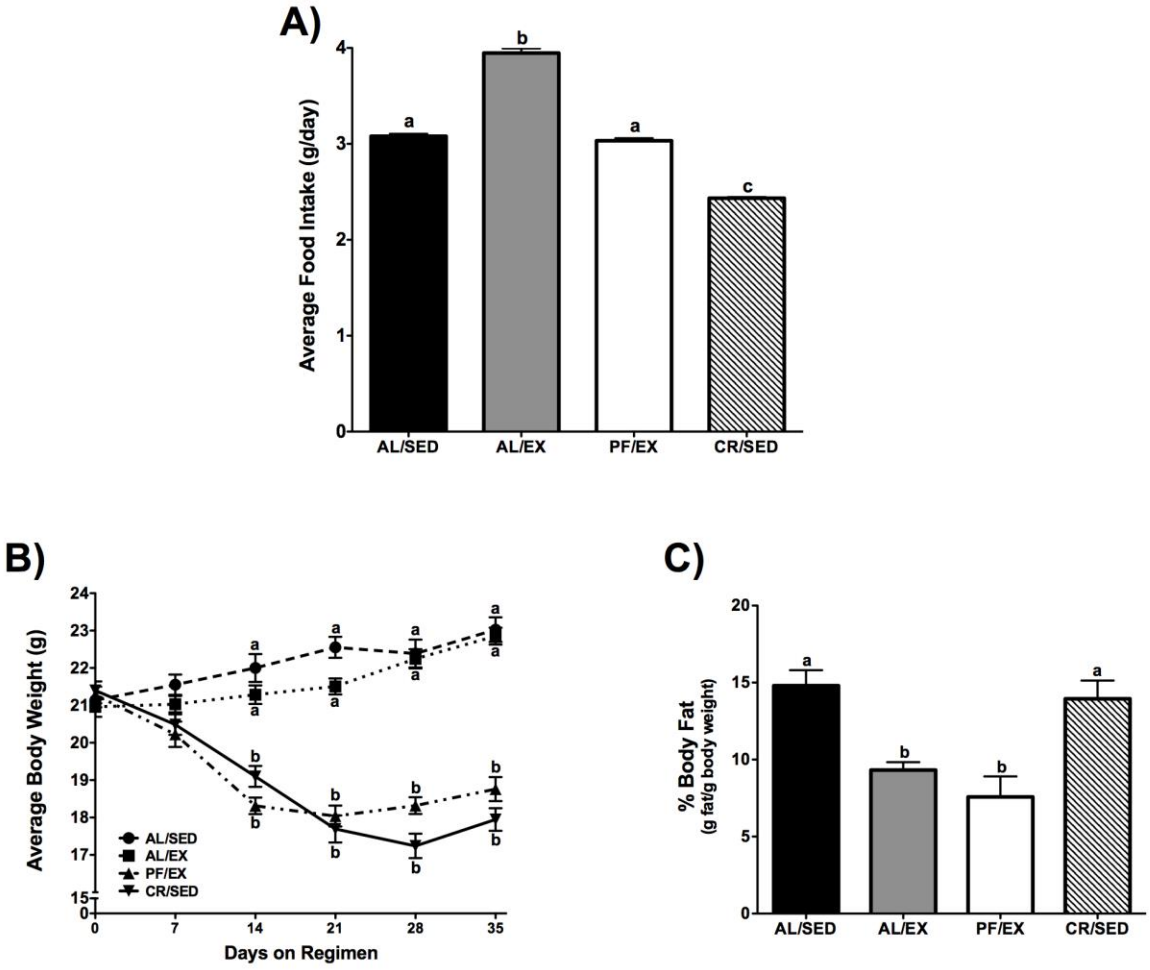

Figure 3: Effect of voluntary wheel running on food intake, percent body fat and body weight in female mice (Ex 2)

Female mice were divided into 4 groups; *ad libitum*-fed and sedentary (AL/SED), *ad libitum*-fed and provided free access to a running wheel (AL/EX), pair-fed to AL/SED and provided free access to a running wheel (PF/EX) and calorie restricted to body weight match the PF/EX group and sedentary (CR/SED). Food was provided once daily at 1200 hours. (A) Food intake was recorded every other day. Data represent the mean food intakes over the 5-week experiment. (B) Body weights were recorded approximately 3 times per week. Data represent the mean weekly body weights. (C) Following euthanization, percent body fat was determined via chemical extraction from the carcass. Values are expressed as means ± SEM, n=15 for each group for food intake and body weight and n=5 to 14 for each group for percent body fat. One-way ANOVA with Tukey's post hoc test was used for all between–group analyses; means not sharing a common letter are significantly different ($p < 0.05$).

All mice remained on their regimens for a total of five weeks at which point they were euthanized and their tissues were collected for cell proliferation analysis. Despite significantly lower percent body fat, there were no differences in cell proliferation rates in any of the cell types analyzed in AL/EX compared to AL/SED mice. Cell proliferation rates were significantly lower in all cell types analyzed in CR/SED mice compared to AL/SED mice (31%, 75%, 62% and 55% lower in keratinocytes, liver, mammary epithelial and splenic T-cells, respectively). Cell proliferation rates were also significantly lower in all cell types analyzed in PF/EX mice compared to AL/SED mice (15%, 36%, 42% and 31% lower in keratinocytes, liver, mammary epithelial and splenic T-cells, respectively). Interestingly, cell proliferation rates in CR/SED mice were significantly lower than in PF/EX mice, to which they were body weight matched (19%, 60%, 34% and 35% lower in keratinocytes, liver, mammary epithelial and splenic T-cells, respectively) (**Fig 4A-D**).

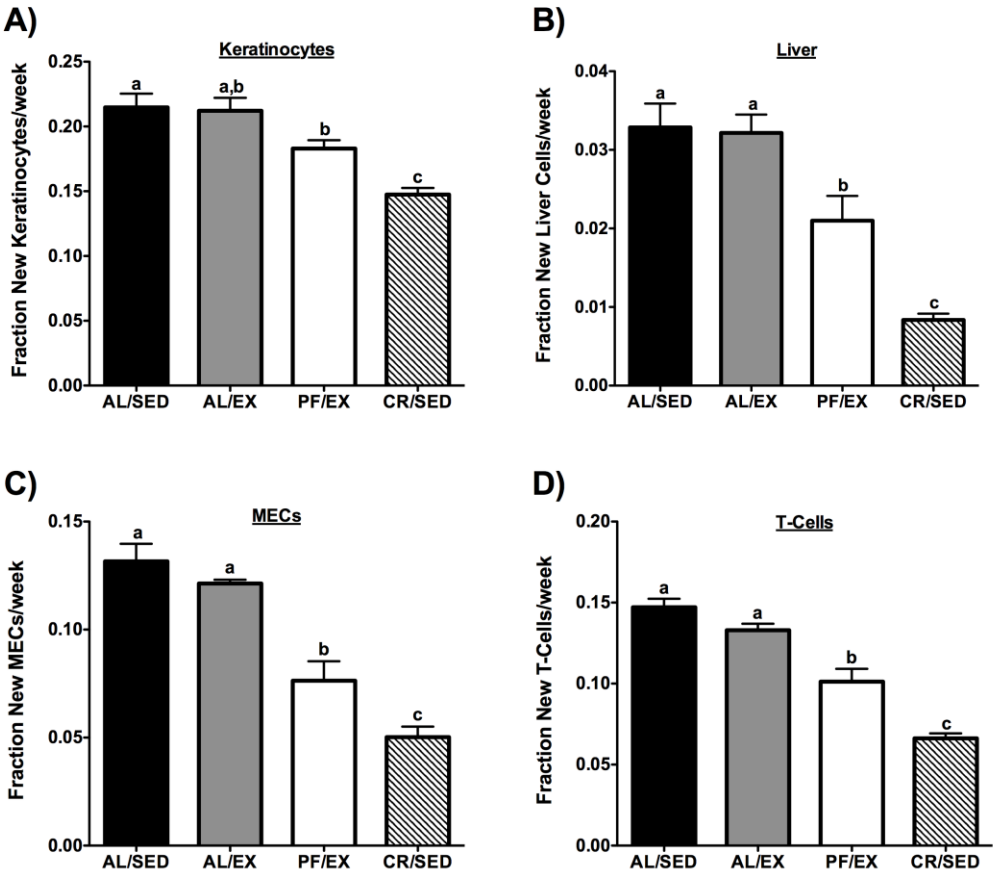

Figure 4: Effect of voluntary wheel running on cell proliferation rates in female mice (Ex 2)

Cell proliferation rates in (A) keratinocytes, (B) liver, (C) mammary epithelial and (D) splenic T-cells. Values are expressed as means ± SEM, n=10 to 15 for each group. One-way ANOVA with Tukey's post hoc test was used for all between–group analyses; means not sharing a common letter are significantly different ($p < 0.05$).

These data suggest that reductions in percent body fat are not sufficient to account for the cell proliferation rate lowering effects of CR, whereas reductions in body weight may be associated with lower rates of cell proliferation. Interestingly, both groups of mice in which we observed an effect of reduced body weight on cell proliferation rates (PF/EX and CR/SED) were food restricted relative to what they would have eaten if fed *ad libitum*. As exemplified by the increased food intake of AL/EX mice, PF/EX mice would have consumed more food had they been given free access and not restricted to the food intake of AL/SED mice. These results suggest that the effects on cell proliferation rates could be due to a "perceived" reduction in energy intake rather than to reduced body weight per se. Accordingly, we designed Experiment 3 with the intention of dissociating reduced body weight from CR.

Experiment 3: *The effect of mimicking physiological adaptations to CR via voluntary wheel running on cell proliferation rates (male mice)*

To determine the effect of reduced body weight on cell proliferation rates in the context of *ad libitum* food intake, male C57BL/6 mice were randomized into one of four groups: *ad libitum*-fed and sedentary (AL/SED), *ad libitum*-fed with free access to a voluntary running wheel (AL/EX), pair-fed to the AL/SED group with free access to a voluntary running wheel (PF/EX) or calorie restricted to body weight match PF/EX mice and sedentary (CR/SED). The rationale for the group design in Experiment 3 was based on the assumption that male AL/EX mice will voluntarily increase their food intake to counter their increased energy expenditure, but will fail to fully compensate energetically and will, therefore, have reduced body weight compared to AL/SED mice. Therefore, Experiments 2 and 3 had identical designs, but utilized differences in food intake and energy balance in response to exercise between female (Experiment 2) and male (Experiment 3) mice.

The average daily food intake of the AL/EX mice was significantly elevated compared to both AL/SED and PF/EX mice (AL/SED: 3.1 ± 0.07, AL/EX: 4.1 ± 0.1, PF/EX 3.2 ± 0.06, CR/SED 2.4 ± 0.01 g/day) (**Fig 5A**). However, AL/EX mice had significantly lower body weight compared to AL/SED mice at the end of the experiment (reduced by 12.4%; AL/SED: 29.8 ± 0.7, AL/EX: 26.1 ± 0.2, PF/EX 20.1 ± 0.2, CR/SED 20.0 ± 0.3 g) (**Fig 5B**). There was no difference in average body weight between PF/EX and CR/SED mice, while mice in these two groups did have significantly lower body weights than both AL/SED and AL/EX mice.

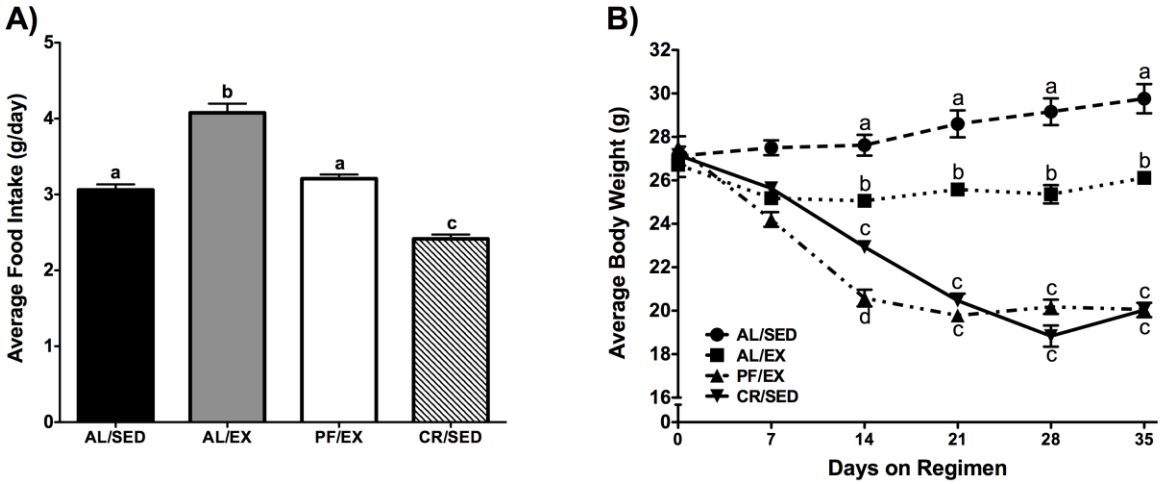

Figure 5: Effect of voluntary wheel running on food intake and body weight in male mice (Ex 3)

Male mice were divided into 4 groups; *ad libitum*-fed and sedentary (AL/SED), *ad libitum*-fed and provided free access to a running wheel (AL/EX), pair-fed to AL/SED and provided free access to a running wheel (PF/EX) and calorie restricted to body weight match the PF/EX group and sedentary (CR/SED). Food was provided once daily at 1200 hours. (A) Food intake was recorded every other day. Data represent the mean food intakes over the 5-week experiment. (B) Body weights were recorded approximately 3 times per week. Data represent the mean weekly body weights. Values are expressed as means ± SEM, n=3 to 5 for each group. One-way ANOVA with Tukey's post hoc test was used for all between–group analyses; means not sharing a common letter are significantly different ($p < 0.05$).

All mice remained on their regimens for a total of five weeks at which point they were euthanized and their tissues were collected for cell proliferation analysis. Interestingly, despite a significant reduction in body weight as compared to AL/SED, AL/EX male mice did not have significant differences in cell proliferation rates in any of the cell types analyzed. Cell proliferation rates were significantly lower in all cell types analyzed in CR/SED mice compared to AL/SED mice (37%, 71% and 51% lower in keratinocytes, liver and splenic T-cells, respectively) (**Fig 6A-D**).

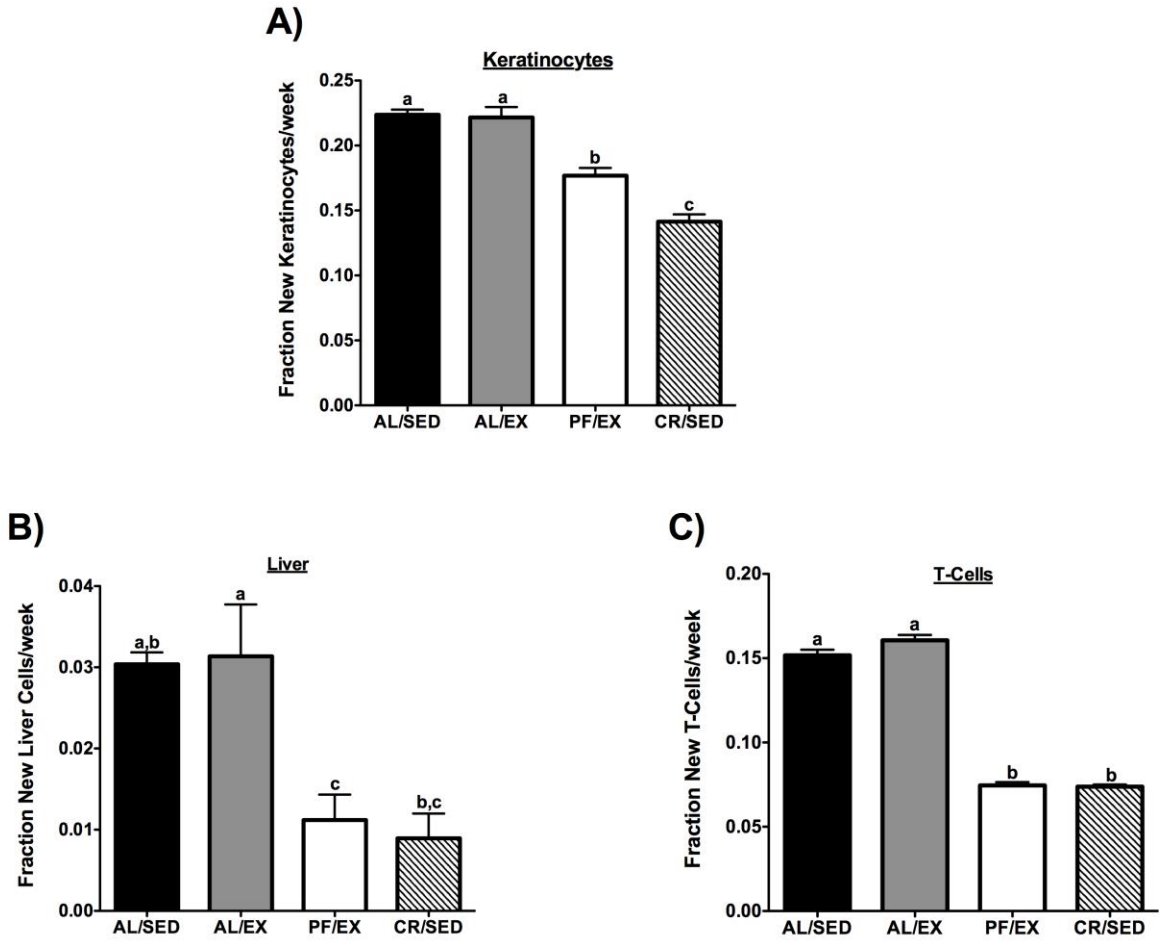

Figure 6: Effect of voluntary wheel running on cell proliferation rates in male mice (Ex 3)

Cell proliferation rates in (A) keratinocytes, (B) liver and (C) splenic T-cells. Values are expressed as means ± SE, n=3 to 5 for each group. One-way ANOVA with Tukey's post hoc test was used for all between–group analyses; means not sharing a common letter are significantly different ($p < 0.05$).

These data suggest that in the context of *ad libitum* food intake, reduced body weight relative to sedentary controls is not sufficient to account for the cell proliferation rate lowering effects of CR. Together, the results from Experiments 1, 2 and 3 (**Fig 7A-C**) suggest that none of the classic adaptations to CR (reductions in food intake, energy expenditure, percent body fat and body weight) are sufficient to account for the reductions in "global" cell proliferation rates observed in CR mice.

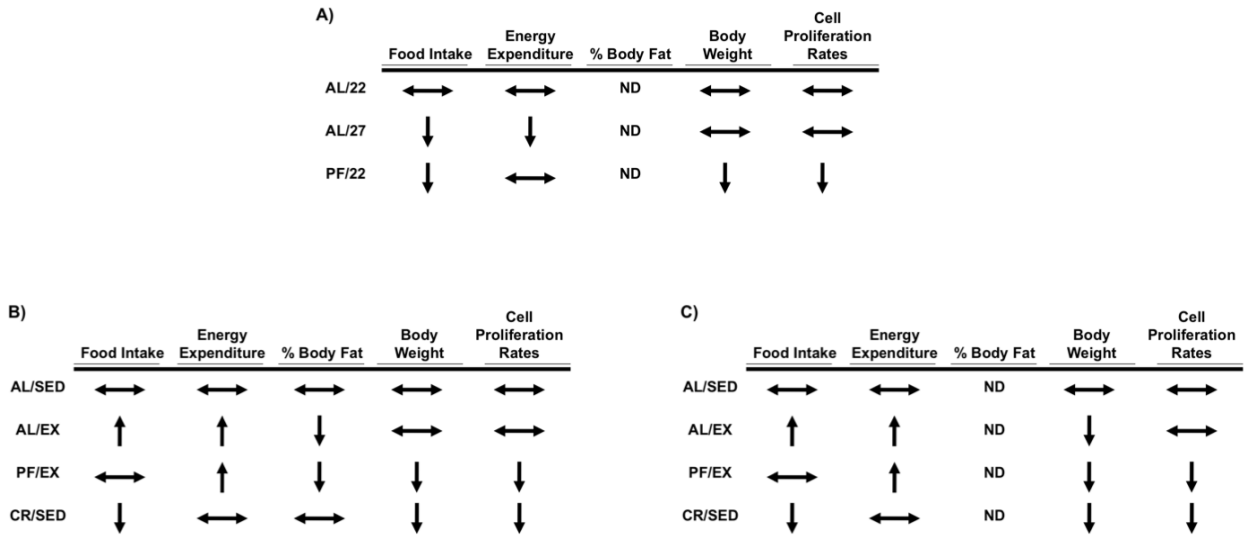

Figure 7: Summary of the effects of the physiological adaptations to CR on cell proliferation rates (Ex 1,2 and 3)

Cell proliferation rates were measured under experimental conditions in which (A) food intake and energy expenditure (Ex 1), (B) percent body fat (Ex 2) or (C) body weight were reduced, relative to *ad libitum*-fed controls, through changes in ambient housing temperature (Ex 1) or voluntary wheel running (Ex 2 and 3), independent of classic CR. Indicated changes in food intake, energy expenditure, percent body fat, body weight and cell proliferation rates are relative to AL/22 (Ex 1) or AL/SED (Ex 2 and 3) controls. ⍰⍰= no change, ⍰= increased and ⍰= decreased.⍰ND = not determined. Changes in energy expenditure were assumed based on changes in food intake and body weight.

Circulating factors and cell proliferation

To identify circulating factors that may mediate global reductions in cell proliferation rates, we measured the concentrations of several circulating growth factors in mice from Experiments 2 and 3. Insulin-like growth factor binding protein-3 (IGFBP-3), triiodothyronine (T_3) and thyroxine (T_4) serum levels were not different in any group in Experiment 2 (**Table 1**). In contrast, serum insulin-like growth factor-1 (IGF-1) levels were significantly lower in CR/SED compared to both AL groups (**Table 1**). In addition, IGF-1 serum levels correlated positively with cell proliferation rates in all cell types analyzed in all mice in Experiments 2 and 3 (**Fig 8A-D**).

Circulating Factor				
Group	IGF-1	IGFBP-3	T_3	T_4
AL/SED	$163.9 \pm 8.9^{a,b}$	489.2 ± 28.7^{a}	$1.30 \pm 0.07^{a,b}$	49.3 ± 3.4^{a}
AL/EX	182.3 ± 7.6^{a}	501.5 ± 48.6^{a}	1.44 ± 0.07^{a}	46.5 ± 2.3^{a}
PF/EX	$142.1 \pm 10.3^{b,c}$	416.5 ± 26.3^{a}	$1.18 \pm 0.1^{a,b}$	41.6 ± 2.2^{a}
CR/SED	123.1 ± 4.6^{c}	388.3 ± 20.5^{a}	1.14 ± 0.09^{b}	43.1 ± 2.5^{a}

Table 1: Circulating factors (Ex 2)

Serum insulin-like growth factor-1 (IGF-1), insulin-like growth factor binding protein-3 (IGFBP-3), triiodothyronine (T_3) and thyroxine (T_4) levels were determined at the end of the 5-week experiment. Values are expressed as means ± SEM (ng/mL). n=15 (IGF-1), n=15 (IGFBP-3) and n=10 (T_3 and T_4) for each group. One-way ANOVA with Tukey's post hoc test was used for all between–group analyses; means not sharing a common letter are significantly different ($p < 0.05$).

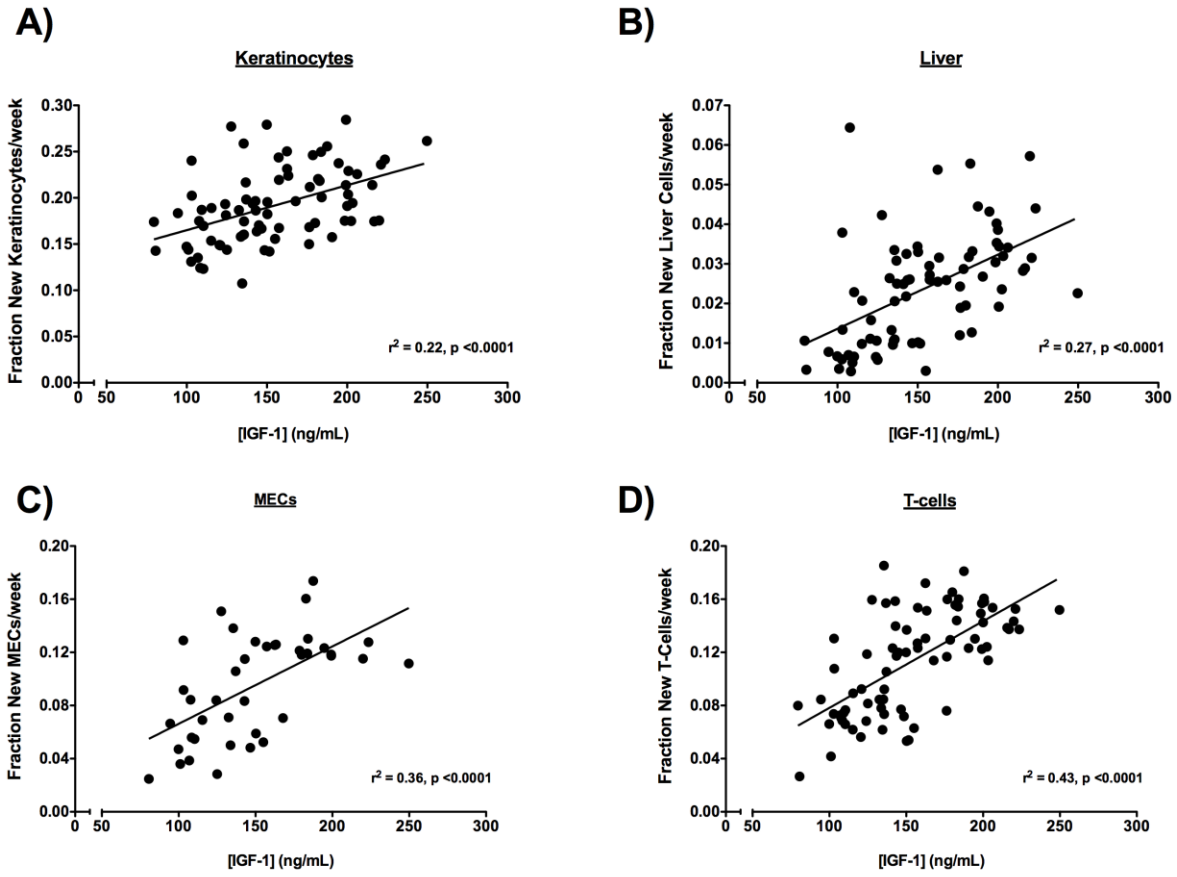

Figure 8: Correlation of serum IGF-1 and cell proliferation (Ex 2 and 3)

Serum IGF-1 levels were determined at the end of the 5-week experiments and correlated to (A) keratinocyte, (B) liver, (C) mammary epithelial (Ex 2 only) and (D) splenic T-cell proliferation rates. Linear regression analyses were performed and coefficient of determination values (r^2) were determined. n = 40 to 80 mice per correlation.

Discussion

The experiments presented here demonstrate that reductions in food intake, energy expenditure, percent body fat or body weight cannot account for the decrease in cell proliferation rates in response to CR (results summarized in **Fig 7**). The unifying feature associated with lower cell proliferation rates among all experiments was restriction of food intake below the level that the animals would have selected if given *ad libitum* access to food. Potential signals mediating these effects were explored and reductions in serum IGF-1 were associated with decreased cell proliferation rates. These data are also consistent with the hypothesis that reduced cell proliferation is a biomarker that correlates with interventions that increase longevity (11).

In all experiments, a ~20% reduction in caloric intake led to reduced cell proliferation rates in keratinocytes, liver cells, MECs and splenic T-cells, as compared to *ad libitum*-fed controls (**Fig 2, 4 & 6**). These data are consistent with previous work showing CR-induced reductions in cell proliferation rates in many tissues. Previous work using ^{3}H-thymidine incorporation, demonstrated decreased cell proliferation rates in the small intestine, colon, bladder, dermis, mammary tissue and esophagus in response to 25% CR in Swiss Webster mice[225] and decreased cell proliferation of primary hepatocytes from calorie restricted F344 rats[266]. Work from our laboratory has confirmed these results in several tissues, based on ^{2}H incorporation from heavy water into the deoxyribose moiety of purine deoxyribonucleosides in DNA, and extended the findings to include lower proliferation rates of keratinocytes and splenic T-cells in CR mice[227,281]. Taken together with the present findings, it is clear that 20-40% CR leads to a robust decrease in cell proliferation rates across many tissues. However, until now, the physiological adaptations to CR that initiate this reduction in cell proliferation rate had not been systematically evaluated.

The overall goal of this work was to determine the effects of the physiological adaptations associated with CR on cell proliferation rates, independent of classical CR. The first adaptation that we examined was food intake. In two separate experiments we found that decreased food intake (Experiment 1) and increased food intake (Experiment 2), while maintaining the same relative body weight as *ad libitum*-fed sedentary controls, had no effect on cell proliferation rates.

While food intake has been previously suggested to mediate the longevity effects of CR[268,269,282], our data on cell proliferation rates are consistent with previous work on spontaneous tumor formation. Huffman et al.[276] demonstrated that prostate tumor development was reduced in CR mice housed at 23°C, but not reduced in *ad libitum*-fed mice housed at 28°C, despite the fact that the latter group consumed the same amount of food as the CR group at 23°C. In conjunction with the present data, it appears that CR-induced reductions in cell proliferation rates and tumor promotion are not mediated by decreased food intake per se.

The second CR-associated physiological adaptation that we examined was whole body energy expenditure. In two separate experiments we demonstrated that neither decreases (Experiment 1) nor increases (Experiment 2) in energy expenditure had any effect on cell proliferation rates. It should be noted that energy expenditure was estimated by energy balance, not directly measured through oxygen consumption. In both Experiment 1 and 2, there were significant changes in food intake, yet no change in body weight, implying that there were also changes in energy expenditure or food absorption. Neither increased housing temperature nor increased wheel running have been reported to affect food absorption, thus we believe changes in energy expenditure are most likely to account for body weight maintenance in these settings of altered food intake.

While reduced energy expenditure has been proposed to mediate the longevity effects of CR, our data on cell proliferation rates are consistent with the current views of energy expenditure and longevity. The "rate of living theory" proposed to explain CR-induced longevity[270] stated that CR animals have reduced metabolic rates and thus longer lifespan. More recent work has suggested that while whole body energy expenditure does decrease in CR rodents[283], metabolic rate is actually increased in CR rodents when

corrected for body weight[269,283,284]. Our data here show that decreases in whole body energy expenditure cannot reproduce the cell proliferation rate lowering effects of CR. Thus, it appears that decreased energy expenditure, either at the level of the whole body or corrected for lean body weight, does not mediate either the cell proliferation or longevity effects of CR.

The third CR-associated physiological adaptation that we examined was percent body fat. In Experiment 2, a reduction in percent body fat had no effect on cell proliferation rates. These findings on cell proliferation rates are consistent with direct work on percent body fat and longevity. Since the first suggestion that decreased body fat could mediate the health benefits of CR[271], several studies have tested the role of percent body fat on longevity, however none have shown a direct role. Bertrand et al.[285] showed no correlation between percent body fat and longevity in *ad libitum*-fed F344 rats, and a positive correlation in those on CR. Testing the hypothesis more directly, Harrison et al.[268] studied lean and ob/ob mice fed *ad libitum* or CR. They reported that ob/ob mice on CR lived longer than lean *ad libitum*-fed mice and as long as lean CR mice, despite having a much higher percent body fat than either lean *ad libitum*-fed or CR mice, again dissociating percent body fat and longevity. Exercise and longevity studies have also shown a dissociation between percent body fat and longevity, where exercised rats have decreased percent body fat, yet no increase in maximal lifespan[286]. Accordingly, it appears that the effects of CR on cell proliferation rates and longevity are not mediated by reductions in percent body fat.

The final CR-associated physiological adaptation that we examined was body weight. From our first two experiments, it appeared that reduced body weight relative to *ad libitum*-fed sedentary controls was associated with lower cell proliferation rates. To determine the effect of reduced body weight relative to *ad libitum*-fed sedentary controls, independent of food restriction, we used male mice provided free access to food and a running wheel. In Experiment 3, AL/EX male mice weighed significantly (12.4%) less than AL/SED control mice (**Fig 5A**), yet there were no differences in cell proliferation rates between these two groups for any cell type analyzed (**Fig 6**). We have previously found that 15% CR results in a 13% reduction in body weight and decreased cell proliferation rates relative to *ad libitum*-fed controls (unpublished data). Therefore, the lack of change in cell proliferation rates observed in AL/EX male mice cannot be attributed to their reduced body weight relative to AL/SED controls. Moreover, in Experiment 2, CR/SED mice had lower cell proliferation rates than PF/EX mice in all cell types analyzed despite being matched for body weight (**Fig 3B and Fig 4**), suggesting that body weight could not fully account for the lower rates of cell proliferation observed in CR/SED mice. These data suggest that lower body weight, relative to *ad libitum*-fed sedentary controls, is not sufficient to account for the lower rates of cell proliferation in CR animals.

Our data on cell proliferation rates and body weight are consistent with previous work evaluating longevity in exercised rats. Since the original CR and longevity work by McCay[95], there has been the notion that decreased body weight, relative to *ad libitum*-fed controls, mediates the longevity effects of CR. Consistent with this hypothesis, several studies have shown that exercise leads to decreased tumor formation and markers of cell proliferation in the context of restricted feeding[287,288]. However, studies investigating the effect of voluntary exercise have shown that while exercise dramatically reduces body

weight in rats, it has no effect on maximal lifespan[286]. Thus, it appears that reduced body weight per se is not sufficient to account for the lower rates of cell proliferation or increased longevity in CR animals. Exercise in the setting of food restriction, however, may lead to improved health.

In contrast to these physiological adaptations to CR, reductions in circulating IGF-1 were associated with decreased cell proliferation rates. In Experiment 2, circulating IGF-1 levels were lower in both CR/SED and PF/EX mice as compared to AL/SED controls (**Table 1**), and in Experiments 2 and 3, IGF-1 levels correlated strongly with cell proliferation rates across all mice in all cell types (**Fig 8**). These data are consistent with many other studies reporting decreased IGF-1 in CR mice[23,230,289]. Interestingly, many of the genetic mouse models of increased longevity have disruptions in the GH/IGF-1 axis, with reduced IGF-1 concentration or signaling[290–294]. The mechanisms connecting IGF-1 and longevity, however, have not been established experimentally. One hypothesis is that reduced IGF-1 signaling could increase longevity by reducing cell proliferation rates in younger animals, which would both preserve the replicative capacity of cells and inhibit tumor growth as animals age. In future studies, it will be informative to assess cell proliferation rates in models of altered longevity and to identify adaptations to CR that reduce IGF-1 signaling.

If reductions in food intake, energy expenditure, percent body fat and body weight are insufficient to account for the decreased cell proliferation rates and the increased longevity in CR animals, what might be the adaptations that signal or mediate these effects? A unifying feature of the interventions that reduced cell proliferation rates here was that food intake was restricted below levels that would have been selected by the animals if allowed *ad libitum* access to food. It is not clear how restriction below *ad libitum* intake could serve as a signal for cellular or biochemical events. However, one possibility is the striking alteration in the pattern of food intake that is observed as an adaptation to CR[295]. In contrast to the relatively constant nibbling pattern of *ad libitum*-fed mice, CR mice consume their total daily allotment of food within several hours[295]. We have shown that this pattern of food intake leads to a dramatic change in fatty acid metabolism, with a short, post-prandial phase of fatty acid synthesis, followed by a prolonged period of fatty acid oxidation[295]. It is possible that this diurnal pattern of repeated fasting may initiate signaling mechanisms that lead to lower rates of cell proliferation and increased longevity. Consistent with this hypothesis, mice on intermittent fasting regimens have reduced rates of cell proliferation and increased maximal lifespan[281,296], despite no change in overall food intake, percent body fat or body weight. In future studies it will be important to investigate mechanisms by which repeated fasting and/or increased fatty acid oxidation might lead to decreased rates of cell proliferation, perhaps through regulation of the GH/IGF-1 axis. In addition it will be interesting to identify adaptations to CR that reduce free IGF-1, perhaps through changes in circulating IGFBP1, a serum factor not assessed in this study.

Finally, these results are consistent with the hypothesis that reductions in cell proliferation rates could serve as a rapidly responsive biomarker of interventions that extend lifespan. Cell proliferation rates have been suggested to mediate the longevity effects of CR, by preserving replicative capacity and reducing tumor promotion[94,267]. Cell proliferation rates are reduced rapidly and persistently in many tissues in response to CR[225,227,266] and alternate day fasting[297], two dietary regimens that extend maximal lifespan. In contrast, several progeroid diseases are associated with increased rates of cell

proliferation in early life[56,218,298,299]. In the present study, we show that the cell proliferation rate response is specific to interventions that have been elsewhere demonstrated to extend maximal lifespan. Indeed, there were no changes in cell proliferation rates in response to increased housing temperature and voluntary wheel running, two interventions that mimic physiological adaptations to CR, but cannot reproduce its health and longevity effects in isolation[276,286]. We also confirmed the rapid response of cell proliferation rates to CR and identified a correlation between cell proliferation rates and circulating IGF-1. Future work investigating the rates of cell proliferation in other models of longevity will be valuable in assessing its utility as a biomarker of aging.

Chapter 2: FGF21 and the IGF-1 and cell proliferation responses to several weeks of moderate calorie restriction in adult mice

Introduction

Calorie restriction (CR), reducing caloric intake without malnutrition, increases maximum lifespan and delays the onset of many age-related diseases in organisms ranging from worms to rodents, and possibly non-human primates [300,301]. Decreased signaling through the somatotropic axis is one mechanism that has been suggested to mediate these effects of CR [23], perhaps through a reduction in cell proliferation, which is predicted to contribute to lifespan extension by delaying replicative senescence and inhibiting the promotional phase of carcinogenesis[267]. Several pieces of evidence have built a strong case for this hypothesis; first, CR in mice leads to a reduction in circulating levels of insulin-like growth factor-1 (IGF-1) in association with reduced rates of proliferation in a number of cell types [99,225–228]. Second, repletion of circulating IGF-1 levels in CR rodents has also been shown to attenuate the CR-induced reduction in cell proliferation [229–231]. Lastly, disruption of IGF-1 signaling in several mouse models mimics many of the effects of CR including, increased maximum lifespan, reduced tumor promotion, delayed replicative senescence and reduced rates of cell proliferation [58,64,267,302–305]. Thus, identifying mechanisms that regulate IGF-1 signaling and cell proliferation in response to CR in mice could provide insight into the basic biology of aging and offer therapeutic targets for treating age-related diseases.

Regulation of hepatic IGF-1 production, the predominant source of circulating levels [162], is well understood under *ad libitum* (AL) feeding conditions. Circulating growth hormone (GH) binds to the GH receptor (GHR) stimulating its association with the intracellular kinase, janus kinase 2 (JAK2), which subsequently autophosphorylates and phosphorylates the GHR creating a binding site for signal transducer and activator of transcription 5 (STAT5). Once bound to the GHR, STAT5 is phosphorylated by JAK2, which stimulates its dimerization and translocation to the nucleus where STAT5 activates the transcription of IGF-1 [163,306]. Based on this mechanism, it might be predicted that reduced circulating IGF-1 in CR mice could simply be due to reduced circulating GH. However, while young mice on a severe CR diet have reduced circulating IGF-1, they actually have increased levels of circulating GH compared to AL controls [70]. High circulating GH levels coincident with low IGF-1 levels have also been observed in humans under conditions of energy restriction [232]. In addition, pulsatile GH secretion appears to be increased in older CR rats, compared to age-matched AL controls [23,239]. Together these observations suggest that CR regulates IGF-1 expression downstream of GH. The mechanisms of CR-induced regulation of IGF-1, however, remain unknown.

Recently, fibroblast growth factor 21 (FGF21), a novel endocrine-like member of the FGF superfamily highly expressed in the liver, has been implicated as a negative regulator of IGF-1 expression and shown to extend maximum lifespan in mice when over-expressed [70–72,74,248]. Indeed, FGF21 transgenic mice are smaller, exhibit reduced hepatic GH sensitivity downstream of JAK2 and have reduced circulating IGF-1 levels compared to WT controls [71,74]. Furthermore, treatment of mice with recombinant human FGF21 has been shown to reduce circulating levels of IGF-1 while treatment of chondrocytes with FGF21 attenuates GH-induced IGF-1 mRNA expression [71,72]. Others have also shown that long-term CR (74wks) increases hepatic mRNA and circulating levels of FGF21 and that FGF21 expression is increased in young developing mice on a severe CR diet compared to AL

controls [70,113]. Importantly, in studies using whole-body FGF21-knock out (FGF21-KO) mice, FGF21 has been shown to be necessary for the full undernutrition-related reduction in hepatic mRNA and circulating levels of IGF-1 [70].

Interestingly, earlier work demonstrated that hepatic FGF21 mRNA expression and circulating protein levels are rapidly increased in response to fasting in a peroxisome proliferator-activated receptor alpha (PPARα)-dependent manner [307–309]. Given the intermittent nature of feeding in CR mice (~1 hour of gorging upon food provision followed by ~23 hours of fasting) [295], FGF21 expression may be increased in mice even after just a few weeks on a moderate CR regimen and this hormonal signaling could lead to the decreases in circulating IGF-1 and cell proliferation rates that are observed in response to several weeks of CR. However, the effect of several weeks of moderate CR in adult mice on FGF21 expression and the role of FGF21 in mediating the IGF-1 and cell proliferation responses to CR have not been previously explored.

Accordingly, the goal of this study was to determine the effect of several weeks of moderate CR on GH secretory dynamics, hepatic GH signaling and FGF21 expression in adult C57BL/6 male mice. In addition, we sought to determine if FGF21 is necessary for the CR-induced reductions in circulating IGF-1 and cell proliferation.

Materials and Methods

Animals

12- to 16-week-old male C57BL/6 mice were used in the initial studies (Jackson Laboratory, Bar Harbor, ME). For the FGF21-KO study, 12- to 17-week-old male control C57BL/6N (WT) mice and 12- to 15-week-old male FGF21-KO mice were used (Taconic Farms Inc., Hudson, NY). All mice were housed individually, provided free access to water and maintained under temperature- and light-controlled conditions (12:12-h light-dark cycle, lights on at 0700hr and off at 1900hr)

FGF21-KO mice were generated as previously described. Briefly, to generate mice with targeted disruption of the FGF21 locus, a 6.5-kbNheI genomic fragment containing all three exons of the mouse FGF21 gene was subcloned and used as a gene targeting vector by replacing part of exon 1 (30 bp downstream of the ATG), all of exon 2, and the 5' region of exon 3 with a neomycin resistance gene (pGTN29; New England Biolabs, Ipswich, MA), thus deleting approximately 1200 bp of the genomic FGF21 sequence and deleting the 3' part of exon 1, all of exon 2, and the 5' region of exon 3. Founder mice were subsequently backcrossed onto the C57BL/6 line at least 10 times before investigation [310].

Diets and feeding regimens

All mice in the AL groups were provided free access to semi-purified AIN-93M diet (Research Diets, New Brunswick, NJ). All mice in the CR groups were provided semi-purified dustless precision AIN-93M diet pellets (Bio-Serv, Frenchtown, NJ). The average daily food intake of the AL groups was determined every 3 to 4 days and the food provided to the corresponding CR groups was adjusted accordingly. All mice in the CR groups were fed daily at 1600hr.

For the initial studies, following one week of acclimation to the AIN-93M diet, mice were randomly assigned to one of two dietary groups: AL or CR. Mice in the CR groups were provided with 75% of the average daily food intake of their AL group counterparts (from the previous 3 to 4 days) and, therefore, were 25% calorie restricted. Mice were kept on their feeding regimens for a total of 4 or 6.5 weeks. The body weight of each mouse was determined at least once per week. Mice in these initial studies were euthanized at 2100hr.

For the FGF21-KO study, following one week of acclimation to the AIN-93M diet, WT and KO mice were randomly assigned to one of two dietary groups: AL or CR. The groups included: WT/AL, WT/CR, FGF21-KO/AL and FGF21-KO/CR. Mice in the CR groups were initially acclimated to the CR regimen over the course of 5 days (10% CR for 2 days, 15% CR for 1 day, 20% CR for 2 days and 25% CR thereon after). All mice were kept on their feeding regimens for a total of six weeks. The body weight of each mouse was determined at least twice per week. Mice in the FGF21-KO study were euthanized at 1500hr or 1900hr.

All protocols and procedures were approved by the University of California Berkeley Animal Use Committee.

^2H_2O labeling

In order to measure global rates of DNA synthesis as a marker of cell proliferation, mice in the FGF21-KO study were labeled with an intraperitoneal injection of 100% ^2H_2O (heavy water) (0.35ml/ 10g body weight) 3 weeks prior to the end of the study and were then provided free access to 8% heavy water as drinking water for the remainder of the study, as previously described [278].

Blood collection, tissue collection and cell isolation

Blood

Upon completion of each study, mice were anesthetized under 3% isoflurane and blood was collected via cardiac puncture, followed by cervical dislocation, tissue collection and in some cases cell isolation.

Keratinocytes

After euthanasia, the back of each mouse was shaved followed by an application of Nair for complete hair removal (Carter Products, New York, NY, USA). A small (3cm^2) piece of the dorsal skin was dissected, washed with PBS (Gibco, Grand Island, NY, USA) and placed in 5mL PBS with 10 units of dispase II (Roche, Indianapolis, IN, USA). Dorsal skins were incubated for ~3 to 4 hours with shaking at 100rpm at 37°C. The epidermis was then peeled from the dermis and collected for DNA isolation.

Liver

Upon dissection, the liver was cut into several small pieces (~15-50mg), which were flash frozen in liquid nitrogen. For DNA synthesis measurements, liver samples were homogenized and total DNA from all liver cells was isolated.

Splenic T-cells

Upon dissection, the spleen was homogenized and passed through a 40μM nylon cell strainer. T-cells were isolated from the single cell suspension using mouse anti-CD90.2 microbeads and the MACS cell separation column following the manufacturer's instructions (Miltenyi Biotec, Auburn, CA, USA), pelleted and then collected for DNA isolation.

Bone marrow cells

Femurs were dissected for isolation of bone marrow cells. Bone marrow cells were flushed from the femurs with 2mL of PBS and were then pelleted and collected for DNA isolation.

DNA isolation

DNA was extracted using DNeasy kits (Qiagen, Valencia, CA, USA). Briefly, isolated keratinocytes, liver, T-cells and bone marrow cells were digested overnight at 37 °C in proteinase K solution followed by DNA isolation according to the manufacturer's instructions and elution into 200ul water.

DNA synthesis measurement

Determination of ^{2}H incorporation into purine deoxyribose (dR) of DNA was performed as previously described (8). Briefly, isolated DNA was hydrolyzed overnight at 37 °C with nuclease S1 and potato acid phosphatase. Hydrolyzates were reacted with pentafluorobenzyl hydroxylamine and acetic acid and then acetylated with acetic anhydride and *1*-methylimidazole. Dichloromethane extracts were dried, resuspended in ethyl acetate and analyzed by GC/MS on a DB-17 column with negative chemical ionization using He as carrier and CH_4 as reagent gas. The enrichment of ^{2}H in purine dR was determined by measuring the fractional molar isotope abundances at m/z 435 (M0 mass isotopomer) and 436 (M1 mass isotopomer) of the pentafluorobenzyl triacetyl derivative of purine dR. Excess fractional M1 enrichment (EM1) was calculated as:

$$\mathrm{EM1} = \frac{(\text{abundance m/z 436})_{\text{sample}}}{(\text{abundance m/z 435 + 436})_{\text{sample}}} - \frac{(\text{abundance m/z 436})_{\text{std}}}{(\text{abundance m/z 435 + 436})_{\text{std}}}$$

where sample and standard (std) refer to the analyzed sample and an unenriched pentafluorobenzyl triacetyl purine dR derivative standard, respectively. The fractional synthetic rate (*f*) of keratinocytes, liver and T-cells was calculated by a comparison to bone marrow cells in the same animal, which represents an essentially fully turned over population of cells.

$$f\,(\%\ \text{new cells}) = \frac{(\mathrm{EM1})_{\text{sample}}}{(\mathrm{EM1})_{\text{bone marrow}}}$$

The replacement rate (*k*, % new cells per day) was calculated as:

$$k\ (\%\ \text{new cells per day}) = \frac{\ln (1\text{-}f)}{\text{-t}}$$

where t is the number of days of exposure to heavy water.

Blood collection for GH measurement

~25ul of blood was collected every 45 min between 15:30hr and 20:45hr via the tail vein. CR mice were fed at their regular feeding time (1600hr) on the day of blood collection for GH measurement.

ELISAs

Following centrifugation of blood, plasma was collected and stored at -20°C. Plasma concentrations of GH (Millipore, Billerica, MA), FGF21 (Millipore, Billerica, MA), IGF-1 (R&D Systems, Minneapolis, MN) and insulin-like growth factor binding protein-1 (IGFBP-1) (Insight Genomics, Falls Church, VA) were measured via ELISA following the manufacturer's instructions.

Western blot analysis

Frozen livers were homogenized in 450ul buffer (10mM Tris-base, 150mM NaCl, pH ~7.5, 1% NP-40, 0.1% SDS, 0.5% sodium deoxycholate, 1mM dithiothreitol, 1mM phenylmethylsulfonyl fluoride, 7.5ug/mL leupeptin, 1.0ug/mL pepstatin, 2.0ug/mL aprotinin and 1 Phosphatase Inhibitor Cocktail tablet (Roche Applied Science, Indianapolis, IN) per 10mL buffer) using a stainless steel bead and a TissueLyserII (Retsch, Newtown, PA) set at 30hz for 1 min. Protein homogenates were sonicated in a sonication bath for 1 min and then centrifuged at 10,000 rcf at 4C for 10 min followed by supernatant collection. Protein concentrations were determined by bicinchoninic acid assay (Pierce, Rockford, IL) and proteins were separated by SDS-PAGE. Proteins were transferred to nitrocellulose membranes (Invitrogen, Grand Island, NY) and immunoblotted with total-Jak2, phospho-JAK2 (Try 1007/1008), total-STAT5, phospho-STAT5 (Tyr694) (Cell Signaling, Danvers, MA) and beta-actin (Santa Cruz Biotechnology, Inc., Santa Cruz, CA) primary antibodies followed by incubation with IRDye®700DX- or IRDye®800CW-conjugated secondary antibodies (Rockland Immunochemicals Inc., Gilbertsville, PA). Protein bands were imaged and densitometry measurements were made using the Odyssey® Infrared Imaging System (LI-COR, Lincoln, NE).

Gene expression

RNA was isolated from snap-frozen liver tissue using RNeasy kits (Qiagen, Valencia, CA) and reverse transcribed with M-MulV reverse transcriptase (New England Biolabs, Ipswich, MA). Next, diluted cDNAs were run on an ABI 7500 Fast Real-Time PCR System using TaqMan gene expression master mix and TaqMan probes for FGF21 (Mm00840165_g1), IGF-1 (Mm00439561_m1), IGFBP-1 (Mm00515154_m1) or 18S rRNA (Mm03928990_g1) according to the manufacturer's instructions (Applied Biosystems,

Carlsbad, CA). Expression of FGF21, IGF-1 and IGFBP-1 was normalized to 18S rRNA expression.

Statistical analyses

All results are presented as mean ± SEM. For initial studies, differences between AL and CR groups were analyzed by Student's unpaired two-tailed *t*-tests. For comparisons between WT and FGF21-KO mice fed AL or CR, to analyze differences in body weight and food intake over time, single time point comparisons were made using a one-way ANOVA followed by a Tukey *post hoc* test. Otherwise, differences between groups were analyzed by a two-way ANOVA followed by a Bonferroni *post hoc* test. When two time points were analyzed, differences between WT and FGF21-KO mice fed AL or CR were analyzed separately at each time point by a two-way ANOVA followed by a Bonferroni *post hoc* test. Data were analyzed using Prism Graphpad software (version 5.0a).

Results

GH secretory dynamics and hepatic GH signaling in CR mice

Initially we set out to map where signaling within the canonical GH-mediated IGF-1 production pathway diverges in CR mice and thus, may account for reported lower IGF-1 levels in CR mice. To confirm previous reports on the GH status of CR rodents and to extend those findings to short-term moderate CR in adult mice, we placed 12- to 16-week-old mice on either an AL or 25% CR diet for a total of 4 or 6.5 weeks.

We measured circulating GH levels eight times over a 5.25hr sampling period in mice fed AL or CR for 6.5 weeks. We found that there were no significant differences in circulating GH levels, described as either the integrated concentration or the maximum pulse amplitude of GH, over the 5.25hr sampling period in CR compared to AL mice (**Fig 1A,B**). These findings are consistent with previous reports in CR rodents that provide evidence that a simple reduction in circulating GH levels cannot explain the reduction in IGF-1 levels in response to CR [23,70].

To determine whether hepatic GHR signaling is blunted in CR mice, we measured JAK2 and STAT5 phosphorylation as surrogates of GHR signaling in this tissue in mice fed AL or CR for 4 weeks. We found that there was no significant difference in hepatic JAK2 phosphorylation in CR compared to AL mice, with a non-significant trend towards higher levels in CR mice, while interestingly, hepatic STAT5 phosphorylation was significantly reduced in CR compared to AL mice (**Fig. 1C,D**). These data suggest that the reduction in IGF-1 production in response to CR is likely via a mechanism downstream of JAK2 signaling and may be mediated through a disruption in STAT5 signaling.

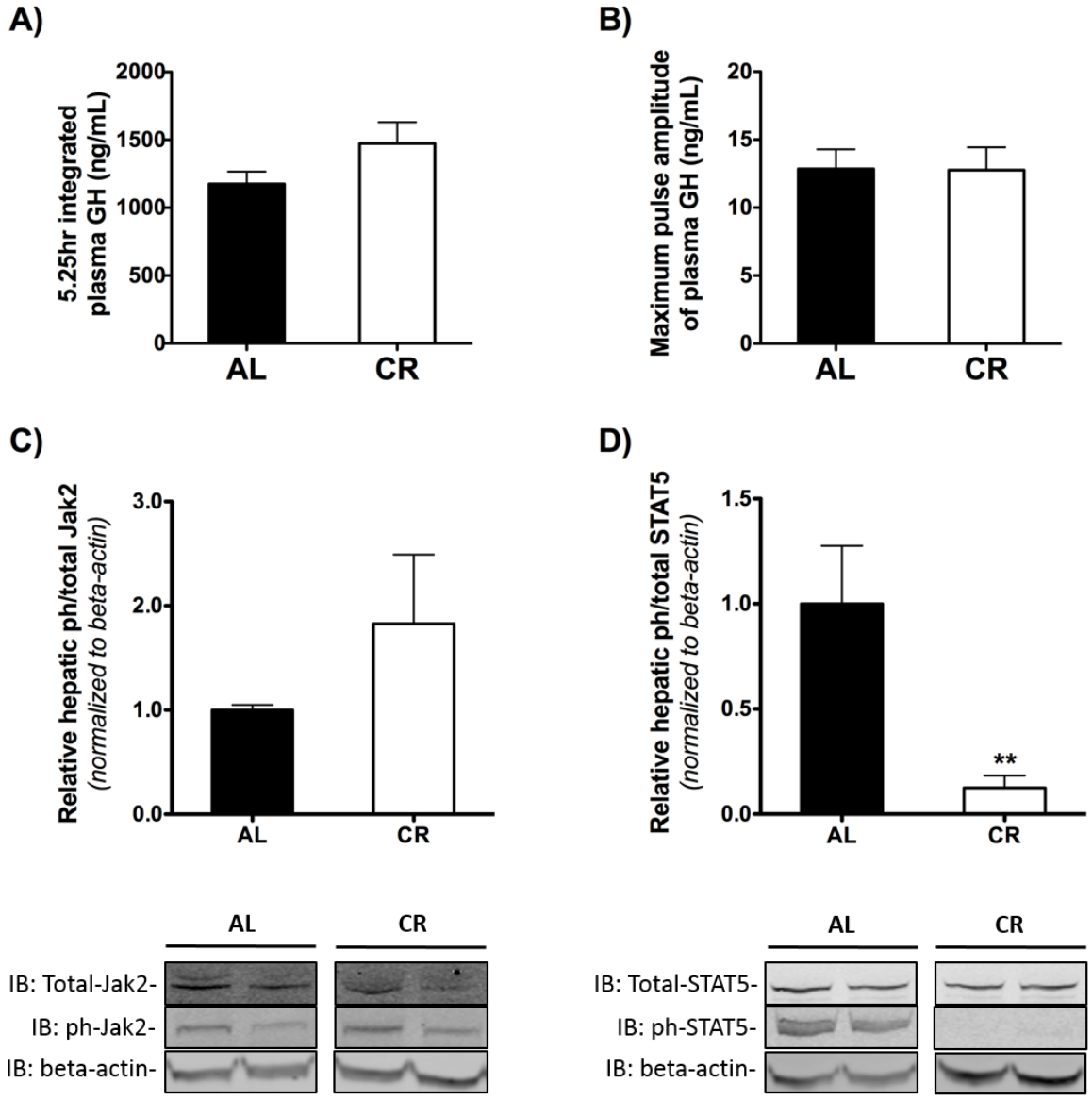

Figure 1: GH secretory dynamics and hepatic GH signaling in CR mice

Plasma GH levels described as A) the integrated concentration or B) the maximum pulse amplitude of GH over the 5.25hr sampling period in AL and CR mice (n = 8 per diet). Hepatic levels of total to phosphorylated C) JAK2 and D) STAT5 in AL and CR mice (n = 5-7 per diet. Data normalized to AL). Student's unpaired two-tailed *t*-tests were used for all between-group analyses (** $p < 0.0066$).

FGF21 expression in CR mice

Previous studies by *Inagaki et al*. and *Kubicky et al.* suggest that the fasting-induced hormone, FGF21, may play an important role in the down-regulation of hepatic IGF-1 production in response to CR, possibly through a STAT5-dependent mechanism [70,71]. Given

these previous findings, we sought to determine whether FGF21 expression was up-regulated in response to several weeks of moderate CR in adult mice and, therefore, whether increased FGF21 might play a role in the IGF-1, and by extension, the cell proliferation response to CR.

Consistent with this hypothesis, we found that circulating and hepatic mRNA levels of FGF21 were significantly increased in CR compared to AL mice (**Fig. 2C,D**). We also confirmed in these mice that circulating and hepatic mRNA levels of IGF-1 were significantly reduced in CR compared to AL mice, as previously observed (**Fig. 2A,B**).

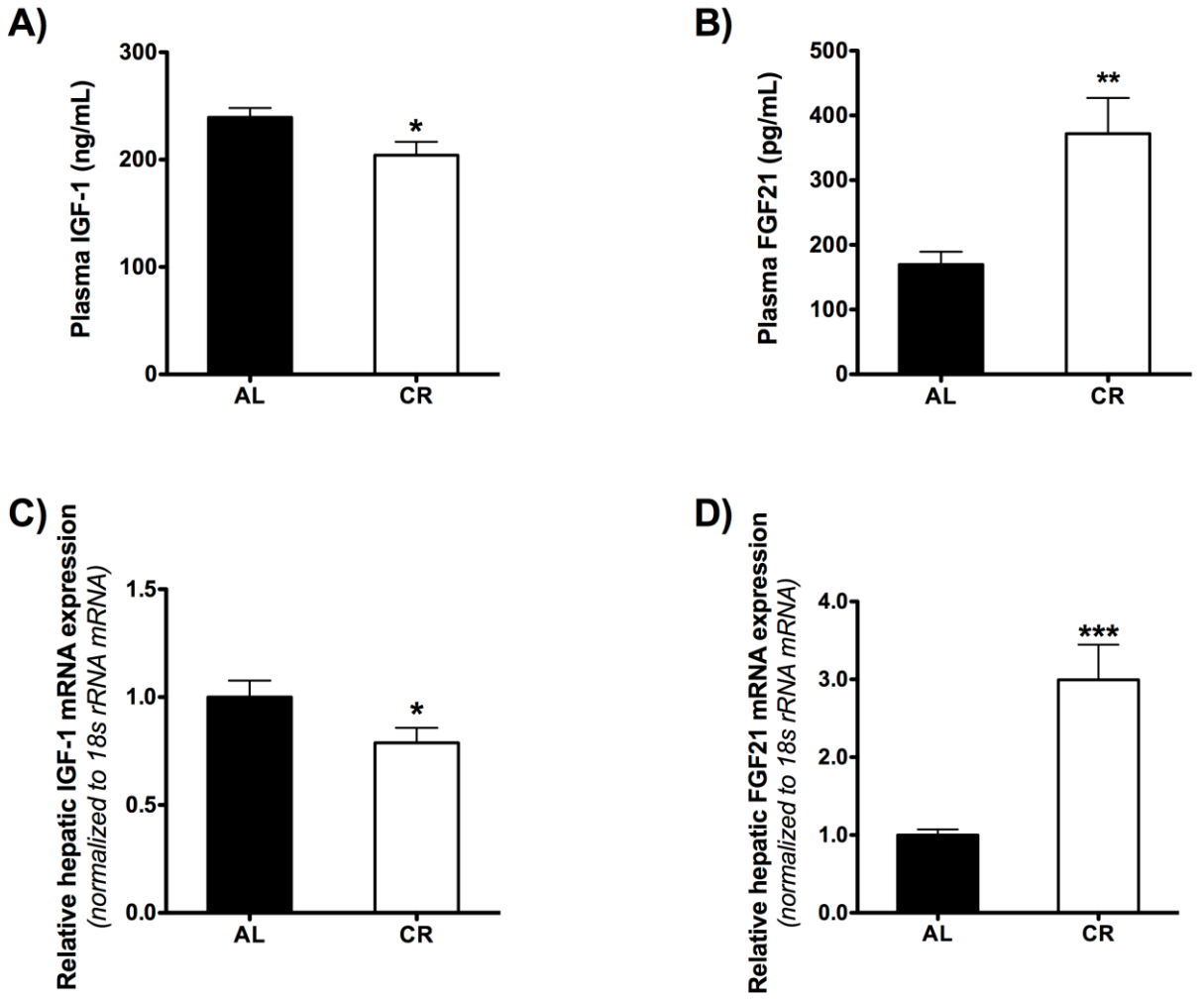

Figure 2: Circulating and hepatic mRNA levels of IGF-1 and FGF21 in CR mice

Plasma A) IGF-1 and B) FGF21 levels in AL and CR mice (n = 16-21 per diet). Relative hepatic mRNA expression levels of C) IGF-1 and D) FGF21 in AL and CR mice (n = 29-31 per diet). Hepatic mRNA expression levels were normalized to 18S rRNA and then normalized to the AL group. Student's unpaired two-tailed *t*-tests were used for all between-group analyses (* $p < 0.05$, ** $p < 0.004$, *** $p < 0.0001$).

FGF21 and the IGF-1 response to CR

Having confirmed that FGF21 expression is in fact up-regulated in adult mice on a moderate CR regimen, we next sought to determine whether FGF21 is necessary for the reductions in circulating IGF-1 and cell proliferation rates in response to several weeks of moderate CR in adult mice. To this end, we placed 12- to 17-week-old WT and FGF21-KO mice on either an AL or 25% CR diet for a total of six weeks and measured circulating and hepatic mRNA levels of IGF-1 and *in vivo* proliferation rates of keratinocytes, liver cells and splenic T-cells.

Consistent with previous findings, FGF21-KO mice weighed significantly more than WT mice on an AL diet [309–311]. Similarly, FGF21-KO mice weighed more than WT mice on a CR diet (**Fig 3A**). There was no difference in the percentage of weight gain over the course of the study between the two AL groups (**Fig 3B**). FGF21-KO mice, however, lost a greater percentage of their body weight on a CR diet than WT mice (**Fig 3B**). Over the course of the study, FGF21-KO mice tended to eat more than WT mice on an AL diet (**Fig 3C**) although there was no significant difference in the overall average food intake between the two AL groups during the study (**Fig 3D**), despite the larger body weight of the FGF21-KO mice.

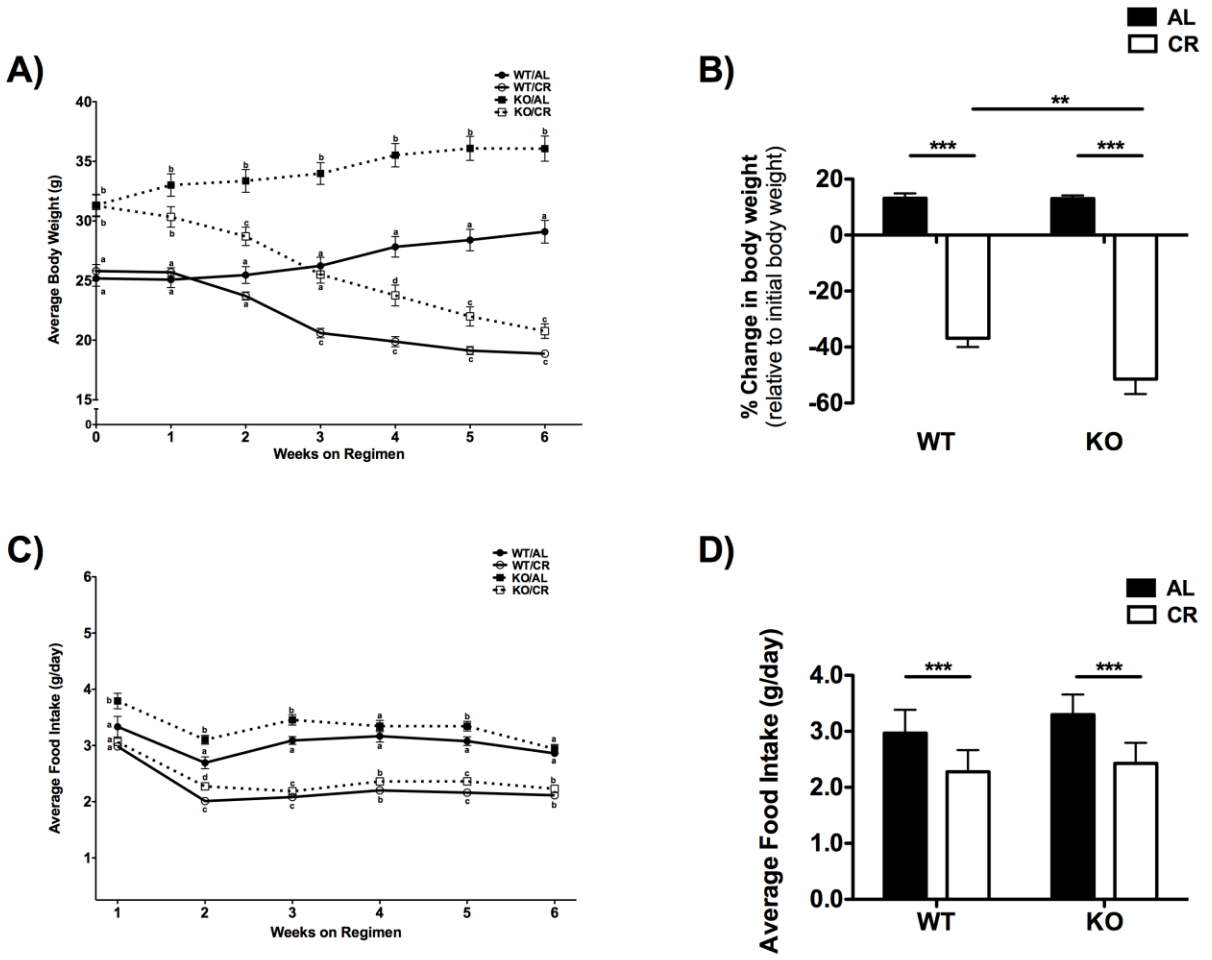

Figure 3: Body weight and food intake in WT and FGF21-KO mice fed AL or CR

A) Body weight trajectories and B) percent body weight change relative to initial body weight over the 6-week study. C) Daily food intake trajectories and D) cumulative average daily food intake over the 6-week study (n = 9-10 per genotype per diet). For A and C, a one-way ANOVA with a Tukey post hoc test was used at each time point for all between-group analyses. Groups not sharing a common letter at a given time point are significantly different ($p < 0.05$). For B and D, a two-way ANOVA with a Bonferroni post hoc test was used for all between-group analyses (** $p < 0.01$, *** $p < 0.001$).

All mice were dosed with heavy water for the last three weeks of the study to allow for global cell proliferation rate measurements, as previously described [278]. To take into account possible circadian fluctuations in the hormones of interest and to account for the fact that CR mice gorge their entire daily allotment of food within ~1hr of food provision, half of the mice in each group were euthanized one hour before (1500hr) and the other half three hours after (1900hr) the scheduled daily feeding of the CR mice (1600hr).

Interestingly, circulating and hepatic mRNA levels of FGF21 exhibited unique circadian fluctuations in WT mice fed an AL or CR diet. Compared to AL mice, circulating and hepatic mRNA levels of FGF21 were lower at 1500hr and higher at 1900hr in CR mice (although the difference in circulating levels of FGF21 at 1500hr in AL compared to CR mice did not reach statistical significance). FGF21 was essentially undetectable in the FGF21-KO mice (**Fig 4 A,D**).

There were no differences in circulating IGF-1 levels between the two AL groups at either time point. Contrary to our expectations, at both time points, circulating IGF-1 levels were reduced to the same extent in WT and FGF21-KO mice fed a CR diet relative to AL controls (**Fig 4B**). These changes in circulating IGF-1 were approximately paralleled by changes in hepatic IGF-1 mRNA expression (**Fig 4E**). These data suggest that FGF21 is not necessary for the reduction in IGF-1 in response to several weeks of moderate CR in adult mice.

Despite comparable levels of circulating IGF-1, it is possible that IGF-1 bioavailability may have differed between WT and FGF21-KO mice in response to CR. Therefore, we measured circulating and hepatic mRNA levels of IGFBP-1, which reduces IGF-1 bioavailability [312–314]. In both WT and FGF21-KO mice, CR led to a robust increase in circulating IGFBP-1 at both time points, although to a lesser extent at 1900hr (**Fig 4C**). While there were no differences in circulating IGFBP-1 levels between WT and FGF21-KO mice on a CR diet at 1900hr, these levels were increased in the FGF21-KO mice at 1500hr. The observed changes in circulating IGFBP-1 were approximately paralleled by changes in hepatic mRNA expression (**Fig 4F**). These data suggest that CR in mice reduces the bioavailability of IGF-1 and that this does not appear to be dependent on FGF21.

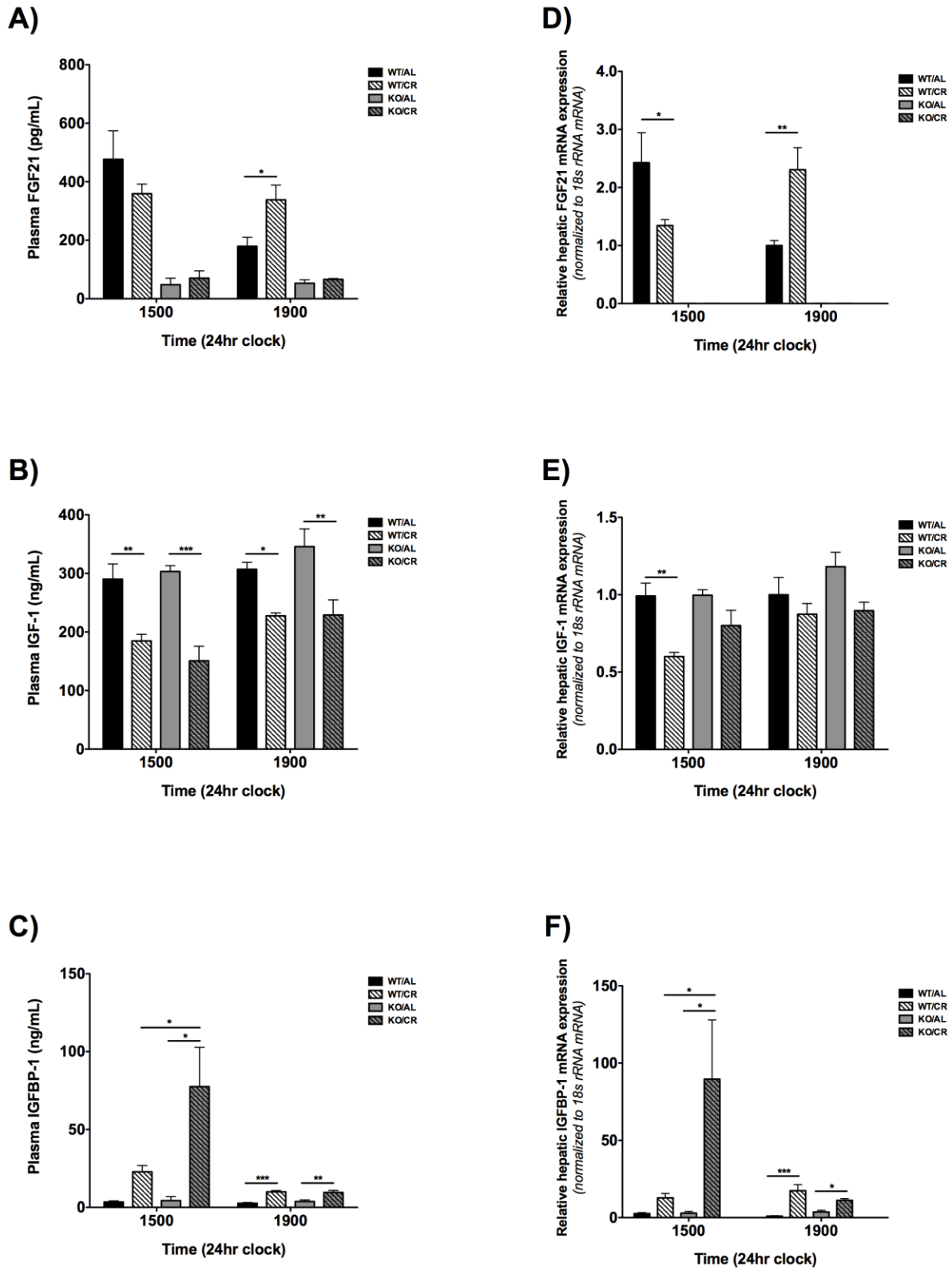

Figure 4: Circulating and hepatic mRNA levels of FGF21, IGF-1 and IGFBP-1 in WT and FGF21-KO mice fed AL or CR

Plasma levels of A) FGF21, B) IGF-1 and C) IGFBP-1 and relative hepatic mRNA expression levels of D) FGF21, E) IGF-1 and F) IGFBP-1 at 1500hr and 1900hr in WT and FGF21-KO mice fed AL or CR (n = 3-12 per genotype per diet per time point). Hepatic mRNA expression levels normalized to 18S rRNA and then normalized to WT/AL mice at 1500hr. All between-group analyses were performed using a two-way ANOVA with a Bonferroni post hoc test at each time point (* $p < 0.05$, ** $p < 0.01$, *** $p < 0.001$).

FGF21 and the cell proliferation response to CR

CR in rodents leads to a robust reduction in global rates of cell proliferation, an effect that has been proposed to confer some of the lifespan benefits of CR by delaying replicative senescence and inhibiting tumor promotion [99,225–228,267]. Importantly, repletion of IGF-1 levels in CR rodents back to AL levels has been shown to attenuate CR-induced reductions in cell proliferation [229–231]. These findings suggest that reduced IGF-1 levels, reduced IGF-1 bioavailability or a combination of both may mediate the cell proliferation effects of CR.

It is important to note that IGF-1 bioavailability is influenced not only by IGFBP-1 levels, as previously mentioned, but also by a variety of other factors including acid-labile subunit (ALS), other IGFBPs and IGFBP proteases [234,235]. Therefore, given the difficulty in assessing IGF-1 bioavailability, to determine the role of FGF21 in CR-induced changes in overall growth status, we measured *in vivo* cell proliferation rates, which serve as an integrated metric of growth stimulation.

We found that the proliferation rates of all three cell types analyzed (keratinocytes, liver cells and splenic T-cells) were reduced in both WT and FGF21-KO mice fed a CR diet relative to AL controls. Interestingly, despite similar levels of food intake and circulating IGF-1 and IGFBP-1 levels, AL-fed FGF21-KO mice exhibited increased rates of proliferation in all three cell types analyzed compared to AL-fed WT mice (**Fig 5A-C**). These data suggest that FGF21 is not necessary for the reduction in global rates of cell proliferation in response to CR but that FGF21 may negatively regulate basal rates of cell proliferation under normal, AL feeding conditions.

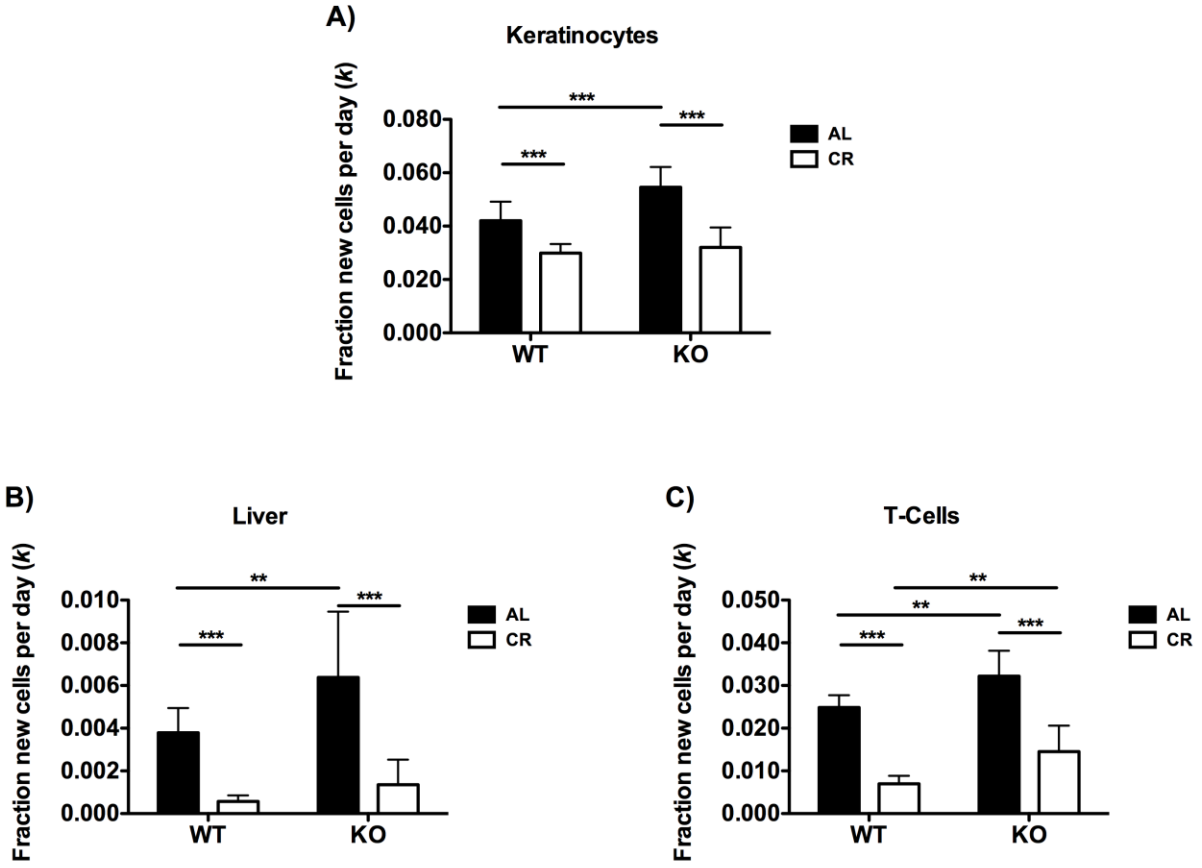

Figure 5: Global cell proliferation rates in WT and FGF21-KO mice fed AL or CR

Fraction of new cells per day for A) keratinocytes, B) liver cells and C) splenic T-cells during the 3 week heavy water labeling period (n = 7-10 per genotype per diet). All between-group analyses were performed using a two-way ANOVA with a Bonferroni post hoc test (* $p < 0.05$, ** $p < 0.01$, *** $p < 0.001$).

Discussion

In the context of several weeks of moderate CR in adult mice, the studies presented here demonstrate the following: 1) Circulating GH levels and hepatic JAK2 phosphorylation levels are unchanged in CR compared to AL-fed mice and, therefore, cannot account for the reduction in IGF-1 in response to CR. 2) A reduction in hepatic STAT5 phosphorylation is the most distal point of somatotropic axis divergence yet reported in CR mice. 3) FGF21 displays an interesting circadian pattern of expression in response to CR, however, ablation of FGF21 has no effect on CR-induced reductions in IGF-1 levels or cell proliferation rates. Together these findings support the conclusion that CR in mice induces some divergence in somatotropic axis signaling that may mediate CR-

induced lifespan extension, perhaps by impacting cell proliferation, however, FGF21 is not necessary for this somatotropic axis divergence.

CR delays aging and extends maximum lifespan across a range of organisms, making it an excellent model for studying the biology of aging. Despite decades of research, the underlying mechanisms that confer delayed aging and maximum lifespan extension in response to CR remain to be fully elucidated. However, there appears to be a consensus in the field of aging research that down-regulation of the somatotropic axis, including a reduction in circulating IGF-1 levels, likely plays an important role [8,23,103,315,316]. Consistent with this, numerous mouse models of extended maximum lifespan are characterized by reduced circulating IGF-1 and somatotropic axis signaling [58]. One proposed mechanism by which a reduction in circulating IGF-1 levels may contribute to delayed aging and maximum lifespan extension in response to CR is by reducing cell proliferation, thereby delaying replicative senescence and inhibiting tumor formation [228,267]. Thus, determining the mechanism (s) by which circulating IGF-1 and cell proliferation are reduced in response to CR could provide insight into the basic biology of aging and offer therapeutic targets for treating age-related diseases.

Under AL feeding conditions, circulating IGF-1 levels are primarily determined by GH signaling in the liver [162,163]. Therefore, GH secretory dynamics and hepatic GH signaling in CR mice were assessed in our initial studies. Data on the effects of short-term moderate CR on circulating GH levels in young rats has been previously described [229,238,239]. It has also been previously shown that short-term severe CR in young developing mice results in an increase in circulating GH while hepatic GH binding and GHR expression are reduced compared to controls [70]. However, to our knowledge, the data presented here represent the first characterization of circulating GH and hepatic GH signaling in response to several weeks of moderate CR in adult mice.

We found that both circulating GH and hepatic JAK2 phosphorylation were unchanged while hepatic STAT5 phosphorylation was reduced in CR compared to AL mice (**Fig 1**) suggesting that the reduction in IGF-1 in response to CR is likely via a mechanism downstream of JAK2 signaling and may be mediated through a disruption in STAT5 signaling. Previous findings in mice by *Inagaki et al.* implicated FGF21 as a negative regulator of IGF-1 expression via a mechanism downstream of JAK2 signaling while findings from *Kuhla et al.* and *Kubicky et al.* have shown that FGF21 expression is increased in long-term CR mice and young mice on a severe CR diet compared to AL controls, respectively [70,71,113]. Consistent with these previous findings, we found that circulating and hepatic mRNA levels of FGF21 were increased in adult mice after several weeks on a moderate CR diet compared to AL-fed controls when measured ~5hrs following food provision to CR mice (**Fig 2**). Together these findings suggested that FGF21 might mediate the reduction in IGF-1 and, therefore, the reduction in cell proliferation rates, in response to CR.

Using FGF21-KO mice, we asked directly whether FGF21 was necessary for the IGF-1 and the cell proliferation responses to several weeks of moderate CR in adult mice. In order to capture possible circadian fluctuations in mRNA and circulating levels of factors of interest, mice were euthanized at two different time points.

We found that circulating and hepatic FGF21 mRNA levels did in fact exhibit unique circadian fluctuations in the context of both an AL and a CR diet in WT mice (**Fig 4 A,D**). The pattern of FGF21 expression in response to CR was unexpected in light of previous observations that FGF21 expression is robustly up-regulated in fasted mice [307–309]. In contrast to these studies, we found that at 1500hr, CR mice, which had essentially been without food for more than 20hrs, had lower levels of FGF21 compared to AL mice. Furthermore, at 1900hr, CR mice, which were in a postprandial state, had higher levels of FGF21 compared to AL mice. These data underscore the fact that CR is not simply repeated fasting and that CR and fasting are two distinct dietary paradigms. The observation that circulating and hepatic mRNA levels of FGF21 are increased in CR mice upon feeding is consistent with previous reports in rats that FGF21 expression in hepatocytes is regulated in part by carbohydrate response element binding protein (ChREBP) [317] and that refeeding after a fast robustly increases circulating and hepatic mRNA FGF21 levels [318]. We also found that the circadian pattern of hepatic FGF21 mRNA expression was inversely correlated with peroxisome proliferator-activated receptor-γ coactivator (PGC)-1α and delta-aminolevulinate synthase-1 (ALAS-1) expression, consistent with previous reports in mouse hepatocytes that PGC-1α, through up-regulation of ALAS-1, represses FGF21 expression [319] (data not shown). Together these data underscore the critical importance of the timing of measurements in the context of AL, as well as non-AL feeding.

This critical timing effect was highlighted in a previous study from our group with regard to hepatic expression of genes involved in *de novo lipogenesis* (DNL). In this study, hepatic mRNA levels of three genes involved in DNL were found to be higher in CR compared to AL mice at two time points during the circadian cycle following food provision to CR mice (consistent with the observation that FA synthesis was higher in CR mice). However, the hepatic mRNA levels of these same three genes was found to be reduced in CR compared to AL mice at another time point approximately 23hrs after food provision to CR mice [295]. With regard to FGF21 expression, it is possible that the apparent absence of any effect of CR on FGF21 expression in previous studies in rodents is due to the timing of tissue collection relative to the time of food provision to CR animals. Consistent with the findings presented here, these previous studies found that FGF21 levels were comparable between AL and CR rodents when tissues were collected ~20hrs after the provision of food to CR animals [74,112].

Despite being higher at 1900hr in CR compared to AL WT mice, FGF21 was not required for the reduction in circulating IGF-1 in response to several weeks of moderate CR (**Fig 4B**). This is in contrast to a recent report showing that FGF21 is necessary for the reduction in circulating IGF-1 in response to under-nutrition in mice [70]. Differences in experimental design likely account for the discrepancies between the results from this previous study and the present study. In the previous study, young (4-week-old) developing mice were placed on a severe CR diet (50% CR) for four weeks while in the present study, adult (12- to 17-week-old) mice were placed on a moderate CR diet (25% CR) for six weeks. The discrepancy between the results of these two studies suggests that i) there may be a threshold of %CR above which the regulatory effects of FGF21 on circulating IGF-1 manifest, ii) FGF21 regulates circulating IGF-1 primarily during development or perhaps iii) a combination of both. Future studies should focus on other

factors that may regulate changes in IGF-1 expression in response to moderate short-term CR in adult mice, including protein intake, insulin and thyroid hormone [232].

We also showed that FGF21 was not required for the reduction in cell proliferation in response to CR (**Fig 5**). An unexpected finding was that despite similar levels of food intake and circulating IGF-1 levels, AL-fed FGF21-KO mice exhibited higher rates of proliferation in all three cell types analyzed compared to AL-fed WT mice. These data are consistent with the reduced susceptibility of transgenic mice over-expressing FGF21 in hepatocytes to diethylnitrosamine (DEN)-induced liver tumor formation [250]. This higher rate of cell proliferation in AL-fed FGF21-KO compared to WT mice suggests that FGF21 may have direct or indirect anti-anabolic effects that are independent of circulating IGF-1 and food intake.

Despite the lack of an effect of FGF21 on the IGF-1 and cell proliferation responses to several weeks of moderate CR in adult mice, FGF21 may have an important role in other responses to this CR regimen. FGF21 is highly expressed in the pancreas and has been shown to have glucose-lowering and insulin-sensitizing effects *in vivo* [247–249,310,320–323]. Given that circulating FGF21 is up-regulated in CR mice after food provision and the gorging of their meal, it will be interesting to determine what if any role FGF21 plays in the well-established glucose-lowering and insulin-sensitizing effects of CR [8,324,325].

In conclusion, we have shown here that several weeks of moderate CR in adult mice results in GH resistance downstream of JAK2 signaling and a unique circadian pattern of FGF21 expression. We have also shown that FGF21 is not necessary for the reductions in IGF-1 or cell proliferation rates in response to several weeks of moderate CR. In addition, in the context of AL feeding, our data provide evidence that FGF21 may have anti-anabolic effects.

While FGF21 does not appear to be necessary for the reduction in circulating IGF-1 in response to several weeks of moderate CR in adult mice, there is evidence to suggest that FGF21 is sufficient to reduce circulating IGF-1 levels given that mice treated with recombinant human FGF21 as well as FGF21 transgenic mice exhibit reduced circulating IGF-1 [71]. Given these observations in conjunction with its glucose-lowering and insulin-sensitizing effects, FGF21 appears to mimic several of the beneficial effects of CR, underscoring its therapeutic potential.

Chapter 3: Reduced *in vivo* protein replacement but not cell proliferation rates are predictive of maximum lifespan extension in mice

Introduction

Age is a major risk factor for numerous diseases including cancer, diabetes and neurodegenerative diseases[326]. In the US, the proportion of the population that is of advanced age (65yr and over) is projected to increase sharply in decades to come and result in a dramatic increase in the prevalence of age-related diseases[7]. The potential social and economic consequences of such an increase have sparked great interest in the development of interventions that promote healthspan, the time in which an individual remains active and in good health. Accordingly, two fundamental goals of gerontological research are to determine the primary physiological, hormonal, cellular and molecular factors that regulate mammalian healthspan determination and to then use this knowledge to identify interventions, be they pharmacological, dietary, genetic or activity-based, that modulate these factors in favor of healthspan promotion.

Broadly speaking, healthspan can be increased in two ways. One way is by curing a single age-related disease which results in an increase in mean lifespan (the age at which 50% of a given population remains alive) but has no effect on maximum lifespan (generally defined as the mean age of the 10% longest-lived individuals in a given population). Healthspan can also be increased by inducing a general slowing of the aging process itself, thereby delaying the onset of a wide range of age-related diseases. A delay in the aging process itself thus results in an increase in not only mean but also maximum lifespan. Importantly, it is the extension of healthspan, not necessarily maximum lifespan in humans that is a primary goal of gerontological research. However, as a means to delay the onset of a wide range of age-related diseases, rather than just one specific age-related disease, it is important to focus on general mechanisms of aging. Therefore, efforts to identify interventions with the potential to extend human healthspan have focused on the extension of maximum lifespan. For a variety of ethical and practical reasons, testing of candidate interventions with the potential to increase maximum lifespan cannot be conducted in humans. Instead, candidate interventions are tested in physiologically relevant organisms, including mice.

Currently, the most robust program for testing candidate interventions (specifically, candidate compounds) with the potential to extend maximum lifespan in mice is the National Institute on Aging's (NIA) Interventions Testing Program (ITP). Conceived of in 2000, this program tests candidate compounds at three sites (the University of Michigan, the University of Texas and the Jackson Laboratory) in genetically heterogeneous mice with enough statistical power to detect 10% changes in lifespan[125,126]. To date, more than 25 compounds have entered the testing pipeline. Two of these compounds, rapamycin and acarbose, have been shown to extend maximum lifespan in both male and female mice[140,142,327]. Rapamycin is an antifungal compound that in mammals reduces the function of mammalian target of rapamycin (mTOR) complex 1 (mTORC1) (and mTORC2 when administered chronically)[129,131,176]. mTORC1 is a central integrator of a variety of signals in the cell including those for nutrient availability, growth factors and stress and mTORC1 signaling promotes among many things, protein synthesis and cell growth[166]. Acarbose inhibits intestinal α-glucosidases, thereby limiting dietary starch and disaccharide absorption[328]. Subsequent ITP studies have shown that rapamycin increases maximum lifespan in both male and female mice in a dose-dependent manner and slows multiple

aspects of aging in mice [141,143]. Several other compounds that have entered the ITP testing pipeline, however, have been shown to have no effect on maximum lifespan or only in one sex [140,151,329].

While these lifespan studies are by definition the gold standard for evaluating changes in lifespan, even when conducted in mice, they are very costly and can take 3 or more years to conduct. Therefore, a robust initial screening process to further refine which candidate interventions should be prioritized for inclusion into lifespan studies in mice represents an attractive strategy for accelerating the identification of interventions that extend maximum lifespan in mice and, therefore, may have the potential to extend healthspan in humans. An ideal initial screening process would be based on a panel of predictive markers of maximum lifespan extension, changes in which i) manifest soon after the initiation of an intervention, ii) are predictive of healthspan and maximum lifespan extension even at early time point measurements and iii) are not sex-, strain- or intervention-specific (**Fig 1**). Efforts to develop such a panel have been underway for over two decades.

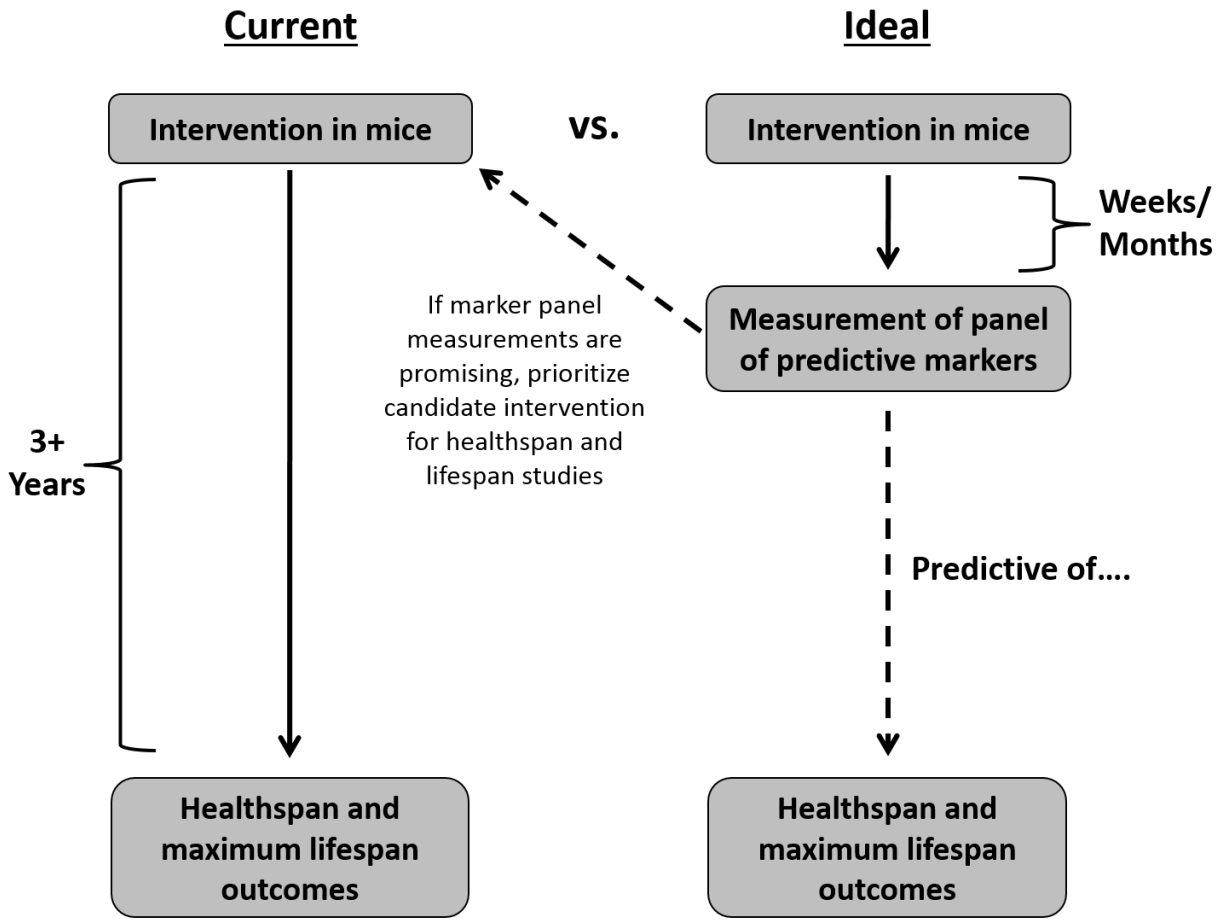

Figure 1: Current vs. ideal practices for screening and prioritizing candidate interventions with the potential to delay aging and extend healthspan and maximum lifespan in mice

In 1988, the NIA, in collaboration with the National Center for Toxicological Research (NCTR), initiated the "Biomarkers of Aging Program" designed to "identify and validate a panel of biomarkers of aging in rodents in order to rapidly test the efficacy and safety of interventions designed to slow aging"[254,255]. At the time, calorie restriction (CR), which is the reduction of caloric intake without malnutrition, was the only known intervention to reliably slow aging and extend maximum lifespan in rodents. Therefore, all rodents entered into the program, totally over 60,000 animals from 4 mouse and 3 rat strains, were fed either an *ad libitum* (AL) or CR diet. At ~6 month intervals, animals were sacrificed and all tissues were examined for the histological presence or absence of various degenerative, neoplastic or proliferative nonneoplastic lesions. Not surprisingly, the development of many lesions was found to increase with age and to be attenuated by CR[257,330]. Others have identified T-cell subsets that at middle age predict lifespan in genetically heterogeneous mice[262]. In addition, lifespan studies in 31 genetically-diverse inbred strains of mice conducted by the Jackson Aging Center revealed that longer-lived inbred strains of mice have lower circulating levels of insulin-like growth-1 (IGF-1) at 6 months of age (although this correlation disappeared when tested at 12 and 18 months of age)[152].

While these and other studies have provided invaluable insight into mammalian aging, none identified robust early predictors of maximum lifespan extension applicable across diverse genetic backgrounds and interventions. Moreover, no potentially translatable biomarkers into humans have been identified. Accordingly, the goal of the work presented here was to evaluate two putative predictive markers of maximum lifespan extension in three unique mouse models of maximum lifespan extension, in genetically diverse mice and at relatively early time points. The two putative predictive markers evaluated here were reduced *in vivo* cell proliferation rates and reduced *in vivo* protein synthesis rates.

A reduction in both of these processes may not only predict maximum lifespan extension but a growing body of evidence suggests that they may also be causally related to maximum lifespan extension. A reduction in cell proliferation rates is predicted to contribute to maximum lifespan extension by inhibiting the promotional phase of carcinogenesis and delaying cellular replicative senescence, thereby delaying the loss of cellular and tissue homeostasis that accompanies aging (**Fig 2**)[267]. CR, which robustly extends maximum lifespan in rodents, also leads to drastic reductions in global cell proliferation rates as well as the preservation of the proliferative capacity of many cell types later in life[99,224–228]. Additionally, numerous genetic mouse models of extended maximum lifespan are characterized by reduced levels of the mitogen IGF-1 and reduced tumor promotion[290,302–305]. In contrast, premature aging and shortened maximum lifespan are associated with early-life hyperproliferation and premature loss of the proliferative capacity of cells in both mice and humans[14,56,218].

A reduction in protein synthesis is predicted to contribute to maximum lifespan extension by preserving proteome homeostasis (proteostasis), which normally declines with age, thereby delaying the loss of cellular and tissue homeostasis that accompanies aging[20]. Proteostasis is achieved through protection against and/or efficient detection, repair and, if necessary, replacement of unfolded, damaged or otherwise abnormal proteins that, if left unchecked, might compromise cellular function[209,331]. A reduction in protein

synthesis rates may preserve proteostasis by limiting the accumulation of unfolded and damaged proteins by increasing chaperone capacity, proteolytic capacity, translational fidelity and by inducing the differential translational upregulation of mRNAs encoding proteins involved in somatic maintenance and stress responses, a phenomenon that occurs when global protein synthesis is inhibited and is regulated by unique 5' untranslated regions (5'UTR) sequences and internal ribosome entry sites (IRES) in some mRNAs (**Fig 2**)[183,332–337]. Consistent with this, numerous models of lifespan extension in yeast, worms, flies and mice are characterized by reduced signaling or expression of machinery involved in protein synthesis as well as enhanced expression of proteins involved in somatic maintenance and stress responses and, therefore, many of these models are resistance to various forms of stress[29,39,41,42,80,142]. In contrast, impaired protein quality control results in features of premature aging and shortened lifespan in mice[210].

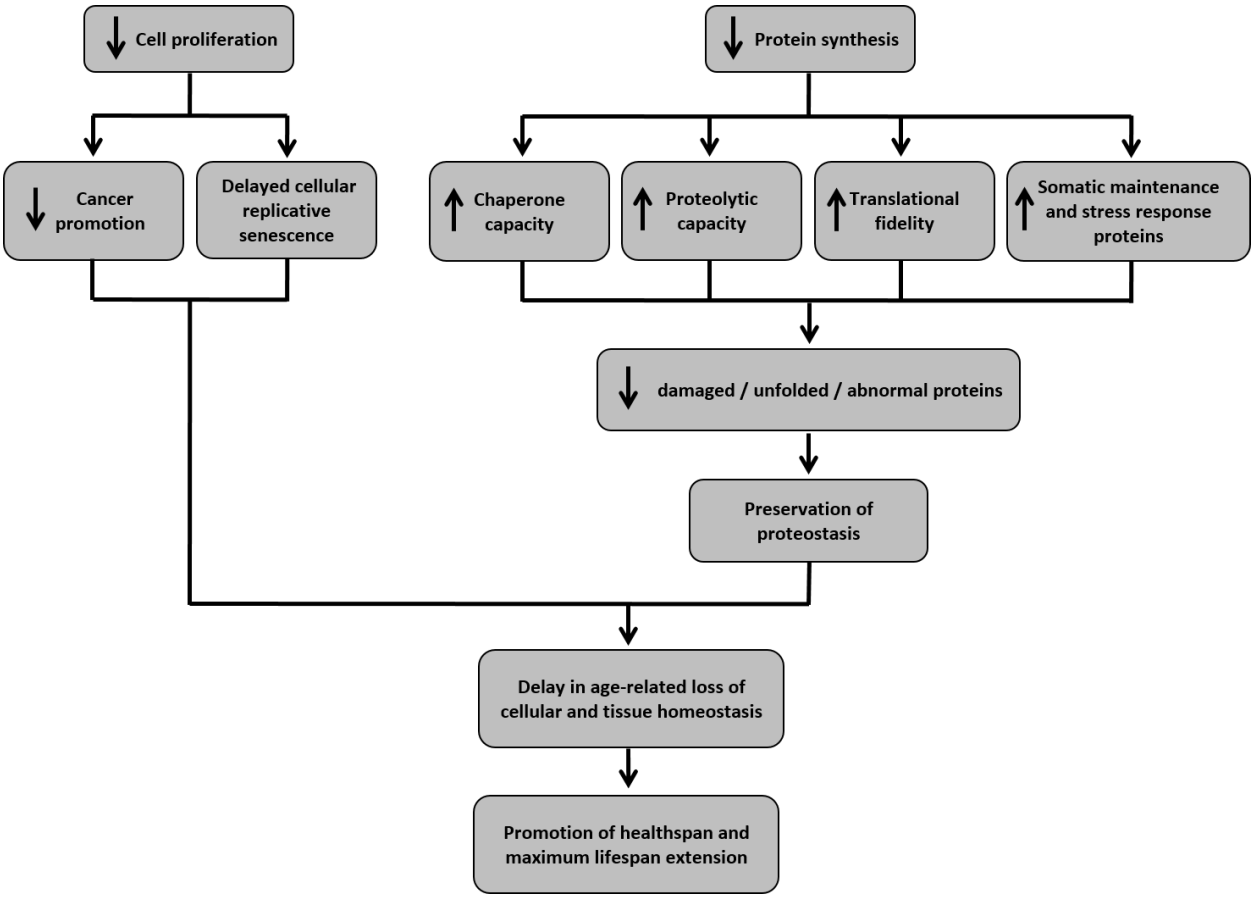

Figure 2: Model of predicted impact of reduced *in vivo* cell proliferation and protein synthesis on healthspan and maximum lifespan in mammals

To evaluate if reduced *in vivo* cell proliferation, reduced protein synthesis and/or other proteome alterations (like altered synthesis of a subset of proteins) are early predictors of maximum lifespan extension in mice, we conducted *in vivo* cell proliferation

and proteome dynamics analyses in three unique mouse models of extended maximum lifespan. Importantly, each model corresponds to a different genetic background of mice. The three models evaluated include: rapamycin treatment, CR and the Snell dwarf [65,140–142,338]. Snell dwarf mice are homozygous for a loss-of-function recessive mutation in the pituitary transcription factor 1 (Pit-1) gene involved in anterior pituitary gland development and, therefore, Snell dwarf mice are prolactin, thyroid stimulating hormone, growth hormone and consequently, IGF-1 deficient [62,63]. Similar to CR and rapamycin-treated mice, Snell dwarf mice exhibit reduced tumor burden as well as several features of delayed aging including a delay in age-related collagen cross-linking and immune system dysfunction [64,68].

In all three models, *in vivo* proliferation rates of keratinocytes, livers cells, mammary epithelial cells (females only) and splenic T-cells as well as the replacement rates, relative pool sizes and within proteome absolute synthesis rates of well over a hundred proteins were measured using a combination of stable heavy isotope labeling, gas and/or liquid chromatography and mass spectrometry. Details regarding the published percent maximum lifespan extension, groups, strain, sex, age at initiation of intervention, duration of intervention and duration of stable isotope labeling for each model for each type of study can be found in **Table 1** (**pg 98**). The cell proliferation data presented here for the CR model was adapted from a previous publication from our group[228]. Similarly, the proteome dynamics data presented here for the CR model was adapted from a previous publication from our group, however, the data reported here include an additional heavy water labeling time point, new protein pool size analyses and a detailed comparison of proteome dynamic alterations in rapamycin-treated, CR, and Snell dwarf mice[339].

Materials and Methods

Mice, husbandry, diets, feeding regimens and heavy water labeling durations

Rapamycin treatment model

The same genetically heterogeneous mouse strain (UM-HET3) and rapamycin-containing diets used in the ITP's lifespan studies were used in the studies presented here [140–142]. Specifically, 4-month-old female UM-HET3 mice (produced from a cross of BALB/cByJ 3 C57BL/6J F1 (CB6F1) females to C3H/ HeJ 3 DBA/2J F1 (C3D2F1) males) were used for all studies. Mice were housed 3-5 per cage. Following ~1 week of acclimation to the animal facility, mice were randomly assigned to diet groups. All mice were kept on their diets for a total of 4 months. The body weight of each mouse was measured once per week.

A total of two independent rapamycin intervention studies were conducted. In the first study, mice were randomly assigned to one of the following two groups: control diet or diet containing 14ppm rapamycin (Rapa (14ppm)). Mice in this study were labeled with heavy water for the last 2, 6, 18 or 24 days of the study. *In vivo* cell proliferation rates were measured in mice from this first study. Mice in this study labeled for 2 days were also used for the initial rapamycin *in vivo* hepatic proteome dynamics study. In the second study, mice were randomly assigned to one of the following four groups: control diet or diet

containing 4.7ppm (Rapa (4.7ppm)), 14ppm (Rapa (14ppm)) or 42 ppm (Rapa (42ppm)) rapamycin. Mice in this study were labeled with heavy water for the last 2 days of the study. Mice in this second study were used for the follow-up rapamycin dose-response *in vivo* hepatic proteome dynamics study.

CR model

For the *in vivo* cell proliferation rate study, 12-week-old male C57BL/6 mice from Charles River (Wilmington, MA) were used. All mice were housed individually. Following ~1 week of acclimation to the animal facility and the AIN-93M diet (Bio-Serv, Frenchtown, NJ), mice were randomly assigned to one of the following two groups: *ad libitum*-fed (AL) or calorie restricted (CR). Mice in the AL group were provided unrestricted access to the AIN-93M diet. Food intake was recorded for each AL mouse every other day. Mice in the CR group were provided with 75% of the average daily food intake of the AL group (from the previous 3 to 4 days) and, therefore, were 25% calorie restricted. CR mice were provided with food daily at 1200h. All mice in this study were kept on their diets for a total of 5 weeks. The body weight of each mouse was measured one to three times per week. Mice in this study were labeled with heavy water for the last 21 days of the study.

For the *in vivo* hepatic proteome dynamics study, 18-month-old male AL and CR C57BL/6 mice were purchased from Charles River (Wilmington, MA), where the NIA Caloric Restricted Mouse Colony is maintained. All mice were housed individually. Mice in the CR group had been on a 40% CR diet since 4 months of age. Mice in the AL group were provided unrestricted access to the NIH-31 diet. Mice in the CR group were provided with 3.0g of the NIH-31/NIA fortified diet daily at 1700hr. The body weight of each mouse was measured once per week. Mice in this study were labeled with heavy water for the last 1, 2, 4, 8, 15 or 32 days of the study.

Snell dwarf model

For all Snell dwarf studies, female heterozygous (Het), wild type (WT) or homozygous (dwarf) DW/J Snell mice were purchased from the NIA Mutant Mouse Aging Colony (Taconic line number 3623). Het and WT Snell mice are phenotypically indistinguishable and, therefore, were combined into one group, Het/WT. For all studies, two Het/WT mice were caged with two dwarf mice and mice were provided NIH-41 diet in pellet and powdered form (in a dish placed on top of the bedding in each cage). The body weight of each mouse was measured one to three times per week.

For the *in vivo* cell proliferation study, ~5- to 6-month old female Het/WT and Snell dwarf mice were used. Mice in this study were labeled with heavy water for the last 19 days of the study. For the *in vivo* hepatic proteome dynamics study, ~4.5- to 6-month old female Het/WT and Snell dwarf mice were used. Mice in this study were labeled with heavy water for the last 0, 1, 2, or 4 days of the study.

All mice in all studies were maintained under temperature- and light-controlled conditions (12:12-h light-dark cycle, lights on at 0700h and off at 1900h). All experiments were performed under the approval of the Institutional Animal Care and Use Committees of the University of California at Berkeley.

$^{2}H_2O$ labeling

In order to measure rates of *in vivo* DNA synthesis and protein replacement, mice were labeled with an intraperitoneal injection of 100% $^{2}H_2O$ (heavy water) (0.35ml/ 10g body weight) at the above specified times prior to the end of the study. Mice were then provided free access to 8% heavy water as drinking water for the remainder of the studies, as previously described [278].

Measurement of $^{2}H_2O$ enrichment in body water

Enrichment of $^{2}H_2O$ in body water (blood) was measured via chemical conversion to tetrabromoethane as previously described [339–341]. Briefly, body water was distilled from blood plasma by pipetting plasma into the caps of inverted tubes and placing these inverted tubes in a ~70-90°C bead bath for ~1hr. The hydrogen atoms in the distilled body water (composed of H_2O and $^{2}H_2O$) were transferred to acetylene via the addition of 2 to 5ul of distilled body water via a syringe to calcium carbide in a sealed vial equipped with a 10-ml syringe inserted into the septum. The resulting acetylene gas was drawn into the syringe and expelled into another sealed vial containing 0.42ml of 0.15M Br_2 (dissolved in CCl_4). After an overnight incubation at room temperature, the remaining Br_2 was reacted with 20ul cyclohexene (99% solution). Following the addition of 400ul ethyl acetate, samples were analyzed via GC-MS. GC-MS analysis was performed with a DB-225 30m column at 220°C using methane chemical ionization with selected ion monitoring. The $C_2H_2Br_3$ fragment (m/z 265 and 266, representing the M0 and the M1 mass isotopomers of the $^{79}Br^{79}Br^{81}Br$ isotopologue) was used for calculating ^{2}H enrichment by means of comparison to standard curves generated by mixing 100% $^{2}H_2O$ with natural abundance H_2O in known proportions. Body water $^{2}H_2O$ enrichment values (p) were used to calculate the fractional synthetic rate (f) of peptides as detailed in a subsequent section.

Blood. plasma and tissue collection and cell isolation

<u>Blood and plasma</u>

Upon completion of each study, mice were anesthetized under 3% isoflurane and blood was collected via cardiac puncture, followed by cervical dislocation, tissue collection and in some cases cell isolation. Following centrifugation of blood, plasma was collected and stored at -20°C.

<u>Keratinocytes</u>

After euthanasia, the back of each mouse was shaved followed by an application of Nair for complete hair removal (Carter Products, New York, NY, USA). A small (3cm^2) piece of the dorsal skin was dissected, washed with PBS (Gibco, Grand Island, NY, USA) and placed in 5mL PBS with 10 units of dispase II (Roche, Indianapolis, IN, USA). Dorsal skins were incubated for ~3 to 4hr with shaking at 100rpm at 37°C. The epidermis was then peeled from the dermis and collected for DNA isolation.

<u>Liver</u>

Upon dissection, the liver was cut into several small pieces (~20-100mg), which were flash frozen in liquid nitrogen. For DNA synthesis measurements, liver samples were

homogenized and total DNA from all liver cells was isolated. Preparation of liver samples for proteome dynamics analysis is described in a subsequent section.

Mammary epithelial cells

Mammary epithelial cells (MECs) were isolated using a protocol adapted from *Fata et al* [279]. Briefly, the 4L and 4R inguinal mammary glands were removed, placed in Dulbecco's Modified Eagle Medium (DMEM; Gibco, Grand Island, NY, USA) and minced. The minced tissue was incubated in 20mL collagenase/trypsin solution (0.2% Collagenase A, 0.2% Trypsin, 5% fetal bovine serum in DMEM) for 20min, shaking at 100 rpm at 37°C. Following digestion, the tissue suspension was centrifuged at 1500 rpm for 10min and the collagenase/trypsin solution and upper fat layer were discarded and the pellet was resuspended in 10mL DMEM. The suspension was pelleted via centrifugation at 1500 rpm for 10min, the DMEM solution and upper residual fat layer were discarded and the pellet was resuspended in 4mL DMEM containing 5ul DNase (≥500U/mL Sigma, D5319), shaken vigorously for 2min and then incubated at room temperature for 5min. 6mL of DMEM were added to the suspension, which was then pelleted via centrifugation at 1500 rpm for 10min. The DMEM/DNase solution was discarded and the pellet was resuspended in 10mL DMEM and the suspension was briefly centrifuged at 1500 rpm and the DMEM solution was discarded. The pellet was subjected to a total of three rounds of this brief differential centrifugation at 1500 rpm. The resulting pellet containing the MECs was then collected for DNA isolation.

Splenic T-cells

Upon dissection, the spleen was homogenized and passed through a 40μM nylon cell strainer. T-cells were isolated from the single cell suspension using mouse anti-CD90.2 microbeads and the MACS cell separation column following the manufacturer's instructions (Miltenyi Biotec, Auburn, CA, USA), pelleted and then collected for DNA isolation.

Bone marrow cells

Femurs were dissected for isolation of bone marrow cells. Bone marrow cells were flushed from the femurs with 2mL of PBS and were then pelleted and collected for DNA isolation.

DNA isolation

DNA was extracted using DNeasy kits (Qiagen, Valencia, CA, USA). Briefly, isolated keratinocytes, liver, MECs, T-cells and bone marrow cells were digested overnight at 37 °C in proteinase K solution followed by DNA isolation according to the manufacturer's instructions and elution into 200ul water.

Measurement of in vivo DNA synthesis

Determination of ^{2}H incorporation into purine deoxyribose (dR) of DNA was performed as previously described[278]. Briefly, isolated DNA was hydrolyzed overnight at 37°C with nuclease S1 and potato acid phosphatase. Hydrolyzates were reacted with pentafluorobenzyl hydroxylamine and acetic acid and then acetylated with acetic anhydride and *1*-methylimidazole. Dichloromethane extracts were dried, resuspended in

ethyl acetate and analyzed by GC-MS on a DB-17 column with negative chemical ionization using He as carrier and CH_4 as reagent gas. The enrichment of ^2H in purine dR was determined by measuring the fractional molar isotope abundances at m/z 435 (M0 mass isotopomer) and 436 (M1 mass isotopomer) of the pentafluorobenzyl triacetyl derivative of purine dR. Excess fractional M1 enrichment (EM1) was calculated as:

$$EM1 = \frac{(\text{abundance m/z } 436)_{\text{sample}}}{(\text{abundance m/z } 435 + 436)_{\text{sample}}} - \frac{(\text{abundance m/z } 436)_{\text{std}}}{(\text{abundance m/z } 435 + 436)_{\text{std}}}$$

where sample and standard (std) refer to the analyzed sample and an unenriched pentafluorobenzyl triacetyl purine dR derivative standard, respectively. The fractional synthetic rate (*f,* % new cells) of keratinocytes, liver cells, MECs and T-cells for each mouse was calculated by a comparison to bone marrow cells in the same animal, which represents an essentially fully turned over population of cells.

$$f\,(\%\text{ new cells}) = \frac{(EM1)_{\text{sample}}}{(EM1)_{\text{bone marrow}}}$$

The replacement rate (*k*, % new cells per day) was calculated as:

$$k\,(\%\text{ new cells per day}) = \frac{\ln(1-f)}{-t}$$

where t is the number of days a given mouse was labeled with heavy water.

Measurement of in vivo proteome dynamics

Sample preparation

-Liver protein preparation

Frozen livers from AL and CR mice labeled with heavy water for 1, 4, 8, 15, or 32 days were prepared and treated as previously described[339]. Frozen livers from AL and CR mice labeled with heavy water for 2 days as well as livers from mice in all rapamycin and Snell dwarf studies were homogenized in ~500ul lysis buffer (10mM Tris-base, 150mM NaCl, 1% NP-40, 0.1% SDS, 0.5% sodium deoxycholate, 1mM dithiothreitol (DTT), 1mM phenylmethylsulfonyl fluoride (PMSF), 7.5ug/mL leupeptin, 1.0ug/mL pepstatin, 2.0ug/mL aprotinin and 1 Phosphatase Inhibitor Cocktail 6t (Roche Applied Science, Indianapolis, IN) per 10mL buffer, pH ~7.5) using a stainless steel bead and a TissueLyserII (Retsch, Newtown, PA) set at 30hz for 1min. Tissue homogenates were sonicated in a sonication

bath for 1min and then centrifuged at 10,000 rcf at 4°C for 10min followed by supernatant collection. Protein concentrations were determined by bicinchoninic acid (BCA) assay (Pierce, Rockford, IL). 100-200ug of protein from these homogenates was uniformly reduced via incubation in 4.8mM tris(2-carboxyethyl)phosphine (TCEP) and SDS-PAGE sample loading buffer for 10min at 70°C. The reduced samples were then alkylated via incubation in 14.3mM iodoacetamide for 1hr in the dark at room temperature.

Proteins from all prepared homogenates were then fractionated by SDS-PAGE (Invitrogen, Grand Island, NY). Prior to blocking, all membranes were and incubated in ~15mL 0.1% Ponceau S (w/). Using in-gel molecular weight markers, each sample was divided into 10 molecular weight regions spanning from 3.5kDa to 160kDa. Select bands were then subjected to overnight trypsin digestion at 37°C (Trypsin Gold, Promega, Madison, WI) (see **Table 1** (**pg 98**) for kDa range analyzed for each study). The peptides from the resulting samples were extracted from the gel, dried, reconstituted in 5% acetonitrile/5% formic acid, and desalted using disposable C18 tips (spec-PT-C18, Fisher Scientific) according to the manufacturer's recommendations. Briefly, the tips were activated using methanol and then washed three times with 5% acetonitrile/5% formic acid, the extracted peptide solution was then passed through the tip, washing three times with 5% acetonitrile/5% formic acid between each pass of the sample. Desalted peptides were eluted from the tip using 80% acetonitrile/5% formic acid. The solvent was evaporated off in a SpeedVac, after which the sample was reconstituted in 25-50ul 0.1% formic acid/99.9% water for analysis via LC-MS.

The relative concentration of proteins in the liver was measured by comparison to exogenously labeled standards mixed into tissue homogenates (**S**table **I**sotope **LA**beling in **M**ammals, SILAM). The exogenously labeled standard was derived from the liver of a C57BL/6 mouse metabolically labeled with ^{15}N (MouseExpress Liver, Cambridge Isotope). Briefly, equal ug amounts of protein derived from the liver homogenates of mice in our studies and protein derived from the SILAM liver were combined prior to protein treatment, fractionation and LC-MS analysis.

-Plasma protein preparation

PMSF and ethylenediaminetetraacetic acid (EDTA) were added to thawed plasmas to a final concentration of 1mM and 3mM, respectively. Protein concentrations of plasmas were determined by BCA assay (Pierce, Rockford, IL). For each sample, 1mg of plasma was passed through a 0.22um filter via centrifugation at 1,000rcf for 1min and then immunodepleted of albumin, transferrin and IgG using the Multiple Affinity Removal System (MARS) Mouse-3 column following the manufacturer's instructions (Agilent, Santa Clara, CA). 20mM tris-HCL (pH ~7.4) was then added to immunodepleted plasmas at three times the volume of the immunodepleted plasmas. Samples were then concentrated to ~100ul via centrifugation at ~3,200rcf at 4°C for ~1-1.5hrs in spin concentrators with a molecular weight cutoff of 5kDa (Agilent, Santa Clara, CA). Protein concentrations of the immunodepleted/concentrated samples were then determined BCA assay (Pierce, Rockford, IL). ~60-250ug of protein was then dried to completion in a SpeedVac and placed at -20°C.

Thawed dried protein samples were then reconstituted, denatured and reduced in a solution containing 48mM ammonium bicarbonate (ABC), 47% trifluoroethanol (TFE)

(Sigma, St. Louis, MO) and 8.8mM DTT for 1hr at 60°C. The reduced samples were then alkylated via incubation in 16mM iodoacetamide for 1hr in the dark at room temperature. Samples were then diluted in ABC to a final concentration of ~25mM ABC and ~4.9% TFE. Samples were then subjected to an overnight in-solution trypsin digestion at 37°C with 1ug of trypsin (Sequencing Grade Modified Trypsin, Promega, Madison, WI) added per 50ug protein. Samples were then dried to completion in a SpeedVac and resuspended in 25-50ul of 0.1% formic acid/3% acetonitrile for analysis via LC-MS.

LC-MS analysis

In-gel digests were analyzed on either Agilent 6520 or 6550 QTOF (quadrupole time-of-flight) mass spectrometer. In-solution digests of plasma were analyzed on the higher-sensitivity Agilent 6550 QTOF mass spectrometer. Both instruments were fitted with a 1260 Chip Cube nano ESI source (Agilent Technologies, Santa Clara, CA, USA). Peptides were separated chromatographically using a Polaris HR chip (Agilent #G4240-62030) consisting of a 360 nL enrichment column and a 0.075 x 150 mm analytical column, each packed with Polaris C18-A stationary phase with 3 μm particle size. Mobile phases were (A) 5% v/v acetonitrile and 0.1% formic acid in deionized water and (B) 95% acetonitrile and 0.1% formic acid in deionized water. Peptides were eluted at a flow rate of 350 nL/min with either a 18 min gradient (gel bands) or a 60 min LC gradient (plasma in-solution digests). Each sample was analyzed twice, once for protein/peptide identification in data-dependent MS/MS mode and once for peptide isotope analysis in MS mode. In MS/MS mode, acquisition rates were 6 Hz for MS and 4 Hz for MS/MS with up to 6 precursors per cycle on 6520 QTOF and 20 precursors per cycle on 6550 QTOF. Acquisition rate in MS mode was 1 Hz on 6520 QTOF and 0.6 Hz on 6550 QTOF. Acquired MS/MS spectra were extracted and searched using Spectrum Mill Proteomics Workbench software (version B.04.00, Agilent Technologies, Santa Clara, CA, USA) and a UniProtKB/Swiss-Prot mouse protein database (16,473 proteins, UniProt.org, release 2012_02). Fixed modifications (carbamidomethylation of cysteine) and variable modifications (oxidized methionine, pyroglutamic acid, hydroxylation of proline) were enabled with up to two missed cleavages permitted. Search results were autovalidated with a global false discovery rate of 1%. Results were searched again allowing for non-specific cleavage of protein. A list of peptides with scores greater than 6 and scored peak intensities greater than 50% was exported from Spectrum Mill and condensed into a non-redundant peptide formula database using Excel. This database, containing peptide elemental composition, mass, and retention time was used to extract peptide mass isotope abundances (M0-M3) of each peptide from corresponding MS-only acquisition files with the Find-by-Formula algorithm in Mass Hunter (version B.05.00, Agilent Technologies, Santa Clara, CA, USA). Software developed at KineMed, Inc. was used to calculate peptide elemental composition and curve-fit parameters for determining peptide isotope enrichment (EM0) based on precursor $^{2}H_2O$ enrichment in body water (p) and the number (n) of amino acid C–H positions per peptide actively incorporating hydrogen (H) and deuterium (^{2}H) from body water. Subsequent data handling was performed using Microsoft Excel templates, with input of precursor $^{2}H_2O$ enrichment in body water (p) for each mouse, to yield fractional synthesis rate (FSR or *f*) data at the protein level. Details of FSR calculations and data filtering criteria have been described previously[342]. The kinetic data were filtered to

exclude protein measurements with fewer than two peptide isotope measurements per protein.

Calculation of replacement rate (k), relative pool size (RPS) and within proteome absolute synthesis rates (WPASR) for individual proteins

Protein replacement rates (*k* , % new protein per day) were calculated as:

$$k\ (\%\ \text{new protein per day}) = \frac{\ln(1\text{-}f)}{\text{-t}}$$

where t is the number of days a given mouse was labeled with heavy water. The relative pool size for each protein (RPS) in a given mouse was calculated as:

$$\text{RPS} = \text{Average L:H}$$

where L is the abundance of the light version of a given protein coming from our sample and H is the abundance of the heavy version of that same protein coming from the internal heavy SILAM standard.

For each study, if *k* (or RPS) data was derived for a given protein for both the control and the experimental group (defined as the longer-lived group in each of the three models), an average *k* (or RPS) value was calculated for that protein for each group. Proteins that failed to meet certain criteria were excluded from each study. These criteria included: i) identification of the protein in two or more mice per group, ii) a corresponding average *f* value of less than 0.75 and a coefficient of variation (CV%) for *k* (or RPS) data of less than 30% for each group and iii) a mean peptide count of two or more.

For those proteins for which both average *k* and RPS data was derived in both groups, the within proteome absolute synthesis rates of those proteins were calculated as:

$$\text{WPASR} = k_{\text{n}} \times \frac{\text{RPS}_{\text{n}}}{\text{RPS}_{\text{Control}}}$$

where n corresponds to the control or experimental group.

Western blot analysis

Frozen livers were homogenized in 350-400ul lysis buffer (10mM Tris-base, 150mM NaCl, 1% NP-40, 0.1% SDS, 0.5% sodium deoxycholate, 1mM DTT, 1mM PMSF, 7.5ug/mL leupeptin, 1.0ug/mL pepstatin, 2.0ug/mL aprotinin and 1 Phosphatase Inhibitor Cocktail

tablet (Roche Applied Science, Indianapolis, IN) per 10mL buffer, pH ~7.5) using a stainless steel bead and a TissueLyserII (Retsch, Newtown, PA) set at 30hz for 1 min. Tissue homogenates were tip-sonicated on ice for 3 x 15sec pulses at 10% amplitude with 10sec pauses in between pulses. Protein concentrations were determined by BCA assay (Pierce, Rockford, IL) and proteins were separated by SDS-PAGE (Invitrogen, Grand Island, NY). Prior to blocking, all membranes were incubated in ~15mL 0.1% Ponceau S (w/v) and 5.0% acetic Acid (w/v) for 15-20min. Membranes were then partially destained in dH_20 to bring out Ponceau S stained bands before imaging. Membranes were then completely distained via incubation in 0.1M NaOH for 30sec followed by 2 minutes of rinsing under running dH_2O. Following blocking, membranes were immunoblotted with glucose-regulated protein 78 (GRP78, also known as BiP), GRP94 and heat shock protein 90-β (Hsp90-β) (Cell Signaling, Danvers, MA) primary antibodies followed by incubation with IRDye®700DX-conjugated secondary antibodies (Rockland Immunochemicals Inc., Gilbertsville, PA). BiP, GRP94 and Hsp90-β protein bands were imaged and densitometry measurements were made using the Odyssey® Infrared Imaging System (LI-COR, Lincoln, NE). The total amount of protein loaded per lane was used as a loading control. Total protein per lane was quantified by taking densitometry measurements of Ponceau S staining for each lane using Image J (National Institutes of Health, Bethesda, Maryland).

Pathway analyses

An in-house Python script was developed to determine which Kyoto Encyclopedia of Genes and Genomes (KEGG) pathway (s) identified proteins mapped to[343,344].

Statistical analyses

Cell proliferation and western blot data are expressed as the mean ± SEM and Student's unpaired two-tailed *t*-tests were used for all between-group analyses. For pathway analyses, when WPASRs of proteins within a given pathway were compared between control and experimental groups, the data are expressed as the mean ± SEM and Student's paired two-tailed *t*-tests were used for all between-group analyses. When experimental WPASR to control WPASR ratios were compared between proteins mapping to a specified pathway and all other proteins, the data are expressed as the mean ± SEM and Student's unpaired two-tailed *t*-tests with Welch's correction were used for all between-group analyses. For correlation between % maximum lifespan extension vs. median experimental *k* to control *k* ratio for those proteins identified in all three models, a linear regression analysis was performed and a coefficient of determination value (R^2) and p value were determined. All data were analyzed by Prism Graphpad software (version 5.0a.

Results

In vivo cell proliferation rates

To determine the extent to which a reduction in *in vivo* cell proliferation may be an early predictor of maximum lifespan extension in mice, we measured changes in *in vivo* proliferation rates of keratinocytes, liver cells, MECs and splenic T-cells in rapamycin-treated, CR and Snell dwarf mice.

Cell proliferation rates were measured in 8-month-old female UM-HET3 mice after 4 months on either a control diet or a diet containing 14ppm rapamycin (Rapa (14ppm)). We found that there were no significant differences in the proliferation rates of any of cell type analyzed in Rapa (14ppm) compared to control mice, although there was a trend towards a reduction in the proliferation rates of splenic T-cells ($p < 0.12$)(**Fig 3A**). The lack of any significant effect of rapamycin treatment on the proliferation rates of any of the cell type analyzed was surprising given reports that rapamycin reduces the proliferation rates of numerous cell types including HepG2 liver cells, splenic T-cells *ex vivo* as well as heart and skeletal muscle cells *in vivo*[132,133,135–138,345]. The discrepancies between these previously published results and the results presented here may be due to differences in the dose and method of rapamycin administration, differences in the *in vitro/*ex vivo versus the *in vivo* effects of rapamycin as well as differences in the effect of rapamycin on various cell types. However, our observation that the *in vivo* proliferation rate of liver cells is unchanged in female UM-HET3 mice consuming a diet containing 14ppm rapamycin compared to control-fed mice is consistent with a previous report using a very similar study design[345].

Cell proliferation rates were measured in 3-month-old male C57BL/6 mice after 5 weeks on either an AL or 25% CR diet, as previously described[228]. Consistent with previous reports of the effects of CR on global cell proliferation rates, we found that the proliferation rates of keratinocytes, liver cells and splenic T-cells were significantly reduced in CR compared to AL mice (50.4%, 71.6% and 60.0% reduced, respectively)(**Fig 3B**) (no data on MEC).

Cell proliferation rates were measured in 6- to 7-month-old female Snell Het/WT and dwarf mice. We found that the proliferation rates of liver cells, MECs and splenic T-cells were significantly reduced in Snell dwarf compared to Het/WT mice (39.5%, 41.5% and 32.5% reduced, respectively). However, there was no difference in the proliferation rates of keratinocytes in Snell dwarf compared to Het/WT mice (**Fig 3C**).

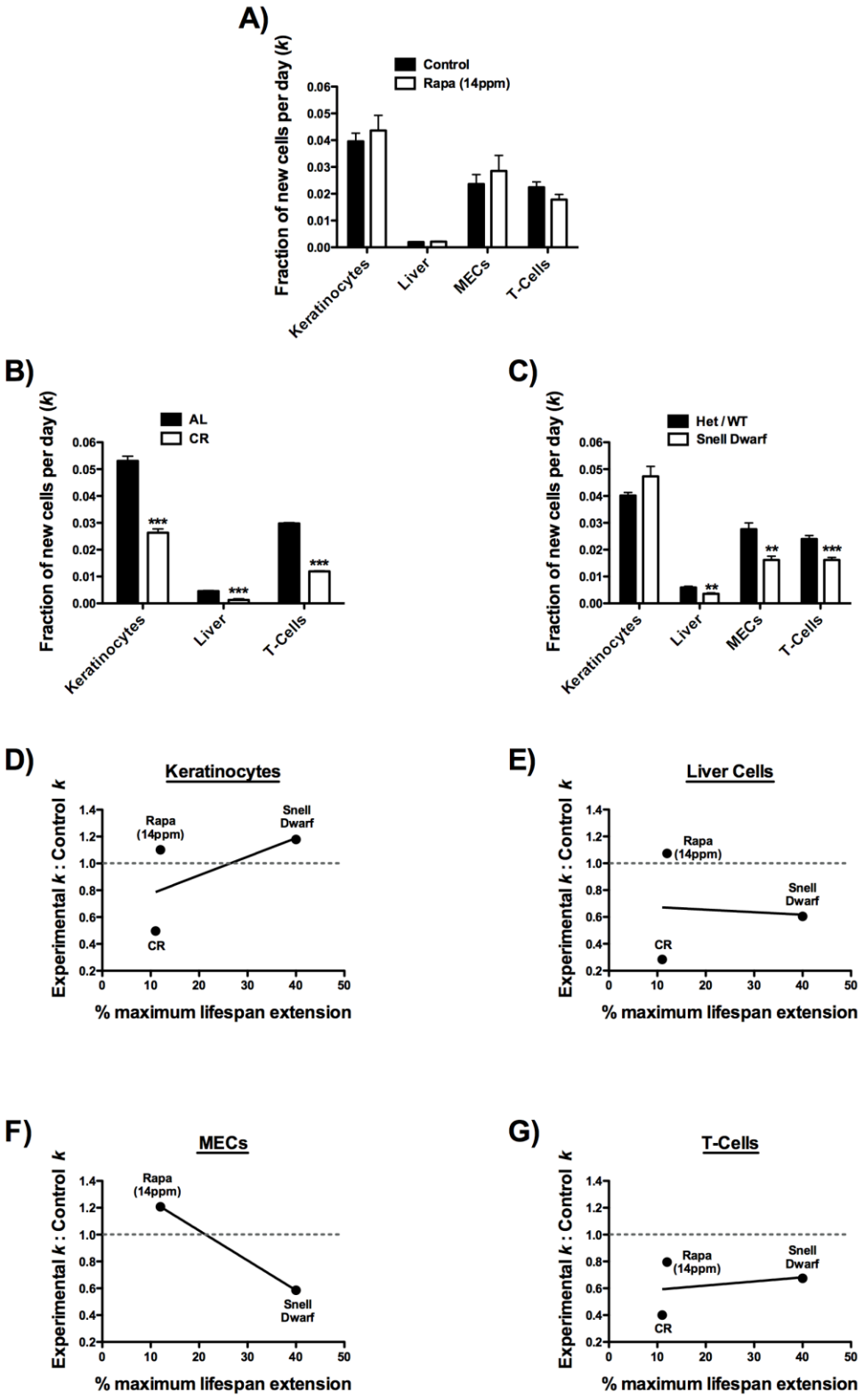

Figure 3: Global *in vivo* cell proliferation rates

Fraction of newly divided keratinocytes, liver cells, MECs and splenic T-cells per day (*k*) in A) control vs. Rapa (14ppm) (n = 5-12 per group), B) AL vs. CR (no MEC data) (n = 2-5 per group) and C) Snell Het/WT vs. dwarf mice (n = 5-6 per group). Values are expressed as the mean ± SEM. Student's unpaired two-tailed *t*-tests were used for all between-group analyses (** $p < 0.003$, *** $p < 0.0008$). % maximum lifespan extension vs. experimental *k* : control *k* ratio for for D) keratinocytes, E) liver cells, F) MECs and G) splenic T-cells. % maximum lifespan extension in CR model estimated to be 11%.

Together the data from these three models suggest that a reduction in *in vivo* cell proliferation rates is not a consistent or sensitive early predictor of maximum lifespan extension in mice. Treatment of mice with 14ppm rapamycin had no effect on the proliferation rates of any of the cell types analyzed and there was no effect on the proliferation rates of keratinocytes in Snell dwarf mice, despite the well-documented increase in maximum lifespan in rapamycin-treated and Snell dwarf mice compared to their control counterparts[65,140–142].

It is important to note that an increase in maximum lifespan has not been documented for the specific CR regimen and diet used for the cell proliferation studies presented here. However, 40% CR started at 4 months of age increases maximum lifespan by 18% in the same strain of mice used in the present study[338]. Therefore, based on reports that CR increases maximum lifespan in a dose-dependent manner, it is reasonable to assume that the 25% CR regimen used for the cell proliferation studies present here would increase maximum lifespan by no more than 18%, and likely by less[346]. Estimating an 11% extension in maximum lifespan in response to the 25% CR regimen used here, we found that there was no correlation between the degree of maximum lifespan extension across the three models and changes in the proliferation rates of any of the four cell types analyzed (**Fig 3D-G**).

In vivo hepatic proteome dynamics

To determine the extent to which a general reduction in *in vivo* protein synthesis and/or alterations in the synthesis of subsets of related proteins may be early predictors of maximum lifespan extension in mice, we measured changes in *in vivo* hepatic proteome dynamics in rapamycin-treated, CR and Snell dwarf mice. To capture changes in both the replacement rates (*k*) and relative pool sizes (RPS) of individual proteins, we combined heavy water labeling, SILAM and LC-MS/MS. We also calculated the within proteome absolute synthesis rates (WPASR) for those proteins for which both *k* and RPS data were derived.

Hepatic proteome dynamic analyses were initially conducted in 8-month-old female UM-HET3 mice after 4 months on either a control diet or a diet containing 14ppm rapamycin (Rapa (14ppm)). We determined *k* values for 270 proteins and RPS values for 254 proteins in both control and Rapa (14ppm) mice. We also calculated WPASR values for the 199 proteins for which we derived both *k* and RPS data. Defining a change as plus or minus 10% of control, we found that 32.6% of the identified proteins exhibited a reduction in *k* while only 10.4% were increased in Rapa (14ppm) compared to control mice. 10.2% of the identified proteins exhibited a reduction in RPS while 31.9% were increased in Rapa (14ppm) compared to control mice. Surprisingly, we found that the percentage of

identified proteins that exhibited a reduction in WPASR in Rapa (14ppm) compared to control mice was very similar to the percentage that were increased, with 24.6% exhibiting a reduction in WPASR and 27.7% exhibiting an increase (**Fig 4A-C and Table 2** (**pg 99**)). The median Rapa (14ppm) WPASR to control WPASR ratio was 0.994, suggesting that the overall rate of hepatic protein synthesis is unchanged in response to rapamycin treatment. A study by another group using a different treatment regimen also found that chronic rapamycin treatment has no effect on hepatic protein synthesis in mice, as measured by ribosome activity[347]. This is in contrast to acute rapamycin treatment, which reduces *in vivo* hepatic protein synthesis in mice and reduces protein synthesis *in vitro* in mouse embryonic fibroblasts (MEFs)[180,347].

In the study presented here, while there was no effect of chronic rapamcyin treatment on the overall rate of hepatic protein synthesis, protein replacement rates were affected. The median Rapa (14ppm) *k* to control *k* ratio was 0.945, consistent with a modest but general reduction in hepatic protein replacement rates in response to chronic rapamycin treatment (**Table 2** (**pg 99**)). This finding in the liver is consistent with the *in vivo* effects of chronic 14ppm rapamycin treatment on global skeletal muscle protein replacement rates (as measured by alanine turnover), which are reduced by ~9% in rapamycin-treated compared to control mice[345]. Our finding is also consistent with the *in vivo* effects of 10 weeks of 14ppm rapamycin treatment in old mice (27mn) on global cardiac protein replacement rates (as measured by deuterated-leucine labeling), which are reduced by ~10% in rapamycin-treated compared to control mice[348].

Hepatic proteome dynamic analyses were conducted in 18-month-old male C57BL/6 mice after 14 months on either an AL or 40% CR diet. Data from these AL and CR mice were reported previously, however, the data presented here include an additional heavy water labeling time point (2 days) as well as a new SILAM analysis[339]. We determined *k* values for 98 proteins and RPS values for 242 proteins in both AL and CR mice. We also calculated WPASR values for the 84 proteins for which we derived both *k* and RPS data. We found that 60.2% of the identified proteins exhibited a reduction in *k* while only 1.0% were increased in CR compared to AL mice. 38.0% of the identified proteins exhibited a reduction in RPS while 19.8% were increased in CR compared to AL mice. We also found that 72.6% of the identified proteins exhibited a reduction in WPASR while just 4.8% were increased in CR compared to AL mice (**Fig 4D-F and Table 2** (**pg 99**)). The median CR WPASR to AL WPASR ratio was 0.818 and the median CR *k* to AL *k* ratio was 0.859, suggesting that the overall rates of both hepatic protein synthesis and protein replacement are reduced in response to CR (**Table 2** (**pg 99**)). Our findings are consistent with the *in vivo* effects of 10 weeks of 40% CR in old mice (27mn) on global cardiac protein replacement rates (as measured by deuterated-leucine labeling), which are reduced by ~23% in CR compared to AL mice[348]. However, our findings are in contrast to previous studies in rats and isolated hepatocyte which report that both protein synthesis and replacement rates become higher with age in CR compared to AL controls[349–351].

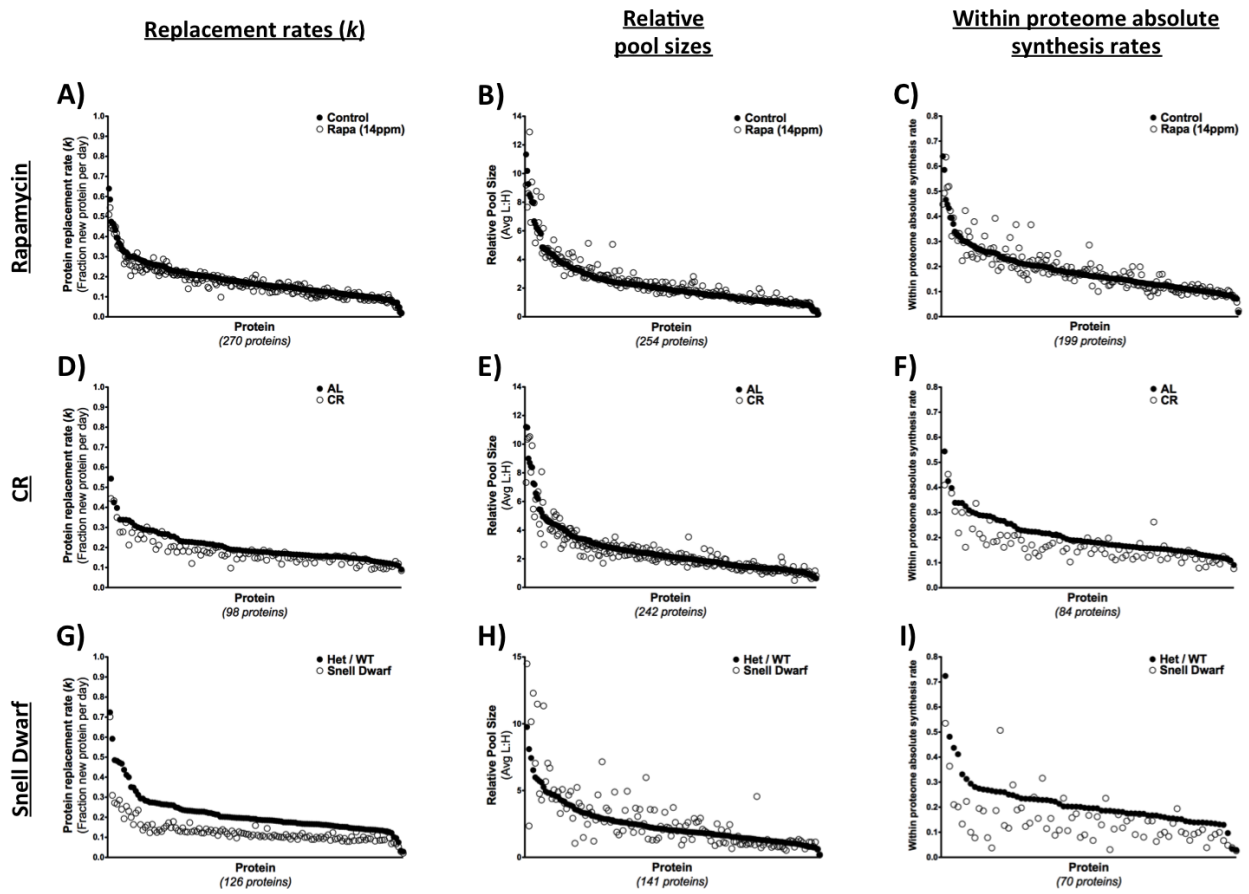

Figure 4: *In vivo* hepatic proteome dynamics

Replacement rates (*k*), relative pool sizes (RPS) and within proteome absolute synthesis rates (WPASR) of hepatic proteins in A-C) control vs. Rapa (14ppm) (n = 2-3 per group), D-F) AL vs. CR (n = 2-12 per group) and G-I) Snell Het/WT vs. dwarf mice (n = 2-6 per group). For each model, each vertical pair of solid and open symbols represents the mean *k*, RPS or WPASR value for an individual protein in the control and experimental group, respectively (where the experimental group refers to the longer-lived group within each model). For clarity, protein names are not listed and proteins are sorted in descending order based on control group values.

Hepatic proteome dynamic analyses were also conducted in 5.5- to 7-month-old female Snell Het/WT and dwarf mice. We determined *k* values for 126 proteins and RPS values for 141 proteins in both Het/WT and dwarf mice. We also calculated WPASR values for the 70 proteins for which we derived both *k* and RPS data. We found that almost all (97.6%) of the identified proteins exhibited a reduction in *k* while no proteins were increased in Snell dwarf compared to Het/WT mice. 35.5% of the identified proteins exhibited a reduction in RPS while 40.4% were increased in Snell dwarf compared to Het/WT mice. Lastly, we found that 86.0% of the identified proteins exhibited a reduction in WPASR while 10.0% were actually increased in Snell dwarf compared to Het/WT mice

(**Fig 4G-I and Table 2** (**pg 99**)). The median dwarf WPASR to Het/WT WPASR ratio was 0.671 and the median dwarf *k* to Het/WT *k* ratio was 0.591, suggesting that the overall rates of both hepatic protein synthesis and protein replacement are drastically reduced in Snell dwarf compared to Het/WT mice (**Table 2** (**pg 99**)). These findings are consistent with reports of reduced translation initiation signaling and reduced global rates of hepatic protein synthesis and replacement, as measured by [4-^{3}H]-phenylalanine incorporation, in Snell dwarf compared to WT mice[352,353].

It is possible that the overall global reduction in hepatic protein synthesis observed in CR and Snell dwarf mice was a consequence of an accumulation of unfolded proteins in these mice leading to a global suppression of protein synthesis, rather than a consequence of a general decrease in protein synthetic burden[205]. Therefore, we measured via western blot the levels of several chaperones in the livers of these mice including BiP (also known as glucose-regulated protein 78 (GRP78)) and GRP94, both of which reside in the endoplasmic reticulum (ER), as well as heat shock protein 90-β (Hsp90-β), which resides in the cytosol. The function of these chaperones is to facilitate the proper folding of proteins and in the context of an accumulation of unfolded proteins, the levels of these chaperones would be expected to increase[354,355]. We found that the levels of BiP were reduced while the levels of GRP94 were unchanged in CR compared to AL mice, consistent with previous findings (**Fig 5D,E**)[356]. Hsp90-β levels were also unchanged in CR compared to AL mice (**Fig 5F**). We found that the levels of BiP, GRP94 and Hsp90-β were all reduced in Snell dwarf compared to Het/WT mice (**Fig 5G-I**). These data suggest that the overall global reduction in hepatic protein synthesis in CR and Snell dwarf mice is not a consequence of an accumulation of unfolded proteins in these mice. We also found that the levels of BiP and Hsp90-β were unchanged, while the levels of GRP94 were reduced in Rapa (14ppm) compared to control mice (**Fig 5A-C**).

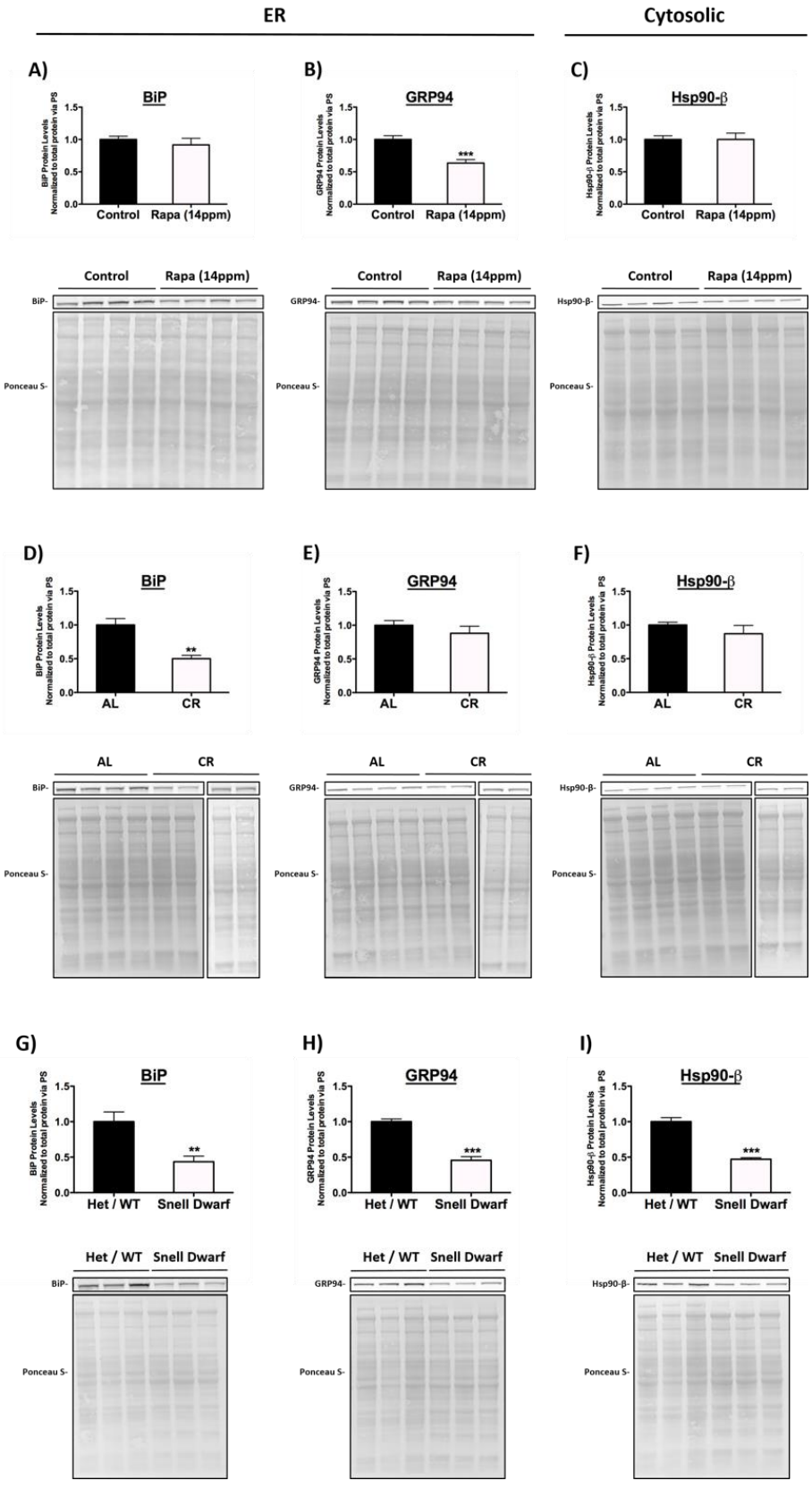
ER
Cytosolic
A)
BiP
BiP Protein Levels Normalized to total protein via PS
Control
Rapa (14ppm)
B)
GRP94
GRP94 Protein Levels Normalized to total protein via PS
***
C)
Hsp90-β
Hsp90-β Protein Levels Normalized to total protein via PS
BiP-
GRP94-
Hsp90-β-
Ponceau S-
D)
**
AL
CR
E)
F)
G)
Het / WT
Snell Dwarf
H)
I)

Figure 5: Chaperone levels in the liver

Western blot images, Ponceau S (PS) stain images and corresponding normalized densitometry for levels of hepatic BiP, GRP94 and Hsp90-β in A-C) control vs. Rapa (14ppm) (n = 8-12 per group), D-F) AL vs. CR (n = 4-8 per group) and G-I) Snell Het/WT vs. dwarf mice (n = 5-6 per group). Total protein within a given lane, as determined by PS staining, was used as the loading control. Values are expressed as the mean ± SEM. Student's unpaired two-tailed *t*-tests were used for all between-group analyses (** $p < 0.006$, *** $p < 0.0001$).

Next we determined if the overall synthesis (WPASR) of any subset of related proteins was reduced in all three models. We found that the WPASR of only those proteins involved in protein processing in the ER (PPER) were reduced in all three models, although this reduction did not reach statistical significance in Rapa (14ppm) compared to control mice ($p = 0.077$)(**Fig 6A-C**). Importantly, we found that in all three models the WPASR of PPER proteins was reduced to an even greater extent than the WPASR of all other identified proteins (**Fig 6D-F**). These findings are consistent with our western blot data showing that the levels of ER chaperones tend to be reduced in all three models. These data suggest that the demand for the machinery involved in protein folding and quality control in the ER are reduced in all three models. This could potentially be due to a general reduction in protein synthetic burden in the ER or a more efficient folding environment in the ER. Overall our finding that the synthesis of PPER proteins is reduced in all three models is consistent with conserved transcriptional changes in worm, fly and other mouse models of extended maximum lifespan, which include reduced transcription of genes encoding proteins involved in protein biosynthesis[39].

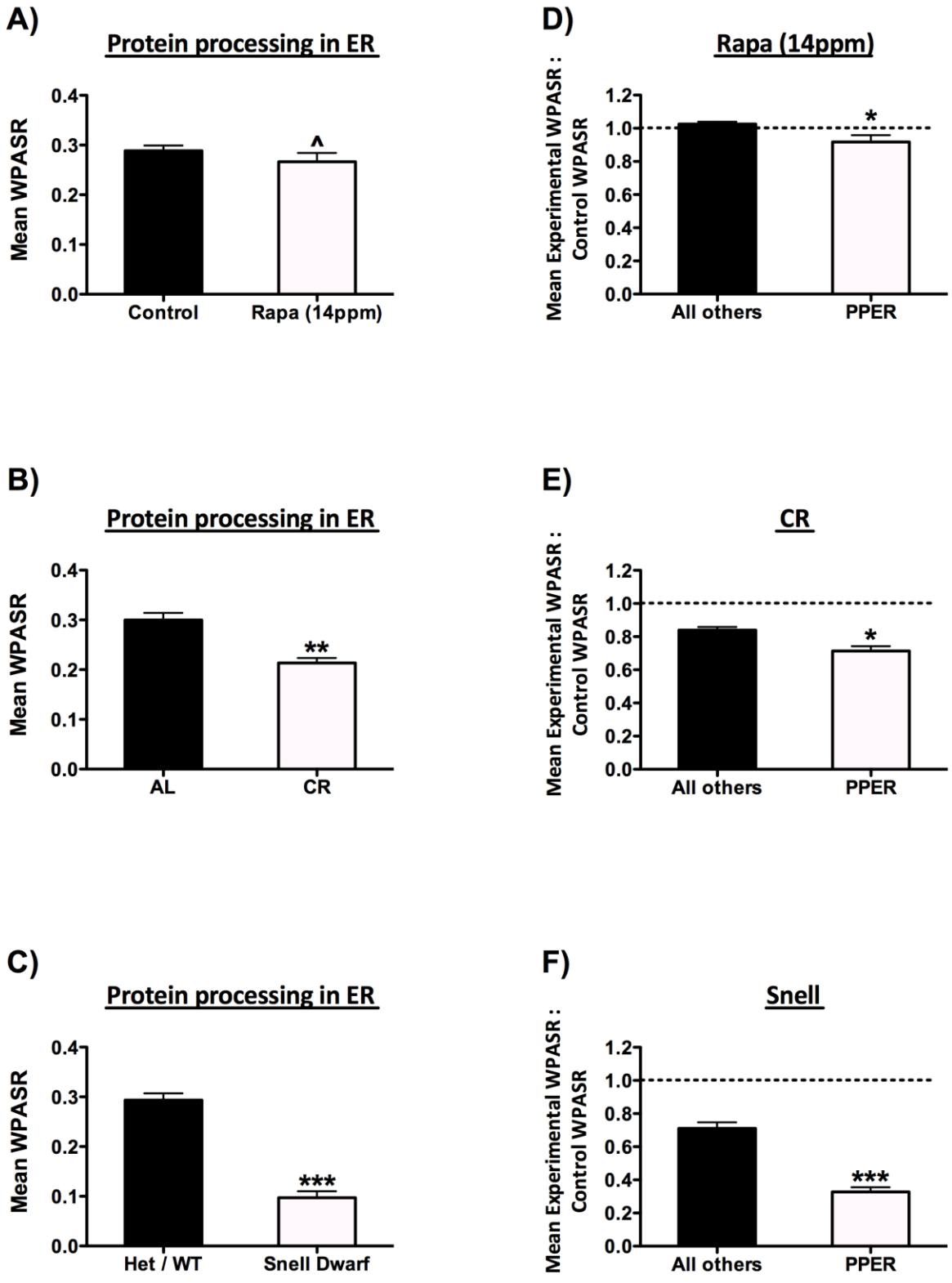

Figure 6: Hepatic synthesis of proteins involved in protein processing in the ER (PPER)

Within proteome absolute synthesis rate (WPASR) of proteins involved in PPER in A) control vs. Rapa (14ppm) (n = 3 per group, total of 11 PPER proteins), B) AL vs. CR (n = 4-9 per group, total of 4 PPER proteins) and C) Snell Het/WT vs. dwarf mice (n = 3-6 per group, total of 4 PPER proteins). Values are expressed as the mean ± SEM. Student's paired two-tailed *t*-tests were used for all between-group analyses (^ $p = 0.077$, ** $p < 0.006$, *** $p < 0.0001$). Experimental WPASR to control WPASR ratio (where the experimental group refers to the longer-lived group within each model) for proteins involved in PPER compared to all other proteins identified in the D) Rapa (14ppm) (total of 11 PPER proteins and 188 other proteins), E) CR (total of 4 PPER proteins and 80 other proteins) and F) Snell dwarf models (total of 4 PPER proteins and 66 other proteins). Values are expressed as the mean ± SEM. Student's unpaired two-tailed *t*-tests with Welch's correction were used for all between-group analyses (* $p < 0.028$, *** $p < 0.0001$). PPER proteins identified include: 78 kDa glucose-regulated protein (UniProt accession #P20029, identified in Rapa (14ppm), CR and Snell dwarf models), 94 kDa glucose-regulated protein (UniProt accession #P08113, identified in Rapa (14ppm) model), Glucosidase 2 subunit beta (UniProt accession #O08795, identified in Rapa (14ppm) model), Heat shock cognate 71 kDa protein (UniProt accession #P63017, identified in Rapa (14ppm), CR and Snell dwarf models), Heat shock protein HSP 90-alpha (UniProt accession #P07901, identified in Rapa (14ppm) model), Heat shock protein HSP 90-beta (UniProt accession #P11499, identified in Rapa (14ppm) model), Hypoxia up-regulated protein 1 (UniProt accession # Q9JKR6, identified in Rapa (14ppm) model), Neutral alpha-glucosidase AB (UniProt accession #Q8BHN3, identified in Rapa (14ppm) model), Protein disulfide-isomerase (UniProt accession # P09103, identified in Rapa (14ppm), CR and Snell dwarf models), Protein disulfide-isomerase A3 (UniProt accession #P27773, identified in Rapa (14ppm), CR and Snell dwarf models) and Transitional endoplasmic reticulum ATPase (UniProt accession #Q01853, identified in Rapa (14ppm) model).

Next we determined if the overall synthesis (WPASR) of any subset of related proteins was increased in all three models. While we did not identify any subset of related proteins for which the WPASR was increased in all three models, we did find a striking increase in or preservation of the WPASR of glutathione S-transferases (GSTs). We found that the WPASR of GSTs was increased in Rapa (14ppm) compared to control mice and that there was a trend towards an increase in CR compared to AL mice (**Fig 7A,B**). Importantly, we found that the WPASR of GSTs was greater than the WPASR of all other proteins identified in Rapa (14ppm) and Snell dwarf mice, while there was a trend towards a greater WPASR of GSTs compared to all other proteins identified in CR mice ($p = 0.167$)(**Fig 7D-F**). GSTs play critical protective roles within cells by inactivating molecules capable of damaging various cellular components including proteins. These damaging molecules include electrophilic xenobiotics as well as endogenously produced α,β-unsaturated aldehydes, quinones, epoxides and hydroperoxides formed as secondary metabolites during oxidative stress[357]. Our finding that the synthesis of GST proteins is either increased or preserved in all three models is consistent with previous reports of increased GST mRNA expression in Snell dwarf mice and attenuated age-related decline in GST mRNA expression in CR rodents[358–360]. Our findings are also consistent with conserved transcriptional changes in worm, fly and other mouse models of extended maximum lifespan, which include increased transcription of genes encoding GSTs[39]. This finding also

suggests that damage to cellular components, including proteins, may be reduced in the Rapa (14ppm), CR and Snell dwarf mice used in our studies, something that has been previously reported in Snell Dwarf mice and CR rodents, although differences in protein damage in AL compared to CR rodents may depend on the cellular fraction (soluble or insoluble) assayed[64,361–363]. Consistent with this, the common global hepatic proteome alteration in all three models was a reduction in protein replacement rates, which may reflect a general reduction in the demand for protein renewal, possibly due to reduced protein damage.

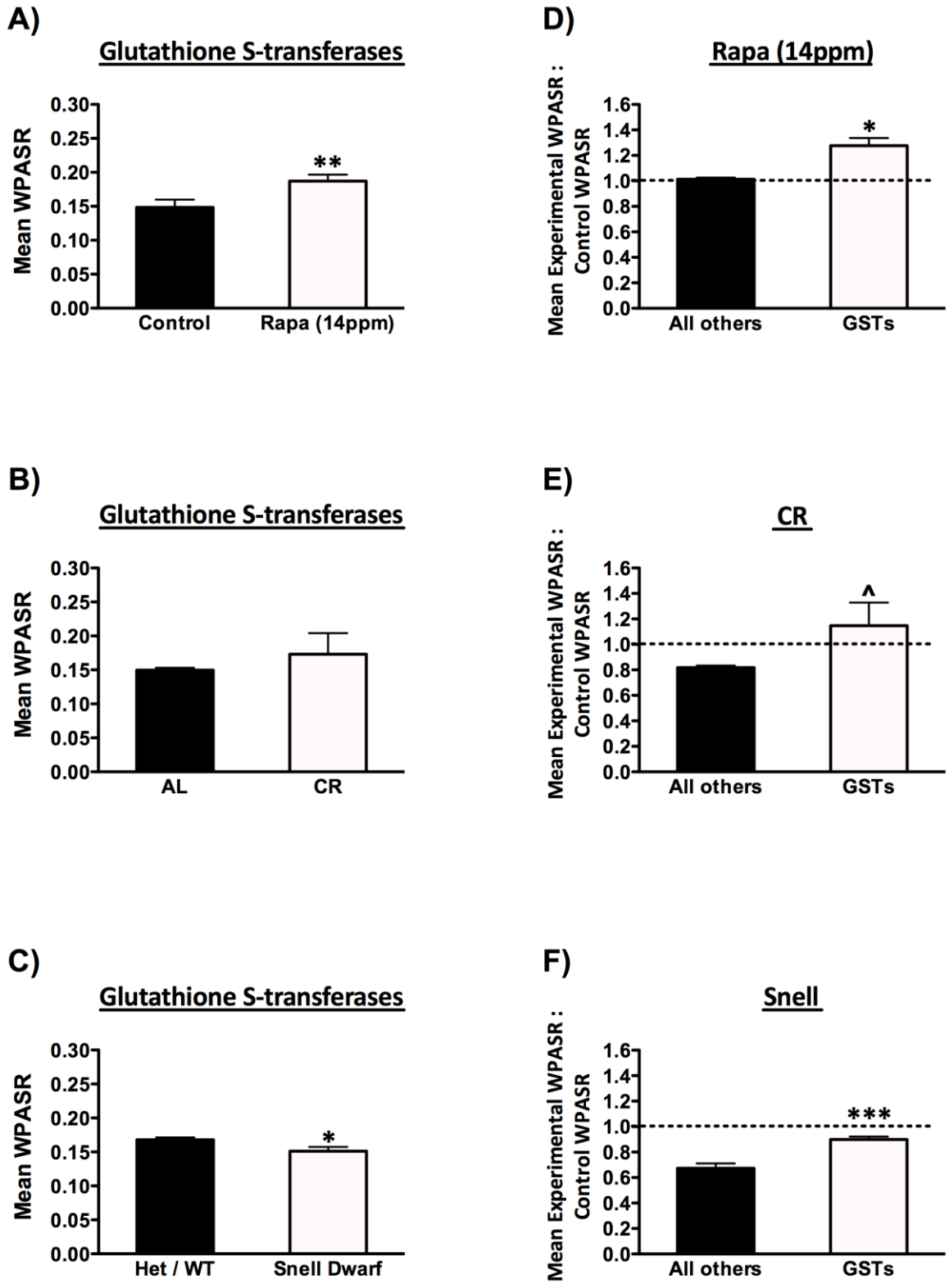

Figure 7: Hepatic synthesis of glutathione S-transferase (GST) proteins

Within proteome absolute synthesis rate (WPASR) of GSTs in A) control vs. Rapa (14ppm) (n = 2-3 per group, total of 5 GSTs), B) AL vs. CR (n = 3-10 per group, total of 4 GSTs) and C) Snell Het/WT vs. dwarf mice (n = 2-4 per group, total of 5 GSTs). Values are expressed as the mean ± SEM. Student's paired two-tailed *t*-tests were used for all between-group analyses (* $p < 0.011$, ** $p < 0.006$). Experimental WPASR to control WPASR ratio (where the experimental group refers to the longer-lived group within each model) for GSTs compared to all other proteins identified in the D) Rapa (14ppm) (total of 5 GST proteins and 194 other proteins), E) CR (total of 4 GST proteins and 80 other proteins) and F) Snell dwarf models (total of 5 GST proteins and 65 other proteins). Values are expressed as the mean ± SEM. Student's unpaired two-tailed *t*-tests with Welch's correction were used for all between-group analyses (^ $p = 0.167$, * $p < 0.013$, *** $p < 0.0001$). GST proteins identified include: Glutathione S-transferase A1 (UniProt accession #P13745, identified in CR and Snell dwarf models), Glutathione S-transferase A3 (UniProt accession #P30115, identified in Rapa (14ppm), CR and Snell dwarf models), Glutathione S-transferase A4 (UniProt accession #P24472, identified in Rapa (14ppm) model), Glutathione S-transferase Mu 1 (UniProt accession #P10649, identified in Rapa (14ppm), CR and Snell dwarf models), Glutathione S-transferase Mu 2 (UniProt accession #P15626, identified in Rapa (14ppm) and Snell dwarf models), Glutathione S-transferase Mu 7 (UniProt accession #Q80W21, identified in Snell dwarf model) and Glutathione S-transferase P 2 (UniProt accession #P19157, identified in Rapa (14ppm) and CR models).

By comparing the 54 proteins for which we derived replacement rate data for in all three models, we found a striking correlation between the degree of maximum lifespan extension and the degree of hepatic protein replacement rate reduction. We found that the degree of hepatic protein replacement rate reduction was smallest in response to 14ppm rapamycin treatment, which increases maximum lifespan by 12%, and greatest in Snell dwarf mice which live 40% longer than their Het/WT counterparts, while hepatic protein replacement rates were reduced to an intermediate level, in response to CR which increases maximum lifespan by 18% (**Fig 8**)[65,140–142,338]. These data suggest that a reduction in hepatic protein replacement rates, but not overall absolute protein synthesis rates, may be a sensitive and early predictor of maximum lifespan extension in mice.

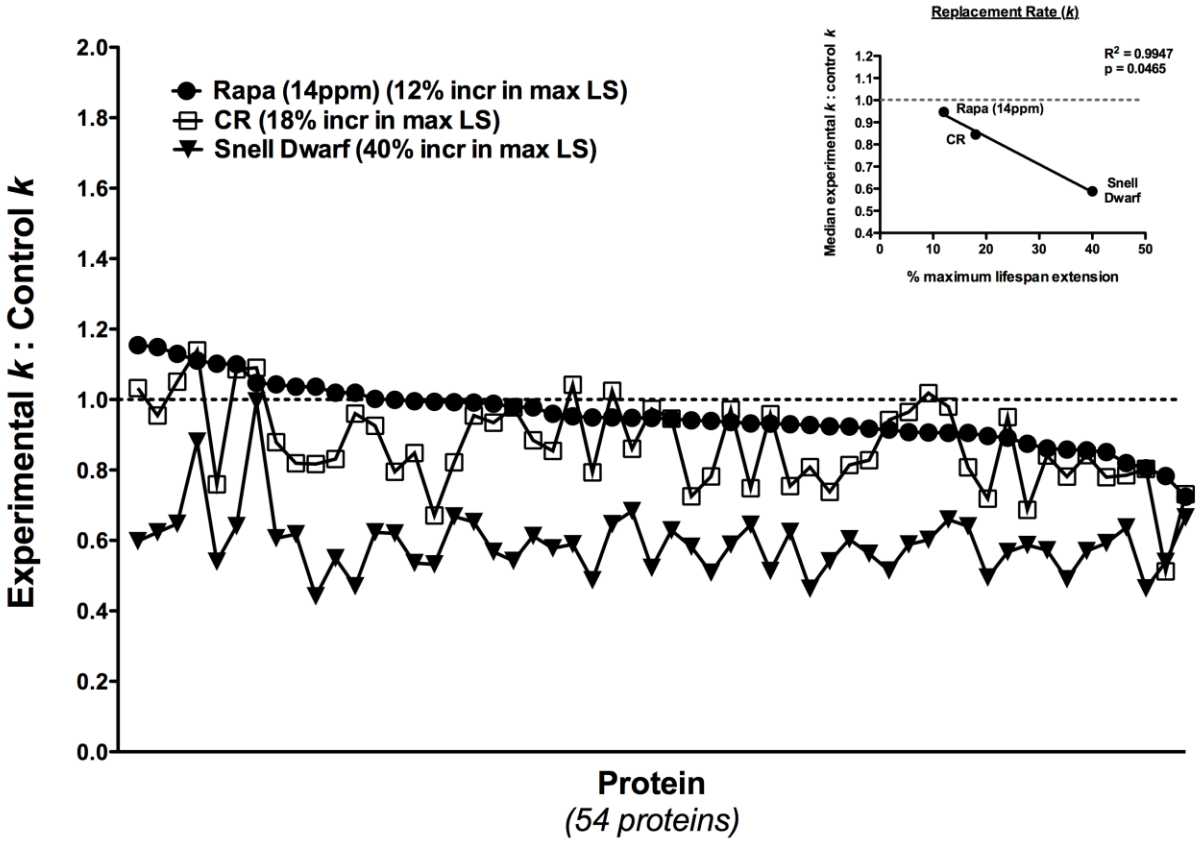

Figure 8: Comparison of the degree of change in the replacement rates (*k*) of hepatic proteins identified in all three models

Experimental *k* to control *k* ratio (where the experimental group refers to the longer-lived group within each model) of each of the 54 proteins identified in all three models. Each symbol represents the mean experimental *k* : control *k* ratio for a given protein in a given model. For clarity, proteins are sorted in descending order based on Rapa (14ppm) model values. The number in parentheses represents the % maximum lifespan extension in each model. Inset: % maximum lifespan extension vs. median experimental *k* : control *k* ratio for only those proteins identified in all three models. R^2 and p values were derived from linear regression analyses.

To test this hypothesis further, we measured hepatic protein replacement rates in response to three different doses of rapamycin. A recent ITP study found that rapamycin treatment extends maximum lifespan in mice in a dose-dependent manner at doses of 4.7ppm to 14ppm but that there is no additional extension of maximum lifespan at 42ppm relative to 14ppm rapamycin (**Fig 9A**)[141]. The question we were specifically addressing in this study was whether changes in hepatic protein replacement rates were predictive of the degree of maximum lifespan extension at these different doses of rapamycin. Strikingly, we found that, indeed, the degree of hepatic protein replacement rate reduction would have predicted the degree of maximum lifespan extension in response to these three different doses of rapamycin. We found that while hepatic protein replacement rates were reduced

in a dose-dependent manner at the 4.7ppm and 14ppm doses, there was essentially no additional reduction in hepatic protein replacement rates in response to 42ppm relative to 14ppm rapamycin (**Fig 9B**). These data provide additional evidence that a reduction in hepatic protein replacement rates may be a sensitive and early predictor of maximum lifespan extension in mice.

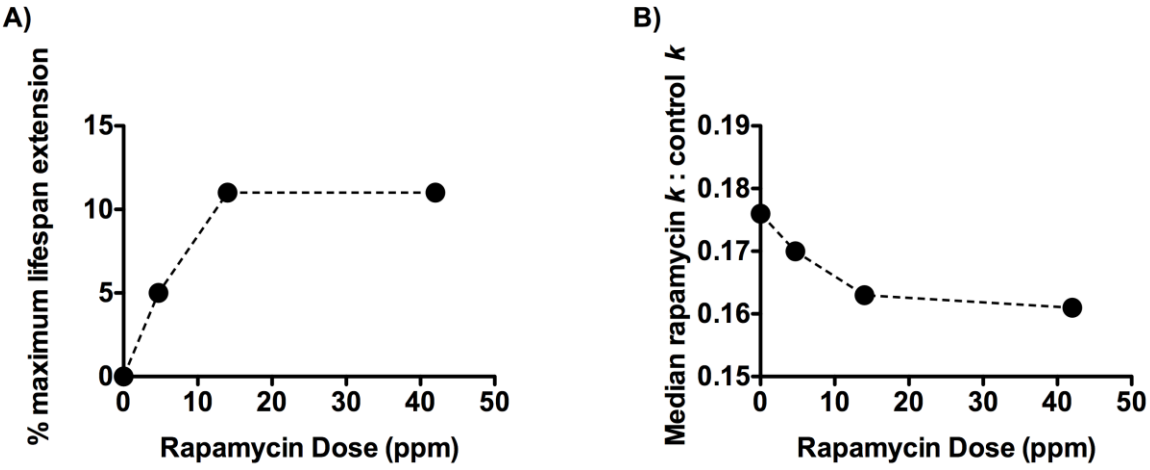

Figure 9: Effects of different doses of rapamycin on maximum lifespan and *in vivo* hepatic protein replacement rates (*k*)

A) Rapamycin dose (ppm) vs. % maximum lifespan extension (adapted from *Miller et al*[141]) and B) rapamycin dose (ppm) vs. median rapamycin (at X ppm) *k* to control *k* ratio (where X = dose of rapamyin in ppm). A total of 150 proteins were identified in all four dosage groups (n = 2-5 per group).

In vivo plasma proteome dynamics

In general, any biological measurement should ideally be minimally invasive and amenable to high-throughput screening. Therefore, we wanted to determine if the replacement rates of plasma proteins were reduced in all three models in a manner similar to that observed for hepatic proteins. Plasmas from mice from all three models were prepped via in-solution trypsin digestion as opposed to fractionation via SDS-PAGE followed by in-gel trypsin digestion. This method of preparation resulted in a very low number of protein identifications in plasma samples compared to the liver samples, likely due to the absence of a fractionation step prior to LC-MS/MS analysis. We identified 25, 27, and 21 plasma proteins in the Rapa (14ppm), CR and Snell dwarf models, respectively, with 7 of these proteins being common to the datasets for all three models.

We found that the median experimental *k* to control *k* ratio for these 7 proteins was, 0.826, 0.873 and 0.391 for the Rapa (14ppm), CR and Snell dwarf models, respectively. Therefore, similar to hepatic proteins, plasma proteins in all three models exhibit reduced replacement rates. A comparison of and the degree of maximum lifespan extension and the degree of plasma protein replacement rate reduction in each model revealed that the degree of replacement rate reduction is not as predictive in plasma proteins as it is in hepatic proteins. Consistent with our findings in the liver, the degree of plasma protein

replacement rate reduction is greatest in the Snell dwarf model, which exhibits the greatest degree of maximum lifespan extension (40%). However, the degree of plasma protein replacement rate reduction in the Rapa (14ppm) and CR models is comparable despite the fact that Rapa (14ppm) mice exhibit a 12% increase in maximum lifespan while CR mice exhibit an 18% increase in maximum lifespan (**Fig 10**).

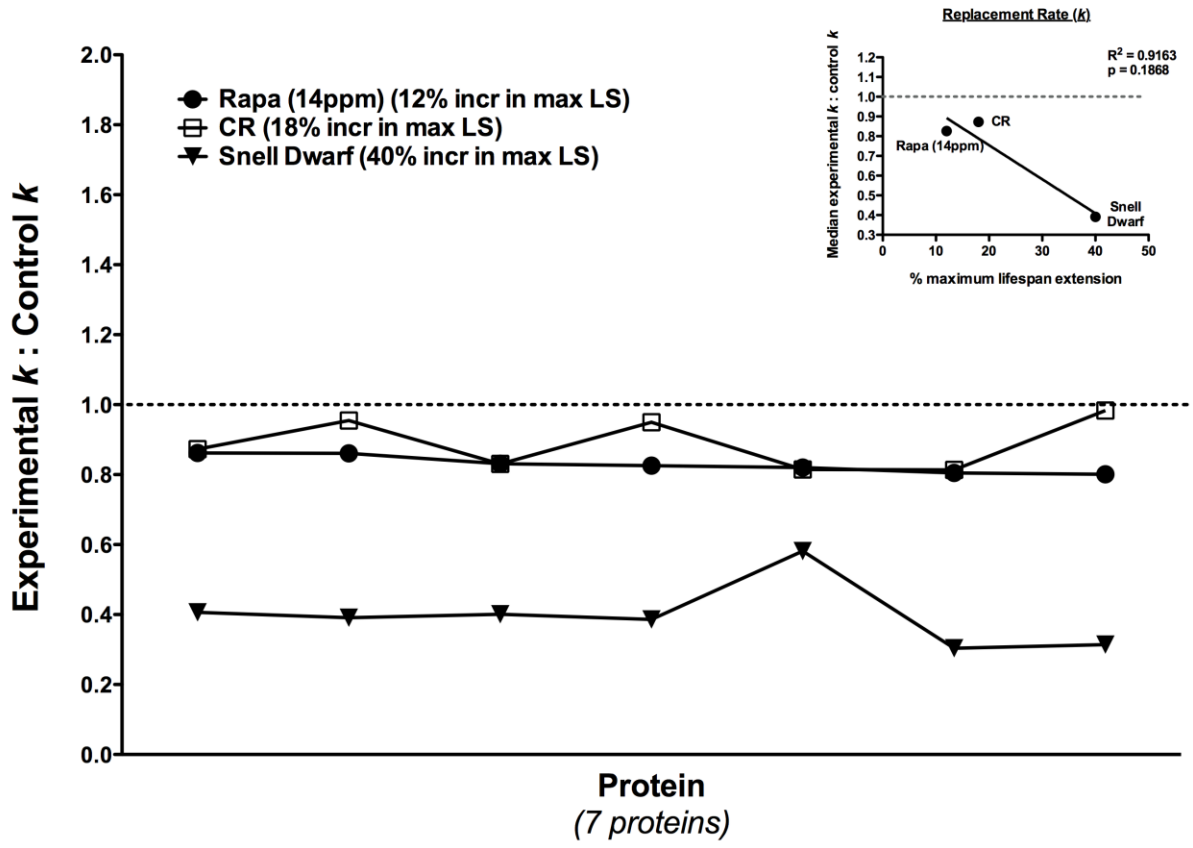

Figure 10: Comparison of the degree of change in the replacement rates (*k*) of plasma proteins identified in all three models

Experimental *k* to control *k* ratio (where the experimental group refers to the longer-lived group within each model) of each of the 7 proteins identified in all three models. Each symbol represents the mean experimental *k* : control *k* ratio for a given protein in a given model. For clarity, proteins are sorted in descending order based on Rapa (14ppm) model values. The number in parentheses represents the % maximum lifespan extension in each model. Inset: % maximum lifespan extension vs. median experimental *k* : control *k* ratio for only those proteins identified in all three models. R^2 and p values were derived from linear regression analyses.

It is possible that once more plasma proteins can be identified in all three models that we will be able to parse out differences in the degree of replacement rate reductions between the Rapa (14ppm) and CR models, if indeed differences exist. However, our initial analysis here of a small number of plasma proteins suggests that the degree of hepatic

protein replacement rate reduction may be a more sensitive predictor or maximum lifespan extension in mice than the degree of plasma protein replacement rate reduction

Model	Type of intervention	Study	% Maximum lifespan extension[a]	Groups	Strain (Sex)	Age at initiation of intervention	Duration of intervention	^2H_2O duration (days)	kDa range of proteins analyzed
Rapamycin Treatment	Pharmacological	CP and PD[b]	12% (14ppm)[140–142]	Control or Rapamycin	UM-HET3 (F)	4m	4m	2[c], 6, 18, 24	3.5 – 160
		PD[d]	5% (4.7ppm)[141] 12% (14ppm)[140–142] 11% (42ppm) [141]	Control or Rapamycin	UM-HET3 (F)	4m	4m	2	20 - 40
CR	Dietary	CP[e]	ND	AL or CR[f]	C57BL/6 (M)	3m	5wk	21	NA
		PD[g]	18%[338]	AL or CR[h]	C57BL/6 (M)	4m	14m	1, 2, 4, 8, 15, 32	3.5 - 160
Snell Dwarf	Monogenetic[i]	CP	40%[65]	Het / WT or Snell Dwarf	DW/J (F)	Birth	6 -7mn[j]	19	NA
		PD	40%[65]	Het / WT or Snell Dwarf	DW/J (F)	Birth	5.5-7mn[j]	1, 2, 4	10 - 80

Table 1: Summary of studies conducted

a Relative to control counterparts.
b Rapamcyin proteome dynamics study 1.
c 2 day labeled mice used for proteome dynamics study 1.
d Rapamycin proteome dynamics study 2.
e Adapted from Bruss et al[228].
f 25% calorie restricted relative to AL.
g Adapted from Price et al[339].
h 40% calorie restricted relative to AL.
i Homozygous for loss of function recessive mutation in Pit1 gene.
j Duration of intervention taken to be the age of the animals at the time of euthanasia.
CP = Cell proliferation.
PD = Proteome dynamics.
ND = No data on maximum lifespan in mice on this specific CR regimen.
NA = Not applicable.

Model	Median Experimental : Control		# of proteins for which data was collected for specified parameter			# of proteins with ≥ 10% reduction in specified parameter (%)			# of proteins with ≥ 10% increase in specified parameter (%)		
	k	**WPASR**	***k***	**RPS**	**WPASR**	***k***	**RPS**	**WPASR**	***k***	**RPS**	**WPASR**
Rapa (14ppm)	0.945	0.994	270	254	199	88 (32.6%)	26 (10.2%)	49 (24.6%)	28 (10.4%)	81 (31.9%)	55 (27.7%)
CR	0.859	0.818	98	242	84	59 (60.2%)	92 (38.0%)	61 (72.6%)	1 (1.0%)	48 (19.8%)	4 (4.8%)
Snell Dwarf	0.591	0.671	126	141	70	123 (97.6%)	50 (35.5%)	60 (86.0%)	0 (0.0%)	57 (40.4%)	7 (10.0%)

Table 2: Summary of global changes in *in vivo* hepatic proteome dynamics

Experimental refers to the longer-lived group within each model (Rapa (14ppm), CR or Snell Dwarf) and control refers to the control group within each model (Control, AL or Snell Het/WT, respectively). *k* = Protein replacement rate. RPS = Relative pool size. WPASR = Within proteome absolute synthesis rate.

Protein	UniProt Accession #	Experimental *k* : Control *k*			Slope	R^2	p value
		Rapa (14ppm) (12%)	CR (18%)	Snell dwarf (40%)			
Acetyl-CoA acetyltransferase, cytosolic	Q8CAY6	0.82	0.785	0.637	-0.006589 ± 0.0001632	0.999	0.016
Cytochrome b5	P56395	0.928	0.808	0.463	-0.01637 ± 0.0007462	0.998	0.029
Glutamate dehydrogenase 1, mitochondrial	P26443	0.851	0.779	0.593	-0.009033 ± 0.0006000	0.996	0.042
Homogentisate 1,2-dioxygenase	O09173	0.96	0.854	0.578	-0.01335 ± 0.0008715	0.996	0.042
Microsomal glutathione S-transferase 1	Q91VS7	0.918	0.828	0.562	-0.01253 ± 0.0005032	0.998	0.026
Succinyl-CoA ligase [ADP/GDP-forming] subunit alpha, mitochondrial	Q9WUM5	0.978	0.885	0.613	-0.01285 ± 0.0005557	0.998	0.028
UDP-glucuronosyltransferase 1-6	Q64435	0.858	0.781	0.490	-0.01319 ± 0.00007137	1.000	0.003

Table 3: Hepatic proteins for which the degree of replacement rate reduction is most highly predictive of the degree of maximum lifespan extension across Rapa (14ppm), CR and Snell dwarf models

Experimental refers to the longer-lived group within each model (Rapa (14ppm), CR or Snell Dwarf) and control refers to the control group within each model (Control, AL or Snell Het/WT, respectively). The number in parentheses represents the % maximum lifespan extension in each model. Slope, R^2 and p values were derived from linear regression analyses on % maximum lifespan extension vs. experimental *k* to control *k* ratios for each protein individually.

Protein	UniProt Accession #	*k* at specified rapamycin dose				Slope	R^2	p value
		0ppm (0%)	**4.7ppm** (5%)	**14ppm** (11%)	**42ppm** (11%)			
Acetyl-CoA acetyltransferase, cytosolic	Q8CAY6	0.193	0.230	0.173	0.267	0.001944 ± 0.005352	0.062	0.751
Succinyl-CoA ligase [ADP/GDP-forming] subunit alpha, mitochondrial	Q9WUM5	0.143	0.124	0.121	0.121	-0.001814 ± 0.0005841	0.828	0.090

Table 4: Proteins from Table 3 identified in rapamycin dose-response study

The number in parentheses represents the % maximum lifespan extension relative to 0ppm rapamycin. Slope, R^2 and p values were derived from linear regression analyses on dose (ppm) of rapamycin vs. *k* for each protein individually.

Discussion

In the studies presented here, we evaluated the utility of reduced *in vivo* cell proliferation rates and changes in *in vivo* hepatic proteome dynamics as early predictors of maximum lifespan extension in mice. We did this by assessing both in depth, and at relatively early time points, in three unique mouse models of maximum lifespan extension in mice from diverse genetic backgrounds using stable isotope labeling combined with GC- and LC-MS techniques. The major findings of this work include the following: 1) *In vivo* cell proliferation rates are not consistently reduced at early time points in the three mouse models of maximum lifespan extension evaluated here. Therefore, a reduction in *in vivo* cell proliferation rates is not a robust early predictor of maximum lifespan extension in mice. 2) The common hepatic proteome alterations observed in all three models include: i) a reduction in the synthesis of proteins involved in protein processing in the ER, ii) an increase in or preservation of the synthesis of glutathione S-transferases and iii) a reduction in protein replacement rates. 3) The degree to which hepatic protein replacement rates are reduced correlates strongly with the degree of maximum lifespan extension in the three models evaluated. A reduction in hepatic protein replacement rates, therefore, may represent a novel, sensitive and early predictor of maximum lifespan extension in mice.

The third conclusion is somewhat counterintuitive in light of reports of reduced mTORC1 signaling and enhanced autophagy in rapamycin-treated, CR and Snell dwarf mice[110,131,142,352,364,365]. Autophagy is a lysosomal degradation pathway that degrades various cellular components including proteins and organelles and occurs under basal conditions but is upregulated in response to certain forms of stress including nutrient deprivation[366,367]. Therefore, upregulation of autophagy would be expected to increase protein replacement rates, however, we clearly measured a general reduction in hepatic protein replacement rates in all three models. There are at least three possible explanations for the discordance between the reduction in protein replacement rates observed in the studies presented here and reports of enhanced autophagy in these three models. First, it is possible that flux through the autophagic pathway is not actually enhanced in these three models as many researchers rely on surrogates of autophagic flux, including LC3 (microtubule-associated protein 1 light chain 3) lipidation, as opposed to direct measurements of autophagic flux[368]. Secondly, in eukaryotic cells, protein degradation via the ubiquitin-proteasome system (UPS) predominates over autophagy-mediated protein degradation, therefore, changes in protein replacement rates due to changes in autophagic flux may not be readily measurable against "background" UPS-mediated degradation[369]. Lastly, it is possible that some but not most proteins are *bona fide* autophagy substrates.

Our finding that maximum lifespan extension in mice is associated with a reduction in hepatic protein replacement rates is also counterintuitive given that proteasome activity and, therefore, protein replacement rates, diminish with age. This reduced capacity to replace proteins is believed to contribute to the accumulation of damaged proteins with age[24,370]. Therefore, rather than promoting maximum lifespan extension directly, we hypothesize that the observed reduction in hepatic protein replacement rates in all three

models evaluated here simply reflects a reduced demand for protein renewal, likely due to adaptations that reduce the levels of unfolded, damaged or otherwise abnormal proteins. Importantly, a reduction or attenuated increase in the levels of unfolded and damaged proteins with age is predicted to directly promote healthspan and maximum lifespan extension by preserving the functional capacity of the proteome (maintaining proteostasis), thereby delaying age-related loss of cellular and tissue homeostasis (**Fig 2 and 11**).

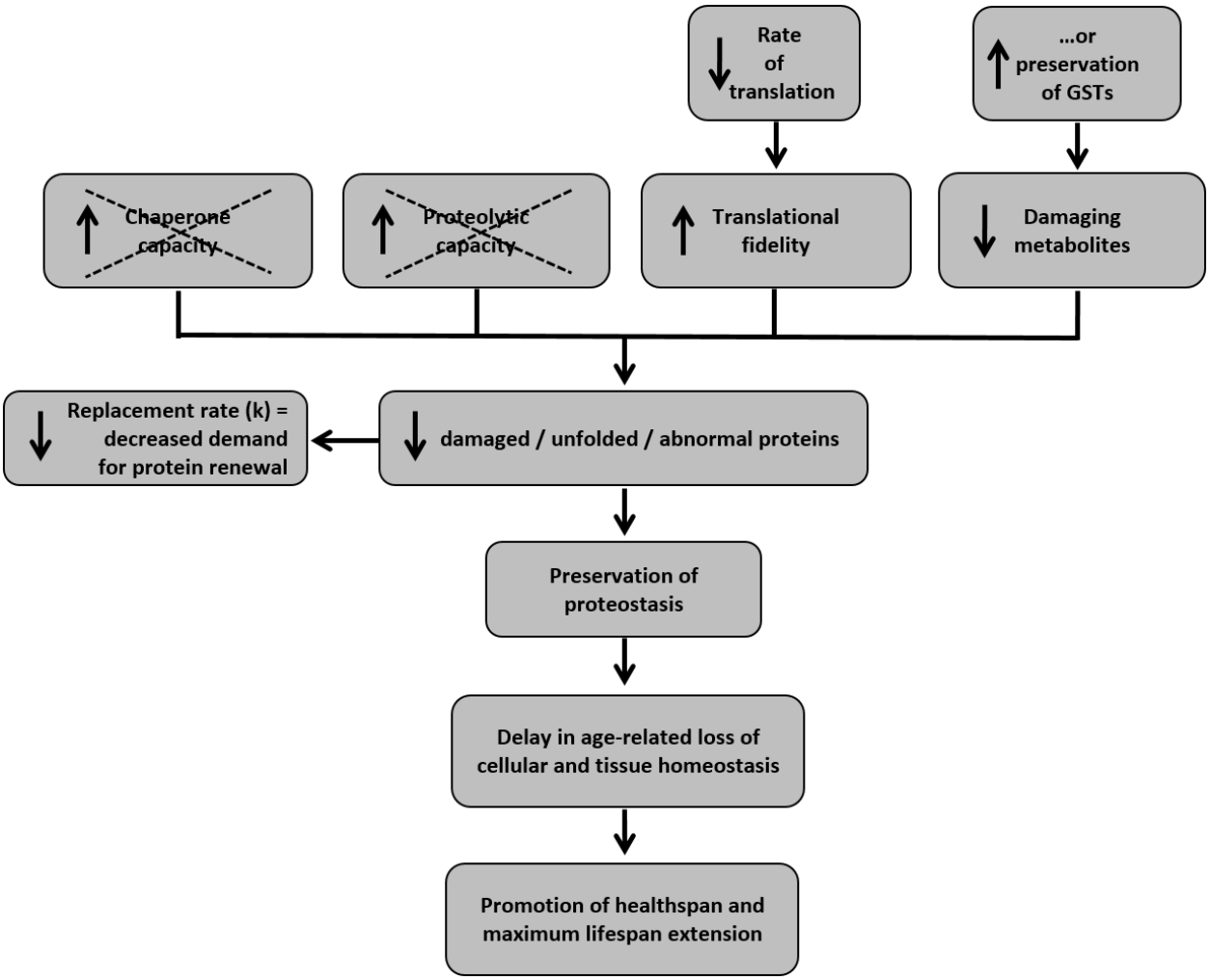

Figure 11: Model of hypothesized explanation for reduction in hepatic protein replacement rates and promotion of healthspan and maximum lifespan extension in Rapa (14ppm), CR and Snell dwarf mice

A variety of cellular adaptations can reduce the levels of unfolded and damaged proteins, including an increase in chaperone capacity, an increase in proteolytic capacity, an increase in translational fidelity as well as a reduction in the levels of damaging metabolites. Our observations that chaperone levels are unchanged or reduced and that

protein replacement rates are reduced (not increased) in all three models evaluated, suggest that neither an increase in chaperone capacity nor an increase in proteolytic capacity can account for a reduction in the levels of unfolded and damaged proteins in these models if a reduction does indeed exist.

Given that mistranslated proteins are more susceptible to unfolding and damage, an increase in translational fidelity is predicted to reduce the levels of unfolded and damaged proteins[193]. Intriguingly, translational fidelity can be increased by simply slowing down the rate of translation[336]. Reducing the rate of translation increases the dwell time of ribosomes, thereby increasing the time ribosomes have to search for the correct/cognate aa-tRNA[334]. While we did not directly measure the rate at which mRNAs were being translated in the three models evaluated here, it is possible that the rate of translation is in fact reduced in these models. This possibility is supported by the fact that inhibition of mTOCR1 via rapamycin treatment *in vitro* reduces the rate of elongation and increases translational fidelity[334]. It remains to be determined whether rapamycin has similar effects *in vivo* and whether translation rates are reduced and translational fidelity is increased in CR and Snell dwarf mice.

Importantly, reducing the rate of translation also reduces the likelihood that chaperones involved in cotranslational folding will become saturated leading to elevated levels of unfolded proteins[335]. We found that the levels of the chaperones BiP, GRP94 and Hsp90-β were either unchanged or decreased across all three models, therefore, if cotranslational folding capacity is enhanced in these three models, it is not through these chaperones. It is, however, possible that the levels of other chaperones not measured in the present study are relatively preserved or increased in these three models and, therefore, may enhance cotranslational folding and reduce the levels of unfolded proteins.

Our data do, however, suggest that levels of unfolded or damaged proteins may be reduced in the three models evaluated due to increased or preserved synthesis of GSTs, which reduce the levels of damaging metabolites (**Fig 11**). Reduced protein damage has been previously reported in Snell dwarf mice and Ames dwarf mice, which like Snell dwarf mice, are pituitary dwarfs and exhibit extended maximum lifespan relative to WT controls[64,290]. Reduced protein damage has also been reported in CR rodents, although there are several notable reports of increased protein damage[108,361–363,371]. Reductions in protein damage have been linked to reduced reactive oxygen species (ROS) production and increased antioxidant enzyme activity in CR rodents and to increased antioxidant enzyme activity in Ames dwarf mice[290,372,373]. In future work it will be important to directly measure levels of damaging metabolites as well as protein damage in soluble and insoluble protein fractions in these three models under the same experimental conditions and at the relatively early time points evaluated here.

Validation of a reduction in hepatic protein replacement rates as a *bona fide* robust sensitive early predictor of maximum lifespan extension in mice requires additional rigorous testing. Specifically, it will be critical to determine if a reduction in hepatic protein replacement rates predicts maximum lifespan extension at earlier time points and in both sexes of the models presented here as well as in other mouse models of maximum lifespan extension. Measuring hepatic protein replacement rates in response to interventions proven to have no effect on maximum lifespan in mice, or only on mean lifespan, will also

be necessary to determine the extent to which this putative predictive marker is specific to maximum lifespan extension. Additionally, it will be important to determine if the degree of replacement rate reduction in any subset of hepatic proteins is as predictive or potentially more predictive than the global degree of hepatic protein replacement rate reduction.

In the studies presented here, we identified seven (out of a total of 54) hepatic proteins for which there was a significant positive correlation between the degree to which their replacement rates were reduced and the degree of maximum lifespan extension in the three models evaluated (**Table 3** (**pg 100**)). Two of these seven proteins were also identified in our study looking at the effects of different doses of rapamycin. However, we found no significant correlation between the degree to which the replacement rates of these two proteins were reduced and the degree of maximum lifespan extension in response to the four doses of rapamycin examined (0, 4.7, 14 and 42ppm) (**Table 4** (**pg 101**)). This comparison, of albeit only two proteins, suggests that it is a reduction in global hepatic protein replacement rates that is a sensitive and early predictor of maximum lifespan extension in mice, rather than a reduction in the replacement rates of specific hepatic proteins. If this is indeed the case, then perhaps for future studies it will only be necessary to measure global protein replacement rates via heavy water labeling and subsequent determination of deuterium incorporation into alanine[374]. However, this technique would prohibit the measurement of the overall synthesis rates (WPASR) of individual proteins, changes in which may ultimately be found to be both predictive and potentially causally related to maximum lifespan extension, as may be the case for increased or preserved synthesis of GST proteins.

In conclusion, the data presented here suggest that maximum lifespan extension in three unique mouse models from diverse genetic backgrounds is associated with a preservation of proteostasis as indicated by a reduced demand for protein replacement. While further validation is still needed, the data presented here also provide evidence that a reduction in global hepatic protein replacement rates may be a sensitive and early predictor of maximum lifespan extension in mice. The development of a panel of early predictive markers of maximum lifespan extension could be used to rapidly screen and prioritize candidate interventions with the potential to modulate the rate of aging in relatively small cohorts of mice for inclusion into healthspan and lifespan studies in much larger cohorts of mice. A reduction in global hepatic protein replacement rates may serve as one such predictive marker.

Discussion and Conclusions

The development of interventions that attenuate aging and extend healthspan in humans is a major goal of gerontological research and would have profound social and economic benefits. The development of such interventions requires a broad understanding of the factors that govern aging and lifespan determination in mammals, as well as a framework for efficiently testing candidate interventions. To this end, the approach taken in the body of work presented here was to use three unique mouse models of maximum lifespan extension to identify physiological, hormonal, cellular and molecular factors with the potential to confer and/or predict maximum lifespan extension and attenuated aging in mammals.

Reduced IGF-1 and mTORC1 signaling are recurring themes across various mouse models of healthspan and maximum lifespan extension[79,80,140–142]. The underlying cellular events that confer healthspan and maximum lifespan extension downstream of reduced IGF-1 and mTORC1 signaling, however, are not completely understood. Chapter 3 describes studies designed to examine two potential cellular alterations down stream of reduced IGF-1 and mTORC1 signaling that may confer as well as predict maximum lifespan extension in mice. The two cellular alterations examined were reduced global cell proliferation rates and reduced protein synthesis rates. Not only are these two cellular alterations tightly linked to reduced IGF-1 and mTORC1 signaling, they have also been linked to maximum lifespan extension across a variety of organisms[29,39,260]. **Figure 2** in Chapter 3 illustrates how reduced cell proliferation and protein synthesis are predicted to promote healthspan and maximum lifespan extension. In the studies described in Chapter 3, we also examined overall alterations in proteome dynamics to determine what if any alterations may confer or predict maximum lifespan extension.

The identification of a panel of predictive markers of maximum lifespan, and therefore, healthspan extension, would greatly accelerate efforts like those spearheaded by the NIA's Interventions Testing Program (ITP), to identify interventions that slow the rate of aging and delay the development of age-related diseases in mice and, therefore, may have therapeutic potential in the fight against age-related diseases in humans[125,126]. Such a panel could be used to screen and prioritize candidate interventions for inclusion in large-scale healthspan and lifespan studies in mice, which are both time and resource intensive. An ideal predictive marker should manifest relatively early on after the initiation of an intervention but should ultimately be predictive of healthspan and maximum lifespan outcomes in a strain- and intervention-independent manner. Therefore, to determine the extent to which a reduction in cell proliferation, a reduction in protein synthesis and/or other proteome alterations may confer or predict maximum lifespan extension, we conducted *in vivo* cell proliferation and proteome dynamics analyses in three unique mouse models of maximum lifespan extension at relatively early time points. These models included rapamycin-treated, CR and Snell dwarf mice, all on unique genetic backgrounds. Using stable isotope labeling combined with GC- and LC-MS/MS techniques, we measured the *in vivo* proliferation rates of three to four cell types as well as three key aspects of protein metabolism, including protein replacement rate, pool size and overall synthesis rate, for hundreds of individual proteins in each model.

In our hepatic proteome dynamics studies we found that a reduction in global protein synthesis is not a consistent predictor of maximum lifespan extension in mice. Global protein synthesis was reduced in CR mice and to an even greater extent in Snell dwarf mice. We assessed the levels of several chaperones, the levels of which increase when unfolded proteins accumulate, and found that they were unchanged or reduced in CR and Snell dwarf mice, thereby ruling out the possibility that the observed reduction in global hepatic protein synthesis in CR and Snell dwarf mice is simply due to an accumulation of unfolded or damaged proteins. Therefore, reduced global protein synthetic burden appears to be a primary response in CR and Snell dwarf mice rather than a secondary response. Surprisingly, we found no evidence of a global reduction in protein synthesis (primary or secondary) in response to 14ppm rapamycin treatment. This finding is, however, consistent with that of another group that demonstrated that chronic rapamycin treatment in mice does not alter global hepatic protein synthesis, as measured by ribosome activity[347]. Interestingly, global hepatic protein synthesis (as measured by ribosome activity) is unchanged in S6K1-/- mice, which exhibit maximum lifespan extension[347]. Therefore, a reduction in global protein synthesis appears to be generally but not universally associated with maximum lifespan extension in mice.

We did, however, identify two subsets of related proteins with synthesis rates similarly differentially affected in all three models, including proteins involved in protein processing in the ER (PPER), the synthesis of which was reduced in all three models. We believe that the reduced synthesis of proteins involved in PPER in CR and Snell dwarf mice may reflect the general reduction in protein synthetic burden in these two models. Additionally, the reduced synthesis of proteins involved in PPER in all three models may reflect a reduced demand for the machinery involved in protein folding and quality control in the ER, possibly to due a more favorable folding environment.

Consistent with this, one of the unifying proteome alterations observed across all three models was a reduction in hepatic protein replacement rates. We believe this reduction in protein replacement rates likely reflects a reduced demand for protein renewal due to reduced levels of unfolded or damaged proteins in all three models. This interpretation is based on previous reports of reduced levels of protein damage in CR and Snell dwarf mice and our observation that chaperones levels are unchanged or reduced in all three models[64,361,362]. In addition, at least in the CR and Snell dwarf models, the levels of damaged proteins my be reduced as a result of enhanced translational fidelity due to reduced rates of protein synthesis (translation) in these models.

Consistent with our interpretation that reduced hepatic protein replacement rates likely reflect a reduced demand for protein renewal due to reduced levels of unfolded or damaged proteins in all three models, we also found that the only other subset of related proteins with synthesis rates similarly differentially affected in all three models was GSTs. We found that the synthesis of GSTs was either increased or preserved in all three models. Given that GSTs play a critical cytoprotective role in cells by reducing the levels of damaging metabolites, this finding it consistent with the hypothesis that the levels of unfolded and damaged proteins are reduced in all three models[357]. In fact, our major finding that protein replacement rates are reduced in all three models is in and of itself indirect evidence that the levels of unfolded and damaged proteins are reduced in these models because protein replacement rates would be expected to be increased in the

context of an accumulation of unfolded or damaged proteins. Our finding that the synthesis of GSTs was either preserved or increased across all three models is also consistent with another recurring theme in maximum lifespan extension from worms, to flies to mammals, which is the recurring theme of enhanced stress resistance and somatic maintenance[37–42,188]. Importantly, enhanced somatic maintenance protects all cellular components from damage, including DNA, and, therefore, is predicted to contribute to lifespan extension not only by preserving proteostasis but also by preserving genomic stability.

Arguably the finding with the most immediate impact from our hepatic proteome dynamics studies was that the degree of hepatic protein replacement rate reduction was highly predictive of the degree of maximum lifespan extension. This was true when replacement rate data were compared between Rapa (14ppm), CR and Snell dwarf mice as well as when replacement rate data were compared across different doses of rapamycin. This finding is highly significant because it provides strong evidence that a reduction in hepatic protein replacement rates could potentially serve as one of ideally several, sensitive and early predictive markers of maximum lifespan extension in large-scale screens designed to identify interventions with the potential to slow the rate of aging in mice. This finding is also consistent with our interpretation that the observed reduction in hepatic protein replacement rates in all three models reflects reduced protein damage. The rationale being that the model with the greatest reduction in protein damage would be expected to exhibit the greatest degree of hepatic protein replacement rate reduction as well as exhibit the greatest degree of maximum lifespan extension due to the greatest preservation of proteostasis. And this is in fact what we found. Of the three models examined, Snell dwarf mice exhibited the greatest degree of hepatic protein replacement rate reduction and, as shown by others, Snell dwarf mice also exhibit the greatest degree of maximum lifespan extension[65]. Importantly, to date, a reduction in hepatic protein replacement rates represents the only known metric that is a sensitive and early predictor of maximum lifespan extension in multiple mouse models of maximum lifespan extension from diverse genetic backgrounds.

Future studies should focus on directly measuring protein damage in Rapa (14ppm), CR and Snell dwarf mice and in response to different doses of rapamycin to test our working hypothesis that the observed reductions in hepatic protein replacement rates reflect reduced protein damage. In addition, it will be important to directly measure translation rates and translational fidelity in these three models to determine if, and to what extent, reduced translation rates and increased translational fidelity contribute to enhanced proteostasis in these models.

To continue to validate reduced hepatic protein replacement rates as a robust and sensitive predictor of maximum lifespan extension in mice, two major hurdles must be overcome. First, it must be shown that hepatic protein replacement rates are reduced in other mouse models of extended maximum lifespan. Second, it must be determined that hepatic protein replacement rates are not reduced in response to interventions that do not extend maximum lifespan, or only extend mean lifespan, to confirm that this marker is specific to maximum lifespan extension and, therefore, specific to interventions that slow the rate of aging.

While hepatic protein replacement rates were measured at relatively early time points in all three models in the work presented here, it will also be important to determine if differences in hepatic protein replacement rates manifest at earlier time points. If this is the case, it would enhance the utility of measuring hepatic protein replacement rates as a means to rapidly screen and prioritize candidate interventions for inclusion in large-scale healthspan and lifespan studies in mice. Finally, future studies should focus on definitively determining if a reduction in plasma protein replacement rates may also serve as a sensitive and early predictor of maximum lifespan extension in mice. This will require the measurement of the replacement rates of many more plasma proteins in rapamycin-treated, CR and Snell dwarf mice than were measured in the work presented here.

In our cell proliferation studies we found that a reduction in global cell proliferation rates is not a consistent predictor of maximum lifespan extension in mice. While proliferation rates were reduced in all cell types analyzed in CR mice and in three of the four cell types analyzed in Snell dwarf mice, rapamycin treatment had no effect on the proliferation rates of any of the cell types analyzed. Therefore, a reduction in global cell proliferation rates appears to be generally but not universally associated with maximum lifespan extension in mice. Comparing cell proliferation rate data between CR and Snell dwarf mice, we also found that the degree of cell proliferation rate reduction was not predictive of the degree of maximum lifespan extension in these two models. Specifically, global cell proliferation rates were reduced to a greater extent in 25% CR mice, which are estimated to exhibit an 11% extension in maximum lifespan, compared to Snell dwarf mice which exhibit a 40% extension in maximum lifespan[65,338]. Nevertheless, there is ample evidence from models of both premature and attenuated aging that global cell proliferation rates are tightly linked to the aging process, with hyperproliferation associated with premature aging and hypoproliferation associated with attenuated aging[14,56,218,260]. The data presented here, however, provide clear evidence that a reduction in global cell proliferation rates is not necessary for maximum lifespan extension in mice but still may have utility, albeit limited, as a metric in a panel of predictive markers of maximum lifespan extension in mice.

While a reduction in global cell proliferation rates is not a universal feature of rapamycin-treated and Snell dwarf mice, it is one of the most robust responses to CR in rodents[224–228]. Importantly, this reduction in global cell proliferation rates has been mechanistically linked to CR-induced lifespan extension through the inhibition of the promotional phase of carcinogenesis and a delay in cellular replicative senescence[94,96,267]. Therefore, identifying upstream physiological inputs or hormonal signals that may mediate reduced cell proliferation rates in response to CR could provide insights into mechanisms of aging and age-related diseases. Several of the physiological responses to CR including reductions in food intake[268,269], energy expenditure[270], percent body fat[83,271,272] and body weight[95,273,274] have been suggested to mediate the effects of CR. However, data definitively demonstrating that any of these physiological adaptations are sufficient to increase lifespan are lacking, in part due to the difficulty in dissociating these various physiological adaptations from classical CR.

Chapter 1 describes experiments employing changes in ambient temperature and exercise designed to isolate these four physiological adaptations from classical CR to determine their effects on global cell proliferation rates. We found that none of these

physiological adaptations, independent of classical CR, could account for the reduction in global cell proliferation rates in response to CR. Given that this reduction in global cell proliferation rates may be mechanistically linked to CR-induced lifespan extension, these findings are consistent with reports that these physiological adaptations cannot account for the reduction in tumor formation or the increase in maximum lifespan in response to CR in rodents[268,269,276,284–288]. Importantly, in each of the three experiments described in Chapter 1, a reduction in global cell proliferation rates was only observed when food intake was below the level that a mouse would select if provided free access to food. It is unclear exactly how this reduction in food intake below some selected threshold is translated into reduced global cell proliferation rates, however, a growing body of evidence implicates a reduction in the circulating levels of IGF-1

We and others have found that circulating IGF-1 levels are reduced in response to CR in rodents[23,228,230]. In the experiments described in Chapter 1, we also found that global cell proliferation rates were significantly positively correlated with circulating levels of IGF-1. This finding is consistent with studies showing that the reduction in cell proliferation rates in CR rodents is attenuated by repletion of IGF-1 levels back to AL levels[229–231].

A reduction in IGF-1 levels (or signaling) is also observed in a variety of mouse models of maximum lifespan extension other then CR[290–294]. Therefore, given this recurring theme of reduced IGF-1 in maximum lifespan extension and evidence of a mechanistic link between reduced circulating IGF-1 levels and reduced global cell proliferation rates in response to CR, the exact mechanism (s) by which IGF-1 levels are reduced in response to CR remains an important unanswered question. Chapter 2 describes studies that directly address this question.

IGF-1 is primarily produced in the liver and GH plays a key role in its production[162,163,306]. We began investigating FGF21, a novel endocrine member of the FGF family, as a potential mediator of the CR-induced reduction in IGF-1 and global cell proliferation rates after published reports that FGF21 is upregulated in response to fasting and negatively regulates IGF-1 production, likely through a mechanism involving the development of hepatic GH resistance[71,307,308]. We first ruled out the possibility that a simple reduction in GH levels in CR mice could account for their reduced circulating IGF-1 levels. Next we identified STAT5 phosphorylation as the most distal point blunted in CR mice within the GH signaling pathway that mediates transcriptional upregulation of IGF-1 in the liver. Consistent with findings in models of long-term CR and undernutrition, we found that indeed, both hepatic mRNA and circulating levels of FGF21 were increased in response to moderate CR in adult mice[70,113].

To then directly determine if FGF21 is necessary for the reduction in IGF-1 and global cell proliferation rates in response to CR, we placed both WT and whole-body FGF21 knockout (FGF21-KO) mice on either an AL or CR diet. We found that FGF21 is not necessary for the reduction in circulating IGF-1 levels in response to CR. These results were surprising given the finding of another group that FGF21 is necessary for the full undernutrition-related reduction in IGF-1 in young developing mice[70]. Given that this other group used young (4-week-old) developing mice on a severe CR diet (50% CR) while we used adult (3-month-old) mice on a moderate CR diet (25%CR), it is possible that

FGF21's effects on IGF-1 only manifest beyond a certain degree of CR and/or only during development.

Another important finding of this study was that FGF21 follows unique diurnal patterns of expression in AL and CR mice. In WT mice, we found that circulating FGF21 levels were higher in AL compared to CR mice at 1500hr (~23hrs after food provision to CR mice) but higher in CR compared to AL at 1900hr (~3hrs after food provision to CR mice). This finding underscores the importance of taking into account the timing of any biological measurement and may explain inconsistencies in reports of the effects of CR on FGF21 levels[70,74,112,113].

In order to evaluate FGF21's role in alterations to overall growth signaling in response to CR, we also measured global cell proliferation rates in WT and FGF21-KO on either an AL or CR diet. We found that global cell proliferation rates were reduced in response to CR to essentially the same extent in WT and FGF21-KO mice. Intriguingly, we found that global cell proliferation rates were higher in AL-fed FGF21-KO mice compared to AL-fed WT mice, despite similar food intakes and circulating IGF-1 levels, providing evidence that FGF21 may have novel anti-anabolic effects.

Regarding FGF21's role in regulating IGF-1 levels in the context of CR, future studies should focus on determining the degree of CR and at what stages of life FGF21's negative regulatory effects on IGF-1 expression manifest. Future studies should also explore the mechanisms underling FGF21's anti-anabolic effects. One possible mechanism could be through alterations in IGFBPs, which influence IGF-1 bioavailability[312–314]. In the studies described in Chapter 2, we ruled out the possibility that IGF-1 bioavailability is increased in FGF21-KO mice due to reduced circulating levels of IGFBP-1 (a binding protein that reduces IGF-1 bioavailability) as circulating IGFBP-1 levels were actually higher in FGF21-KO compared to WT mice on both an AL and CR diet.

Treatment with exogenous FGF21, which reduces circulating IGF-1 levels, still holds promise for therapeutic reduction of IGF-1 levels[71]. In addition, FGF21 has well-documented glucose-lowering and insulin sensitizing effects, providing further evidence of its broad therapeutic potential[247–249,310,320–323]. Regarding other mechanisms by which IGF-1 is reduced in response to CR, future studies should focus on the potential contributions of reduced protein intake, reduced insulin levels, reduced thyroid hormone levels and other IGFBPs that influence the bioavailability and half-life of IGF-1 in circulation.

In closing, the body of work described herein provides additional evidence that reduced circulating IGF-1 levels mediate, at least in part, the CR-induced reduction in global cell proliferation rates, however, reductions in food intake, energy expenditure, body fat and body weight were ruled out as contributing factors to this cellular response in CR mice. In addition, it was determined that STAT5 phosphorylation is the most distal point blunted in hepatic GH-mediated IGF-1 production signaling in CR mice and that FGF21 is not necessary for the reduction in circulating IGF-1 levels or the reduction in global cell proliferation rates in response to several weeks of CR in adult mice. Findings from the hepatic proteome dynamics studies in rapamycin-treated, CR and Snell dwarf mice contribute to the growing body of evidence that reduced protein synthesis rates, enhanced stress resistance, enhanced somatic maintenance and reduced cellular damage take center

stage in the extension of maximum lifespan in mammals. Finally, the data presented here provide strong evidence that a reduction in hepatic protein replacement rates is a sensitive and early predictor of maximum lifespan extension in mice and, therefore, may serve as a tool to identify interventions with the potential to attenuate aging and the development of age-related diseases in humans.

References

1. Yu, B. *Modulation of aging processes by dietary restriction*. (CRC Press, 1994).
2. López-Otín, C., Blasco, M. A., Partridge, L., Serrano, M. & Kroemer, G. The hallmarks of aging. *Cell* **153,** 1194–1217 (2013).
3. Alemayehu, B. & Warner, K. E. The lifetime distribution of health care costs. *Health Serv. Res.* **39,** 627–642 (2004).
4. National Vital Statistics Report Volume 61 No. 4. at </nchs/products/nvsr.htm>
5. Internationale Politik und Gesellschaft : Zeitschrift für globale Trends, Außenpolitik, Internationale Beziehungen, Weltwirtschaft, Länderanalysen. (1985). at <http://www.fes.de/ipg/ipg1_2002/ARTJACOBZONE.htm>
6. WHO | The top 10 causes of death. *WHO* at <http://who.int/mediacentre/factsheets/fs310/en/index1.html>
7. Hobbs, F. & Damon, B. *U.S. Bureau of the Census. Current Population Reports, Special Studies, P23-190, 65+ in the United States.* (U.S. Government Printing Office, Washington, DC, 1996).
8. Masoro, E. J. Overview of caloric restriction and ageing. *Mech. Ageing Dev.* **126,** 913–922 (2005).
9. Olshansky, S. J., Carnes, B. A. & Cassel, C. In search of Methuselah: estimating the upper limits to human longevity. *Science* **250,** 634–640 (1990).
10. Kirkwood, T. B. & Austad, S. N. Why do we age? *Nature* **408,** 233–238 (2000).
11. Medawar, P. B. *An Unsolved Problem of Biology: An Inaugural Lecture Delivered at University College, London, 6 December, 1951*. (H.K. Lewis and Company, 1952).
12. Edney, E. B. & Gill, R. W. Evolution of senescence and specific longevity. *Nature* **220,** 281–282 (1968).
13. Kapahi, P. Protein synthesis and the antagonistic pleiotropy hypothesis of aging. *Adv. Exp. Med. Biol.* **694,** 30–37 (2010).
14. Pendergrass, W. R., Li, Y., Jiang, D. & Wolf, N. S. Decrease in cellular replicative potential in 'giant' mice transfected with the bovine growth hormone gene correlates to shortened life span. *J. Cell. Physiol.* **156,** 96–103 (1993).
15. Kirkwood, T. B. Evolution of ageing. *Nature* **270,** 301–304 (1977).
16. Rose, M. & Charlesworth, B. A test of evolutionary theories of senescence. *Nature* **287,** 141–142 (1980).
17. Partridge, L., Prowse, N. & Pignatelli, P. Another set of responses and correlated responses to selection on age at reproduction in Drosophila melanogaster. *Proc. Biol. Sci.* **266,** 255–261 (1999).
18. Buck, S., Vettraino, J., Force, A. G. & Arking, R. Extended longevity in Drosophila is consistently associated with a decrease in developmental viability. *J. Gerontol. A. Biol. Sci. Med. Sci.* **55,** B292–301 (2000).

19. Stearns, S. C., Ackermann, M., Doebeli, M. & Kaiser, M. Experimental evolution of aging, growth, and reproduction in fruitflies. *Proc. Natl. Acad. Sci. U. S. A.* **97,** 3309–3313 (2000).

20. Rattan, S. I. S. Synthesis, modification and turnover of proteins during aging. *Adv. Exp. Med. Biol.* **694,** 1–13 (2010).

21. Pamplona, R. Membrane phospholipids, lipoxidative damage and molecular integrity: a causal role in aging and longevity. *Biochim. Biophys. Acta* **1777,** 1249–1262 (2008).

22. López-Torres, M., Gredilla, R., Sanz, A. & Barja, G. Influence of aging and long-term caloric restriction on oxygen radical generation and oxidative DNA damage in rat liver mitochondria. *Free Radic. Biol. Med.* **32,** 882–889 (2002).

23. Sonntag, W. E. *et al.* Pleiotropic effects of growth hormone and insulin-like growth factor (IGF)-1 on biological aging: inferences from moderate caloric-restricted animals. *J. Gerontol. A. Biol. Sci. Med. Sci.* **54,** B521–538 (1999).

24. Chondrogianni, N. & Gonos, E. S. Proteasome function determines cellular homeostasis and the rate of aging. *Adv. Exp. Med. Biol.* **694,** 38–46 (2010).

25. Tavernarakis, N. *Protein Metabolism and Homeostasis in Aging*. (Springer, 2011).

26. Kenyon, C., Chang, J., Gensch, E., Rudner, A. & Tabtiang, R. A C. elegans mutant that lives twice as long as wild type. *Nature* **366,** 461–464 (1993).

27. Clancy, D. J. *et al.* Extension of life-span by loss of CHICO, a Drosophila insulin receptor substrate protein. *Science* **292,** 104–106 (2001).

28. Fabrizio, P., Pozza, F., Pletcher, S. D., Gendron, C. M. & Longo, V. D. Regulation of longevity and stress resistance by Sch9 in yeast. *Science* **292,** 288–290 (2001).

29. Kennedy, B. K. & Kaeberlein, M. Hot topics in aging research: protein translation, 2009. *Aging Cell* **8,** 617–623 (2009).

30. Burtner, C. R. & Kennedy, B. K. Progeria syndromes and ageing: what is the connection? *Nat. Rev. Mol. Cell Biol.* **11,** 567–578 (2010).

31. Stenesen, D. *et al.* Adenosine nucleotide biosynthesis and AMPK regulate adult life span and mediate the longevity benefit of caloric restriction in flies. *Cell Metab.* **17,** 101–112 (2013).

32. Kapahi, P. *et al.* Regulation of lifespan in Drosophila by modulation of genes in the TOR signaling pathway. *Curr. Biol. CB* **14,** 885–890 (2004).

33. Zid, B. M. *et al.* 4E-BP extends lifespan upon dietary restriction by enhancing mitochondrial activity in Drosophila. *Cell* **139,** 149–160 (2009).

34. Kenyon, C. J. The genetics of ageing. *Nature* **464,** 504–512 (2010).

35. Kaeberlein, M. & Kennedy, B. K. Protein translation, 2007. *Aging Cell* **6,** 731–734 (2007).

36. Kaeberlein, M. & Kennedy, B. K. Protein translation, 2008. *Aging Cell* **7,** 777–782 (2008).

37. Johnson, T. E. *et al.* Longevity genes in the nematode Caenorhabditis elegans also mediate increased resistance to stress and prevent disease. *J. Inherit. Metab. Dis.* **25,** 197–206 (2002).

38. Cypser, J. R., Tedesco, P. & Johnson, T. E. Hormesis and aging in Caenorhabditis elegans. *Exp. Gerontol.* **41,** 935–939 (2006).

39. McElwee, J. J. *et al.* Evolutionary conservation of regulated longevity assurance mechanisms. *Genome Biol.* **8,** R132 (2007).

40. Jones, L. M. *et al.* Proteomic analyses of Caenorhabditis elegans dauer larvae and long-lived daf-2 mutants implicates a shared detoxification system in longevity assurance. *J. Proteome Res.* **9,** 2871–2881 (2010).

41. Bartke, A., Sun, L. Y. & Longo, V. Somatotropic signaling: trade-offs between growth, reproductive development, and longevity. *Physiol. Rev.* **93,** 571–598 (2013).

42. Le Bourg, E. Hormesis, aging and longevity. *Biochim. Biophys. Acta* **1790,** 1030–1039 (2009).

43. Kennedy, B. K., Steffen, K. K. & Kaeberlein, M. Ruminations on dietary restriction and aging. *Cell. Mol. Life Sci. CMLS* **64,** 1323–1328 (2007).

44. Lucanic, M., Lithgow, G. J. & Alavez, S. Pharmacological lifespan extension of invertebrates. *Ageing Res. Rev.* **12,** 445–458 (2013).

45. Bartke, A. Can growth hormone (GH) accelerate aging? Evidence from GH-transgenic mice. *Neuroendocrinology* **78,** 210–216 (2003).

46. Kajiura, L. J. & Rollo, C. D. A mass budget for transgenic 'Supermice' engineered with extra rat growth hormone genes: evidence for energetic limitation. *Can. J. Zool.* **72,** 1010–1017 (1994).

47. Hauck, S. J. & Bartke, A. Free radical defenses in the liver and kidney of human growth hormone transgenic mice: possible mechanisms of early mortality. *J. Gerontol. A. Biol. Sci. Med. Sci.* **56,** B153–162 (2001).

48. Kuro-o, M. *et al.* Mutation of the mouse klotho gene leads to a syndrome resembling ageing. *Nature* **390,** 45–51 (1997).

49. Kurosu, H. *et al.* Regulation of fibroblast growth factor-23 signaling by klotho. *J. Biol. Chem.* **281,** 6120–6123 (2006).

50. Urakawa, I. *et al.* Klotho converts canonical FGF receptor into a specific receptor for FGF23. *Nature* **444,** 770–774 (2006).

51. Schmid, C., Neidert, M. C., Tschopp, O., Sze, L. & Bernays, R. L. Growth hormone and Klotho. *J. Endocrinol.* **219,** R37–57 (2013).

52. Lanske, B. & Razzaque, M. S. Mineral metabolism and aging: the fibroblast growth factor 23 enigma. *Curr. Opin. Nephrol. Hypertens.* **16,** 311–318 (2007).

53. Shiraki-Iida, T. *et al.* Structure of the mouse klotho gene and its two transcripts encoding membrane and secreted protein. *FEBS Lett.* **424,** 6–10 (1998).

54. Zhang, H., Kieckhaefer, J. E. & Cao, K. Mouse models of laminopathies. *Aging Cell* **12,** 2–10 (2013).

55. Bohr, V. A. Rising from the RecQ-age: the role of human RecQ helicases in genome maintenance. *Trends Biochem. Sci.* **33,** 609–620 (2008).

56. Kill, I. R., Faragher, R. G., Lawrence, K. & Shall, S. The expression of proliferation-dependent antigens during the lifespan of normal and progeroid human fibroblasts in culture. *J. Cell Sci.* **107 (Pt 2),** 571–579 (1994).

57. Kudlow, B. A., Kennedy, B. K. & Monnat, R. J., Jr. Werner and Hutchinson-Gilford progeria syndromes: mechanistic basis of human progeroid diseases. *Nat. Rev. Mol. Cell Biol.* **8,** 394–404 (2007).

58. Liang, H. *et al.* Genetic mouse models of extended lifespan. *Exp. Gerontol.* **38,** 1353–1364 (2003).

59. Godfrey, P. *et al.* GHRH receptor of little mice contains a missense mutation in the extracellular domain that disrupts receptor function. *Nat. Genet.* **4,** 227–232 (1993).

60. Zhou, Y. *et al.* A mammalian model for Laron syndrome produced by targeted disruption of the mouse growth hormone receptor/binding protein gene (the Laron mouse). *Proc. Natl. Acad. Sci. U. S. A.* **94,** 13215–13220 (1997).

61. Chandrashekar, V. & Bartke, A. Induction of endogenous insulin-like growth factor-I secretion alters the hypothalamic-pituitary-testicular function in growth hormone-deficient adult dwarf mice. *Biol. Reprod.* **48,** 544–551 (1993).

62. Li, S. *et al.* Dwarf locus mutants lacking three pituitary cell types result from mutations in the POU-domain gene pit-1. *Nature* **347,** 528–533 (1990).

63. Papaconstantinou, J. *et al.* Hepatic gene and protein expression of primary components of the IGF-I axis in long lived Snell dwarf mice. *Mech. Ageing Dev.* **126,** 692–704 (2005).

64. Flurkey, K., Papaconstantinou, J., Miller, R. A. & Harrison, D. E. Lifespan extension and delayed immune and collagen aging in mutant mice with defects in growth hormone production. *Proc. Natl. Acad. Sci. U. S. A.* **98,** 6736–6741 (2001).

65. Flurkey, K., Papaconstantinou, J. & Harrison, D. E. The Snell dwarf mutation Pit1(dw) can increase life span in mice. *Mech. Ageing Dev.* **123,** 121–130 (2002).

66. Silberberg, R. Articular aging and osteoarthrosis in dwarf mice. *Pathol. Microbiol. (Basel)* **38,** 417–430 (1972).

67. Harrison, D. E. *Genetic Effects on Aging*. (CRC Press, 1990).

68. Vergara, M., Smith-Wheelock, M., Harper, J. M., Sigler, R. & Miller, R. A. Hormone-treated snell dwarf mice regain fertility but remain long lived and disease resistant. *J. Gerontol. A. Biol. Sci. Med. Sci.* **59,** 1244–1250 (2004).

69. Murakami, S., Salmon, A. & Miller, R. A. Multiplex stress resistance in cells from long-lived dwarf mice. *FASEB J. Off. Publ. Fed. Am. Soc. Exp. Biol.* **17,** 1565–1566 (2003).

70. Kubicky, R. A., Wu, S., Kharitonenkov, A. & De Luca, F. Role of fibroblast growth factor 21 (FGF21) in undernutrition-related attenuation of growth in mice. *Endocrinology* **153,** 2287–2295 (2012).

71. Inagaki, T. *et al.* Inhibition of growth hormone signaling by the fasting-induced hormone FGF21. *Cell Metab.* **8,** 77–83 (2008).

72. Wu, S. *et al.* Increased expression of fibroblast growth factor 21 (FGF21) during chronic undernutrition causes growth hormone insensitivity in chondrocytes by inducing leptin receptor overlapping transcript (LEPROT) and leptin receptor overlapping transcript-like 1 (LEPROTL1) expression. *J. Biol. Chem.* **288,** 27375–27383 (2013).

73. Wu, S., Levenson, A., Kharitonenkov, A. & De Luca, F. Fibroblast growth factor 21 (FGF21) inhibits chondrocyte function and growth hormone action directly at the growth plate. *J. Biol. Chem.* **287,** 26060–26067 (2012).

74. Zhang, Y. *et al.* The starvation hormone, fibroblast growth factor-21, extends lifespan in mice. *eLife* **1,** e00065 (2012).

75. Kurosu, H. *et al.* Suppression of aging in mice by the hormone Klotho. *Science* **309,** 1829–1833 (2005).

76. Cha, S.-K. *et al.* Removal of sialic acid involving Klotho causes cell-surface retention of TRPV5 channel via binding to galectin-1. *Proc. Natl. Acad. Sci. U. S. A.* **105,** 9805–9810 (2008).

77. Kuro-o, M. Klotho and aging. *Biochim. Biophys. Acta* **1790,** 1049–1058 (2009).

78. Banerjee, S. *et al.* Klotho ameliorates chemically induced endoplasmic reticulum (ER) stress signaling. *Cell. Physiol. Biochem. Int. J. Exp. Cell. Physiol. Biochem. Pharmacol.* **31,** 659–672 (2013).

79. Wu, J. J. *et al.* Increased mammalian lifespan and a segmental and tissue-specific slowing of aging after genetic reduction of mTOR expression. *Cell Rep.* **4,** 913–920 (2013).

80. Selman, C. *et al.* Ribosomal protein S6 kinase 1 signaling regulates mammalian life span. *Science* **326,** 140–144 (2009).

81. Ortega-Molina, A. *et al.* Pten positively regulates brown adipose function, energy expenditure, and longevity. *Cell Metab.* **15,** 382–394 (2012).

82. Foukas, L. C. *et al.* Long-term p110α PI3K inactivation exerts a beneficial effect on metabolism. *EMBO Mol. Med.* **5,** 563–571 (2013).

83. Blüher, M., Kahn, B. B. & Kahn, C. R. Extended longevity in mice lacking the insulin receptor in adipose tissue. *Science* **299,** 572–574 (2003).

84. Herranz, D. *et al.* Sirt1 improves healthy ageing and protects from metabolic syndrome-associated cancer. *Nat. Commun.* **1,** 3 (2010).

85. Kanfi, Y. *et al.* The sirtuin SIRT6 regulates lifespan in male mice. *Nature* **483,** 218–221 (2012).

86. Michishita, E. *et al.* SIRT6 is a histone H3 lysine 9 deacetylase that modulates telomeric chromatin. *Nature* **452,** 492–496 (2008).

87. Baker, D. J. *et al.* Increased expression of BubR1 protects against aneuploidy and cancer and extends healthy lifespan. *Nat. Cell Biol.* **15,** 96–102 (2013).

88. Schriner, S. E. *et al.* Extension of murine life span by overexpression of catalase targeted to mitochondria. *Science* **308,** 1909–1911 (2005).

89. Migliaccio, E. *et al.* The p66shc adaptor protein controls oxidative stress response and life span in mammals. *Nature* **402,** 309–313 (1999).

90. Gertz, M. & Steegborn, C. The Lifespan-regulator p66Shc in mitochondria: redox enzyme or redox sensor? *Antioxid. Redox Signal.* **13,** 1417–1428 (2010).

91. Jiang, J. C., Jaruga, E., Repnevskaya, M. V. & Jazwinski, S. M. An intervention resembling caloric restriction prolongs life span and retards aging in yeast. *FASEB J. Off. Publ. Fed. Am. Soc. Exp. Biol.* **14,** 2135–2137 (2000).

92. Partridge, L., Piper, M. D. W. & Mair, W. Dietary restriction in Drosophila. *Mech. Ageing Dev.* **126,** 938–950 (2005).

93. Houthoofd, K. & Vanfleteren, J. R. The longevity effect of dietary restriction in Caenorhabditis elegans. *Exp. Gerontol.* **41,** 1026–1031 (2006).

94. Weindruch, R. *The retardation of aging and disease by dietary restriction*. (C.C. Thomas, 1988).

95. McCay, C. M., Crowell, M. F. & Maynard, L. A. The effect of retarded growth upon the length of life span and upon the ultimate body size. 1935. *Nutr. Burbank Los Angel. Cty. Calif* **5,** 155–171; discussion 172 (1989).

96. Weindruch, R., Walford, R. L., Fligiel, S. & Guthrie, D. The retardation of aging in mice by dietary restriction: longevity, cancer, immunity and lifetime energy intake. *J. Nutr.* **116,** 641–654 (1986).

97. Bonkowski, M. S. *et al.* Disruption of growth hormone receptor prevents calorie restriction from improving insulin action and longevity. *PloS One* **4,** e4567 (2009).

98. Mattson, M. P. Emerging neuroprotective strategies for Alzheimer's disease: dietary restriction, telomerase activation, and stem cell therapy. *Exp. Gerontol.* **35,** 489–502 (2000).

99. Wolf, N. S., Penn, P. E., Jiang, D., Fei, R. G. & Pendergrass, W. R. Caloric restriction: conservation of in vivo cellular replicative capacity accompanies life-span extension in mice. *Exp. Cell Res.* **217,** 317–323 (1995).

100. Pendergrass, W. R., Li, Y., Jiang, D., Fei, R. G. & Wolf, N. S. Caloric restriction: conservation of cellular replicative capacity in vitro accompanies life-span extension in mice. *Exp. Cell Res.* **217,** 309–316 (1995).

101. Park, J.-H. *et al.* Calorie restriction alleviates the age-related decrease in neural progenitor cell division in the aging brain. *Eur. J. Neurosci.* **37,** 1987–1993 (2013).

102. Cerletti, M., Jang, Y. C., Finley, L. W. S., Haigis, M. C. & Wagers, A. J. Short-term calorie restriction enhances skeletal muscle stem cell function. *Cell Stem Cell* **10,** 515–519 (2012).

103. Longo, V. D. & Fontana, L. Calorie restriction and cancer prevention: metabolic and molecular mechanisms. *Trends Pharmacol. Sci.* **31,** 89–98 (2010).

104. Harper, J. M. *et al.* Stress resistance and aging: influence of genes and nutrition. *Mech. Ageing Dev.* **127,** 687–694 (2006).

105. HARMAN, D. Aging: a theory based on free radical and radiation chemistry. *J. Gerontol.* **11,** 298–300 (1956).

106. Yu, B. P. Aging and oxidative stress: modulation by dietary restriction. *Free Radic. Biol. Med.* **21,** 651–668 (1996).

107. Pamplona, R. & Barja, G. Highly resistant macromolecular components and low rate of generation of endogenous damage: two key traits of longevity. *Ageing Res. Rev.* **6,** 189–210 (2007).

108. Walsh, M. E., Shi, Y. & Van Remmen, H. The effects of dietary restriction on oxidative stress in rodents. *Free Radic. Biol. Med.* **66,** 88–99 (2014).

109. Masoro, E. J. Caloric restriction-induced life extension of rats and mice: a critique of proposed mechanisms. *Biochim. Biophys. Acta* **1790,** 1040–1048 (2009).

110. Jiang, W., Zhu, Z. & Thompson, H. J. Dietary energy restriction modulates the activity of AMP-activated protein kinase, Akt, and mammalian target of rapamycin in mammary carcinomas, mammary gland, and liver. *Cancer Res.* **68,** 5492–5499 (2008).

111. Masoro, E. J. Retardation of aging processes by food restriction: an experimental tool. *Am. J. Clin. Nutr.* **55,** 1250S–1252S (1992).

112. Sharma, N., Castorena, C. M. & Cartee, G. D. Greater insulin sensitivity in calorie restricted rats occurs with unaltered circulating levels of several important myokines and cytokines. *Nutr. Metab.* **9,** 90 (2012).

113. Kuhla, A. *et al.* Lifelong Caloric Restriction Reprograms Hepatic Fat Metabolism in Mice. *J. Gerontol. A. Biol. Sci. Med. Sci.* (2013). doi:10.1093/gerona/glt160

114. Liao, C.-Y., Rikke, B. A., Johnson, T. E., Diaz, V. & Nelson, J. F. Genetic variation in the murine lifespan response to dietary restriction: from life extension to life shortening. *Aging Cell* **9,** 92–95 (2010).

115. Colman, R. J. *et al.* Caloric restriction delays disease onset and mortality in rhesus monkeys. *Science* **325,** 201–204 (2009).

116. Mattison, J. A. *et al.* Impact of caloric restriction on health and survival in rhesus monkeys from the NIA study. *Nature* **489,** 318–321 (2012).

117. Cava, E. & Fontana, L. Will calorie restriction work in humans? *Aging* **5,** 507–514 (2013).

118. Fontana, L., Partridge, L. & Longo, V. D. Extending healthy life span--from yeast to humans. *Science* **328,** 321–326 (2010).

119. Omodei, D. & Fontana, L. Calorie restriction and prevention of age-associated chronic disease. *FEBS Lett.* **585,** 1537–1542 (2011).

120. Omodei, D., Licastro, D., Salvatore, F., Crosby, S. D. & Fontana, L. Serum from humans on long-term calorie restriction enhances stress resistance in cell culture. *Aging* **5,** 599–606 (2013).

121. Pamplona, R. & Barja, G. Mitochondrial oxidative stress, aging and caloric restriction: the protein and methionine connection. *Biochim. Biophys. Acta* **1757,** 496–508 (2006).

122. Orentreich, N., Matias, J. R., DeFelice, A. & Zimmerman, J. A. Low methionine ingestion by rats extends life span. *J. Nutr.* **123,** 269–274 (1993).

123. Richie, J. P., Jr *et al.* Methionine restriction increases blood glutathione and longevity in F344 rats. *FASEB J. Off. Publ. Fed. Am. Soc. Exp. Biol.* **8,** 1302–1307 (1994).

124. Miller, R. A. *et al.* Methionine-deficient diet extends mouse lifespan, slows immune and lens aging, alters glucose, T4, IGF-I and insulin levels, and increases hepatocyte MIF levels and stress resistance. *Aging Cell* **4,** 119–125 (2005).

125. Warner, H. R., Ingram, D., Miller, R. A., Nadon, N. L. & Richardson, A. G. Program for testing biological interventions to promote healthy aging. *Mech. Ageing Dev.* **115,** 199–207 (2000).

126. Miller, R. A. *et al.* An Aging Interventions Testing Program: study design and interim report. *Aging Cell* **6,** 565–575 (2007).

127. Vézina, C., Kudelski, A. & Sehgal, S. N. Rapamycin (AY-22,989), a new antifungal antibiotic. I. Taxonomy of the producing streptomycete and isolation of the active principle. *J. Antibiot. (Tokyo)* **28,** 721–726 (1975).

128. Heitman, J., Movva, N. R. & Hall, M. N. Targets for cell cycle arrest by the immunosuppressant rapamycin in yeast. *Science* **253,** 905–909 (1991).

129. Chiu, M. I., Katz, H. & Berlin, V. RAPT1, a mammalian homolog of yeast Tor, interacts with the FKBP12/rapamycin complex. *Proc. Natl. Acad. Sci. U. S. A.* **91,** 12574–12578 (1994).

130. Tsang, C. K., Qi, H., Liu, L. F. & Zheng, X. F. S. Targeting mammalian target of rapamycin (mTOR) for health and diseases. *Drug Discov. Today* **12,** 112–124 (2007).

131. Abraham, R. T. Identification of TOR signaling complexes: more TORC for the cell growth engine. *Cell* **111,** 9–12 (2002).

132. Dumont, F. J. *et al.* The immunosuppressive macrolides FK-506 and rapamycin act as reciprocal antagonists in murine T cells. *J. Immunol. Baltim. Md 1950* **144,** 1418–1424 (1990).

133. Varma, S. & Khandelwal, R. L. Effects of rapamycin on cell proliferation and phosphorylation of mTOR and p70(S6K) in HepG2 and HepG2 cells overexpressing constitutively active Akt/PKB. *Biochim. Biophys. Acta* **1770,** 71–78 (2007).

134. Hansel, D. E. *et al.* Mammalian target of rapamycin (mTOR) regulates cellular proliferation and tumor growth in urothelial carcinoma. *Am. J. Pathol.* **176,** 3062–3072 (2010).

135. Pallet, N. *et al.* Rapamycin inhibits human renal epithelial cell proliferation: effect on cyclin D3 mRNA expression and stability. *Kidney Int.* **67,** 2422–2433 (2005).

136. Zahr, E. *et al.* Rapamycin impairs in vivo proliferation of islet beta-cells. *Transplantation* **84,** 1576–1583 (2007).

137. Marx, S. O., Jayaraman, T., Go, L. O. & Marks, A. R. Rapamycin-FKBP inhibits cell cycle regulators of proliferation in vascular smooth muscle cells. *Circ. Res.* **76,** 412–417 (1995).

138. Breslin, E. M., White, P. C., Shore, A. M., Clement, M. & Brennan, P. LY294002 and rapamycin co-operate to inhibit T-cell proliferation. *Br. J. Pharmacol.* **144,** 791–800 (2005).

139. Madke, B. Topical rapamycin (sirolimus) for facial angiofibromas. *Indian Dermatol. Online J.* **4,** 54–57 (2013).

140. Miller, R. A. *et al.* Rapamycin, but not resveratrol or simvastatin, extends life span of genetically heterogeneous mice. *J. Gerontol. A. Biol. Sci. Med. Sci.* **66,** 191–201 (2011).

141. Miller, R. A. *et al.* Rapamycin-mediated lifespan increase in mice is dose and sex dependent and metabolically distinct from dietary restriction. *Aging Cell* (2013). doi:10.1111/acel.12194

142. Harrison, D. E. *et al.* Rapamycin fed late in life extends lifespan in genetically heterogeneous mice. *Nature* **460,** 392–395 (2009).

143. Wilkinson, J. E. *et al.* Rapamycin slows aging in mice. *Aging Cell* **11,** 675–682 (2012).

144. Mendelsohn, A. R. & Larrick, J. W. Dissecting mammalian target of rapamycin to promote longevity. *Rejuvenation Res.* **15,** 334–337 (2012).

145. Lamming, D. W. *et al.* Rapamycin-induced insulin resistance is mediated by mTORC2 loss and uncoupled from longevity. *Science* **335,** 1638–1643 (2012).

146. Rena, G., Pearson, E. R. & Sakamoto, K. Molecular mechanism of action of metformin: old or new insights? *Diabetologia* **56,** 1898–1906 (2013).

147. Anisimov, V. N. *et al.* Metformin slows down aging and extends life span of female SHR mice. *Cell Cycle Georget. Tex* **7,** 2769–2773 (2008).

148. Anisimov, V. N. *et al.* If started early in life, metformin treatment increases life span and postpones tumors in female SHR mice. *Aging* **3,** 148–157 (2011).

149. Martin-Montalvo, A. *et al.* Metformin improves healthspan and lifespan in mice. *Nat. Commun.* **4,** 2192 (2013).

150. Holloszy, J. O. Mortality rate and longevity of food-restricted exercising male rats: a reevaluation. *J. Appl. Physiol. Bethesda Md 1985* **82,** 399–403 (1997).

151. Strong, R. *et al.* Nordihydroguaiaretic acid and aspirin increase lifespan of genetically heterogeneous male mice. *Aging Cell* **7,** 641–650 (2008).

152. Yuan, R. *et al.* Aging in inbred strains of mice: study design and interim report on median lifespans and circulating IGF1 levels. *Aging Cell* **8,** 277–287 (2009).

153. Yuan, R. *et al.* Genetic coregulation of age of female sexual maturation and lifespan through circulating IGF1 among inbred mouse strains. *Proc. Natl. Acad. Sci. U. S. A.* **109,** 8224–8229 (2012).

154. Guevara-Aguirre, J. *et al.* Growth hormone receptor deficiency is associated with a major reduction in pro-aging signaling, cancer, and diabetes in humans. *Sci. Transl. Med.* **3,** 70ra13 (2011).

155. Suh, Y. *et al.* Functionally significant insulin-like growth factor I receptor mutations in centenarians. *Proc. Natl. Acad. Sci. U. S. A.* **105,** 3438–3442 (2008).

156. Bonafè, M. *et al.* Polymorphic variants of insulin-like growth factor I (IGF-I) receptor and phosphoinositide 3-kinase genes affect IGF-I plasma levels and human longevity: cues for an evolutionarily conserved mechanism of life span control. *J. Clin. Endocrinol. Metab.* **88,** 3299–3304 (2003).

157. Willcox, B. J. *et al.* FOXO3A genotype is strongly associated with human longevity. *Proc. Natl. Acad. Sci. U. S. A.* **105,** 13987–13992 (2008).

158. Kuningas, M. *et al.* Haplotypes in the human Foxo1a and Foxo3a genes; impact on disease and mortality at old age. *Eur. J. Hum. Genet. EJHG* **15,** 294–301 (2007).

159. Flachsbart, F. *et al.* Association of FOXO3A variation with human longevity confirmed in German centenarians. *Proc. Natl. Acad. Sci. U. S. A.* **106,** 2700–2705 (2009).

160. Arking, D. E. *et al.* Association of human aging with a functional variant of klotho. *Proc. Natl. Acad. Sci. U. S. A.* **99,** 856–861 (2002).

161. Chen, Y.-F., Wu, C.-Y., Kao, C.-H. & Tsai, T.-F. Longevity and lifespan control in mammals: lessons from the mouse. *Ageing Res. Rev.* **9 Suppl 1,** S28–35 (2010).

162. Yakar, S. *et al.* Normal growth and development in the absence of hepatic insulin-like growth factor I. *Proc. Natl. Acad. Sci. U. S. A.* **96,** 7324–7329 (1999).

163. Rosenfeld, R. G. & Hwa, V. The growth hormone cascade and its role in mammalian growth. *Horm. Res.* **71 Suppl 2,** 36–40 (2009).

164. Ciampolillo, A., De Tullio, C. & Giorgino, F. The IGF-I/IGF-I receptor pathway: Implications in the Pathophysiology of Thyroid Cancer. *Curr. Med. Chem.* **12,** 2881–2891 (2005).

165. Gallagher, E. J. & LeRoith, D. The proliferating role of insulin and insulin-like growth factors in cancer. *Trends Endocrinol. Metab. TEM* **21,** 610–618 (2010).

166. Wullschleger, S., Loewith, R. & Hall, M. N. TOR signaling in growth and metabolism. *Cell* **124,** 471–484 (2006).

167. Sakharova, A. A. *et al.* Role of growth hormone in regulating lipolysis, proteolysis, and hepatic glucose production during fasting. *J. Clin. Endocrinol. Metab.* **93,** 2755–2759 (2008).

168. Vijayakumar, A., Novosyadlyy, R., Wu, Y., Yakar, S. & LeRoith, D. Biological effects of growth hormone on carbohydrate and lipid metabolism. *Growth Horm. IGF Res. Off. J. Growth Horm. Res. Soc. Int. IGF Res. Soc.* **20,** 1–7 (2010).

169. Berryman, D. E. *et al.* Comparing adiposity profiles in three mouse models with altered GH signaling. *Growth Horm. IGF Res. Off. J. Growth Horm. Res. Soc. Int. IGF Res. Soc.* **14,** 309–318 (2004).

170. Bartke, A. & Westbrook, R. Metabolic characteristics of long-lived mice. *Front. Genet.* **3,** 288 (2012).

171. Markowska, A. L., Mooney, M. & Sonntag, W. E. Insulin-like growth factor-1 ameliorates age-related behavioral deficits. *Neuroscience* **87,** 559–569 (1998).

172. Thornton, P. L., Ingram, R. L. & Sonntag, W. E. Chronic [D-Ala2]-growth hormone-releasing hormone administration attenuates age-related deficits in spatial memory. *J. Gerontol. A. Biol. Sci. Med. Sci.* **55,** B106–112 (2000).

173. Ramsey, M. M., Weiner, J. L., Moore, T. P., Carter, C. S. & Sonntag, W. E. Growth hormone treatment attenuates age-related changes in hippocampal short-term plasticity and spatial learning. *Neuroscience* **129,** 119–127 (2004).

174. Sonntag, W. E. *et al.* The effects of growth hormone and IGF-1 deficiency on cerebrovascular and brain ageing. *J. Anat.* **197 Pt 4,** 575–585 (2000).

175. Laplante, M. & Sabatini, D. M. mTOR signaling in growth control and disease. *Cell* **149,** 274–293 (2012).

176. Sarbassov, D. D. *et al.* Prolonged rapamycin treatment inhibits mTORC2 assembly and Akt/PKB. *Mol. Cell* **22,** 159–168 (2006).

177. Stanfel, M. N., Shamieh, L. S., Kaeberlein, M. & Kennedy, B. K. The TOR pathway comes of age. *Biochim. Biophys. Acta* **1790,** 1067–1074 (2009).

178. Ma, X. M. & Blenis, J. Molecular mechanisms of mTOR-mediated translational control. *Nat. Rev. Mol. Cell Biol.* **10,** 307–318 (2009).

179. Zoncu, R., Efeyan, A. & Sabatini, D. M. mTOR: from growth signal integration to cancer, diabetes and ageing. *Nat. Rev. Mol. Cell Biol.* **12,** 21–35 (2011).

180. Thoreen, C. C. *et al.* A unifying model for mTORC1-mediated regulation of mRNA translation. *Nature* **485,** 109–113 (2012).

181. Hamilton, T. L., Stoneley, M., Spriggs, K. A. & Bushell, M. TOPs and their regulation. *Biochem. Soc. Trans.* **34,** 12–16 (2006).

182. Iadevaia, V., Caldarola, S., Tino, E., Amaldi, F. & Loreni, F. All translation elongation factors and the e, f, and h subunits of translation initiation factor 3 are encoded by 5'-terminal oligopyrimidine (TOP) mRNAs. *RNA N. Y. N* **14,** 1730–1736 (2008).

183. Yamasaki, S. & Anderson, P. Reprogramming mRNA translation during stress. *Curr. Opin. Cell Biol.* **20,** 222–226 (2008).

184. Wek, R. C., Jiang, H.-Y. & Anthony, T. G. Coping with stress: eIF2 kinases and translational control. *Biochem. Soc. Trans.* **34,** 7–11 (2006).

185. Gebauer, F. & Hentze, M. W. Molecular mechanisms of translational control. *Nat. Rev. Mol. Cell Biol.* **5,** 827–835 (2004).

186. Baird, T. D. & Wek, R. C. Eukaryotic initiation factor 2 phosphorylation and translational control in metabolism. *Adv. Nutr. Bethesda Md* **3,** 307–321 (2012).

187. Komar, A. A. & Hatzoglou, M. Cellular IRES-mediated translation: the war of ITAFs in pathophysiological states. *Cell Cycle Georget. Tex* **10,** 229–240 (2011).

188. Rogers, A. N. *et al.* Life span extension via eIF4G inhibition is mediated by posttranscriptional remodeling of stress response gene expression in C. elegans. *Cell Metab.* **14,** 55–66 (2011).

189. Hartl, F. U., Bracher, A. & Hayer-Hartl, M. Molecular chaperones in protein folding and proteostasis. *Nature* **475,** 324–332 (2011).

190. Ellis, R. J. & van der Vies, S. M. Molecular chaperones. *Annu. Rev. Biochem.* **60,** 321–347 (1991).

191. Braakman, I. & Hebert, D. N. Protein folding in the endoplasmic reticulum. *Cold Spring Harb. Perspect. Biol.* **5,** a013201 (2013).

192. Kikis, E. A., Gidalevitz, T. & Morimoto, R. I. Protein homeostasis in models of aging and age-related conformational disease. *Adv. Exp. Med. Biol.* **694,** 138–159 (2010).

193. Dukan, S. *et al.* Protein oxidation in response to increased transcriptional or translational errors. *Proc. Natl. Acad. Sci. U. S. A.* **97,** 5746–5749 (2000).

194. Pickering, A. M. & Davies, K. J. A. Degradation of damaged proteins: the main function of the 20S proteasome. *Prog. Mol. Biol. Transl. Sci.* **109,** 227–248 (2012).

195. Paravicini, T. M. & Touyz, R. M. NADPH oxidases, reactive oxygen species, and hypertension: clinical implications and therapeutic possibilities. *Diabetes Care* **31 Suppl 2,** S170–180 (2008).

196. Raha, S. & Robinson, B. H. Mitochondria, oxygen free radicals, disease and ageing. *Trends Biochem. Sci.* **25,** 502–508 (2000).

197. Petropoulos, I. & Friguet, B. Maintenance of proteins and aging: the role of oxidized protein repair. *Free Radic. Res.* **40,** 1269–1276 (2006).

198. Nedelsky, N. B., Todd, P. K. & Taylor, J. P. Autophagy and the ubiquitin-proteasome system: collaborators in neuroprotection. *Biochim. Biophys. Acta* **1782,** 691–699 (2008).

199. Brooks, P., Murray, R. Z., Mason, G. G., Hendil, K. B. & Rivett, A. J. Association of immunoproteasomes with the endoplasmic reticulum. *Biochem. J.* **352 Pt 3,** 611–615 (2000).

200. Ngo, J. K. & Davies, K. J. A. Importance of the lon protease in mitochondrial maintenance and the significance of declining lon in aging. *Ann. N. Y. Acad. Sci.* **1119,** 78–87 (2007).

201. He, C. & Klionsky, D. J. Regulation mechanisms and signaling pathways of autophagy. *Annu. Rev. Genet.* **43,** 67–93 (2009).

202. Ravikumar, B. *et al.* Regulation of mammalian autophagy in physiology and pathophysiology. *Physiol. Rev.* **90,** 1383–1435 (2010).

203. Scherz-Shouval, R. & Elazar, Z. Regulation of autophagy by ROS: physiology and pathology. *Trends Biochem. Sci.* **36,** 30–38 (2011).

204. Olzmann, J. A., Kopito, R. R. & Christianson, J. C. The mammalian endoplasmic reticulum-associated degradation system. *Cold Spring Harb. Perspect. Biol.* **5,** (2013).

205. Todd, D. J., Lee, A.-H. & Glimcher, L. H. The endoplasmic reticulum stress response in immunity and autoimmunity. *Nat. Rev. Immunol.* **8,** 663–674 (2008).

206. Velichko, A. K., Markova, E. N., Petrova, N. V., Razin, S. V. & Kantidze, O. L. Mechanisms of heat shock response in mammals. *Cell. Mol. Life Sci. CMLS* **70,** 4229–4241 (2013).

207. Haynes, C. M. & Ron, D. The mitochondrial UPR - protecting organelle protein homeostasis. *J. Cell Sci.* **123,** 3849–3855 (2010).

208. Powers, E. T., Morimoto, R. I., Dillin, A., Kelly, J. W. & Balch, W. E. Biological and chemical approaches to diseases of proteostasis deficiency. *Annu. Rev. Biochem.* **78,** 959–991 (2009).

209. Koga, H., Kaushik, S. & Cuervo, A. M. Protein homeostasis and aging: The importance of exquisite quality control. *Ageing Res. Rev.* **10,** 205–215 (2011).

210. Min, J.-N. *et al.* CHIP deficiency decreases longevity, with accelerated aging phenotypes accompanied by altered protein quality control. *Mol. Cell. Biol.* **28,** 4018–4025 (2008).

211. Zhang, C. & Cuervo, A. M. Restoration of chaperone-mediated autophagy in aging liver improves cellular maintenance and hepatic function. *Nat. Med.* **14,** 959–965 (2008).

212. Cohen, E. *et al.* Reduced IGF-1 signaling delays age-associated proteotoxicity in mice. *Cell* **139,** 1157–1169 (2009).

213. Mimeault, M. & Batra, S. K. Aging of tissue-resident adult stem/progenitor cells and their pathological consequences. *Panminerva Med.* **51,** 57–79 (2009).

214. Jones, D. L. & Rando, T. A. Emerging models and paradigms for stem cell ageing. *Nat. Cell Biol.* **13,** 506–512 (2011).

215. Ruzankina, Y., Asare, A. & Brown, E. J. Replicative stress, stem cells and aging. *Mech. Ageing Dev.* **129,** 460–466 (2008).

216. HAYFLICK, L. THE LIMITED IN VITRO LIFETIME OF HUMAN DIPLOID CELL STRAINS. *Exp. Cell Res.* **37,** 614–636 (1965).

217. Harrison, D. E. & Astle, C. M. Loss of stem cell repopulating ability upon transplantation. Effects of donor age, cell number, and transplantation procedure. *J. Exp. Med.* **156,** 1767–1779 (1982).

218. Bridger, J. M. & Kill, I. R. Aging of Hutchinson-Gilford progeria syndrome fibroblasts is characterised by hyperproliferation and increased apoptosis. *Exp. Gerontol.* **39,** 717–724 (2004).

219. Campisi, J. & d' Adda di Fagagna, F. Cellular senescence: when bad things happen to good cells. *Nat. Rev. Mol. Cell Biol.* **8,** 729–740 (2007).

220. Campisi, J. Aging, cellular senescence, and cancer. *Annu. Rev. Physiol.* **75,** 685–705 (2013).

221. Jackson, J. G. & Pereira-Smith, O. M. p53 is preferentially recruited to the promoters of growth arrest genes p21 and GADD45 during replicative senescence of normal human fibroblasts. *Cancer Res.* **66,** 8356–8360 (2006).

222. Narita, M. *et al.* Rb-mediated heterochromatin formation and silencing of E2F target genes during cellular senescence. *Cell* **113,** 703–716 (2003).

223. Fumagalli, M. *et al.* Telomeric DNA damage is irreparable and causes persistent DNA-damage-response activation. *Nat. Cell Biol.* **14,** 355–365 (2012).

224. BULLOUGH, W. S. The effect of a restricted diet on mitotic activity in the mouse. *Br. J. Cancer* **3,** 275–282 (1949).

225. Lok, E. *et al.* Dietary restriction, cell proliferation and carcinogenesis: a preliminary study. *Cancer Lett.* **38,** 249–255 (1988).

226. Lok, E. *et al.* Calorie restriction and cellular proliferation in various tissues of the female Swiss Webster mouse. *Cancer Lett.* **51,** 67–73 (1990).

227. Hsieh, E. A., Chai, C. M. & Hellerstein, M. K. Effects of caloric restriction on cell proliferation in several tissues in mice: role of intermittent feeding. *Am. J. Physiol. Endocrinol. Metab.* **288,** E965–972 (2005).

228. Bruss, M. D., Thompson, A. C. S., Aggarwal, I., Khambatta, C. F. & Hellerstein, M. K. The effects of physiological adaptations to calorie restriction on global cell proliferation rates. *Am. J. Physiol. Endocrinol. Metab.* **300,** E735–745 (2011).

229. Hursting, S. D., Switzer, B. R., French, J. E. & Kari, F. W. The growth hormone: insulin-like growth factor 1 axis is a mediator of diet restriction-induced inhibition of mononuclear cell leukemia in Fischer rats. *Cancer Res.* **53,** 2750–2757 (1993).

230. Dunn, S. E. *et al.* Dietary restriction reduces insulin-like growth factor I levels, which modulates apoptosis, cell proliferation, and tumor progression in p53-deficient mice. *Cancer Res.* **57,** 4667–4672 (1997).

231. Mendenhall, C. L., Roselle, G. A., Gartside, P. & Grossman, C. J. Effects of recombinant human insulin-like growth factor-1 and recombinant human growth hormone on anabolism and immunity in calorie-restricted alcoholic rats. *Alcohol. Clin. Exp. Res.* **21,** 1–10 (1997).

232. Thissen, J. P., Ketelslegers, J. M. & Underwood, L. E. Nutritional regulation of the insulin-like growth factors. *Endocr. Rev.* **15,** 80–101 (1994).

233. Cohen, K. L. & Nissley, S. P. The serum half-life of somatomedin activity: evidence for growth hormone dependence. *Acta Endocrinol. (Copenh.)* **83,** 243–258 (1976).

234. Boisclair, Y. R., Rhoads, R. P., Ueki, I., Wang, J. & Ooi, G. T. The acid-labile subunit (ALS) of the 150 kDa IGF-binding protein complex: an important but forgotten component of the circulating IGF system. *J. Endocrinol.* **170,** 63–70 (2001).

235. Lelbach, A., Muzes, G. & Feher, J. The insulin-like growth factor system: IGFs, IGF-binding proteins and IGFBP-proteases. *Acta Physiol. Hung.* **92,** 97–107 (2005).

236. Lee, P. D., Giudice, L. C., Conover, C. A. & Powell, D. R. Insulin-like growth factor binding protein-1: recent findings and new directions. *Proc. Soc. Exp. Biol. Med. Soc. Exp. Biol. Med. N. Y. N* **216,** 319–357 (1997).

237. Ho, K. Y. *et al.* Fasting enhances growth hormone secretion and amplifies the complex rhythms of growth hormone secretion in man. *J. Clin. Invest.* **81,** 968–975 (1988).

238. Armario, A., Montero, J. L. & Jolin, T. Chronic food restriction and the circadian rhythms of pituitary-adrenal hormones, growth hormone and thyroid-stimulating hormone. *Ann. Nutr. Metab.* **31,** 81–87 (1987).

239. Sonntag, W. E., Xu, X., Ingram, R. L. & D'Costa, A. Moderate caloric restriction alters the subcellular distribution of somatostatin mRNA and increases growth hormone pulse amplitude in aged animals. *Neuroendocrinology* **61,** 601–608 (1995).

240. Itoh, N. The Fgf families in humans, mice, and zebrafish: their evolutional processes and roles in development, metabolism, and disease. *Biol. Pharm. Bull.* **30,** 1819–1825 (2007).

241. Dostálová, I., Haluzíková, D. & Haluzík, M. Fibroblast growth factor 21: a novel metabolic regulator with potential therapeutic properties in obesity/type 2 diabetes mellitus. *Physiol. Res. Acad. Sci. Bohemoslov.* **58,** 1–7 (2009).

242. Goetz, R. *et al.* Molecular insights into the klotho-dependent, endocrine mode of action of fibroblast growth factor 19 subfamily members. *Mol. Cell. Biol.* **27,** 3417–3428 (2007).

243. Ogawa, Y. *et al.* BetaKlotho is required for metabolic activity of fibroblast growth factor 21. *Proc. Natl. Acad. Sci. U. S. A.* **104,** 7432–7437 (2007).

244. Kharitonenkov, A. *et al.* FGF-21/FGF-21 receptor interaction and activation is determined by betaKlotho. *J. Cell. Physiol.* **215,** 1–7 (2008).

245. Wu, X. *et al.* FGF19-induced hepatocyte proliferation is mediated through FGFR4 activation. *J. Biol. Chem.* **285,** 5165–5170 (2010).

246. Moyers, J. S. *et al.* Molecular determinants of FGF-21 activity-synergy and cross-talk with PPARgamma signaling. *J. Cell. Physiol.* **210,** 1–6 (2007).

247. Xu, J. *et al.* Acute glucose-lowering and insulin-sensitizing action of FGF21 in insulin resistant mouse models----Association with liver and adipose tissue effects. *Am. J. Physiol. Endocrinol. Metab.* (2009). doi:10.1152/ajpendo.00348.2009

248. Fon Tacer, K. *et al.* Research resource: Comprehensive expression atlas of the fibroblast growth factor system in adult mouse. *Mol. Endocrinol. Baltim. Md* **24,** 2050–2064 (2010).

249. Kharitonenkov, A. *et al.* FGF-21 as a novel metabolic regulator. *J. Clin. Invest.* **115,** 1627–1635 (2005).

250. Huang, X. *et al.* Forced expression of hepatocyte-specific fibroblast growth factor 21 delays initiation of chemically induced hepatocarcinogenesis. *Mol. Carcinog.* **45,** 934–942 (2006).

251. Nishimura, T., Nakatake, Y., Konishi, M. & Itoh, N. Identification of a novel FGF, FGF-21, preferentially expressed in the liver. *Biochim. Biophys. Acta* **1492,** 203–206 (2000).

252. Rico-Bautista, E., Flores-Morales, A. & Fernández-Pérez, L. Suppressor of cytokine signaling (SOCS) 2, a protein with multiple functions. *Cytokine Growth Factor Rev.* **17,** 431–439 (2006).

253. Butler, R. N. Commentary: a brief history of geriatrics. *J. Gerontol. A. Biol. Sci. Med. Sci.* **59,** 1158–1159; discussion 1132–1152 (2004).

254. Turturro, A. *et al.* Growth curves and survival characteristics of the animals used in the Biomarkers of Aging Program. *J. Gerontol. A. Biol. Sci. Med. Sci.* **54,** B492–501 (1999).

255. Sprott, R. L. Biomarkers of aging. *J. Gerontol. A. Biol. Sci. Med. Sci.* **54,** B464–465 (1999).

256. Sprott, R. L. Biomarkers of aging and disease: introduction and definitions. *Exp. Gerontol.* **45,** 2–4 (2010).

257. Lipman, R. D., Dallal, G. E. & Bronson, R. T. Lesion biomarkers of aging in B6C3F1 hybrid mice. *J. Gerontol. A. Biol. Sci. Med. Sci.* **54,** B466–477 (1999).

258. Bekaert, S., De Meyer, T. & Van Oostveldt, P. Telomere attrition as ageing biomarker. *Anticancer Res.* **25,** 3011–3021 (2005).

259. Boonekamp, J. J., Simons, M. J. P., Hemerik, L. & Verhulst, S. Telomere length behaves as biomarker of somatic redundancy rather than biological age. *Aging Cell* **12,** 330–332 (2013).

260. Wolf, N. S. & Pendergrass, W. R. The relationships of animal age and caloric intake to cellular replication in vivo and in vitro: a review. *J. Gerontol. A. Biol. Sci. Med. Sci.* **54,** B502–517 (1999).

261. Liu, L. & Rando, T. A. Manifestations and mechanisms of stem cell aging. *J. Cell Biol.* **193,** 257–266 (2011).

262. Miller, R. A. Biomarkers of aging: prediction of longevity by using age-sensitive T-cell subset determinations in a middle-aged, genetically heterogeneous mouse population. *J. Gerontol. A. Biol. Sci. Med. Sci.* **56,** B180–186 (2001).

263. Rattan, S. I. S. in *Protein Metab. Homeost. Aging* (Tavernarakis, N.) 1–13 (Springer US, 2010). at <http://link.springer.com/chapter/10.1007/978-1-4419-7002-2_1>

264. Jacob, K. D., Noren Hooten, N., Trzeciak, A. R. & Evans, M. K. Markers of oxidant stress that are clinically relevant in aging and age-related disease. *Mech. Ageing Dev.* **134,** 139–157 (2013).

265. Vestergaard, P. F. *et al.* Serum levels of bioactive IGF1 and physiological markers of ageing in healthy adults. *Eur. J. Endocrinol. Eur. Fed. Endocr. Soc.* **170,** 229–236 (2014).

266. Shaddock, J. G., Chou, M. W. & Casciano, D. A. Effects of age and caloric restriction on cell proliferation in hepatocyte cultures from control and hepatectomized Fischer 344 rats. *Mutagenesis* **11,** 281–284 (1996).

267. De Magalhães, J. P. & Faragher, R. G. A. Cell divisions and mammalian aging: integrative biology insights from genes that regulate longevity. *BioEssays News Rev. Mol. Cell. Dev. Biol.* **30,** 567–578 (2008).

268. Harrison, D. E., Archer, J. R. & Astle, C. M. Effects of food restriction on aging: separation of food intake and adiposity. *Proc. Natl. Acad. Sci. U. S. A.* **81,** 1835–1838 (1984).

269. McCarter, R., Masoro, E. J. & Yu, B. P. Does food restriction retard aging by reducing the metabolic rate? *Am. J. Physiol.* **248,** E488–490 (1985).

270. Masoro, E. J. & Austad, S. N. *Handbook of the Biology of Aging*. (Academic Press, 2011).

271. BERG, B. N. & SIMMS, H. S. Nutrition and longevity in the rat. II. Longevity and onset of disease with different levels of food intake. *J. Nutr.* **71,** 255–263 (1960).

272. Picard, F. *et al.* Sirt1 promotes fat mobilization in white adipocytes by repressing PPAR-gamma. *Nature* **429,** 771–776 (2004).

273. Holehan, A. M. & Merry, B. J. The control of puberty in the dietary restricted female rat. *Mech. Ageing Dev.* **32,** 179–191 (1985).

274. Miller, R. A., Harper, J. M., Galecki, A. & Burke, D. T. Big mice die young: early life body weight predicts longevity in genetically heterogeneous mice. *Aging Cell* **1,** 22–29 (2002).

275. Holloszy, J. O. Exercise increases average longevity of female rats despite increased food intake and no growth retardation. *J. Gerontol.* **48,** B97–100 (1993).

276. Huffman, D. M. *et al.* Cancer progression in the transgenic adenocarcinoma of mouse prostate mouse is related to energy balance, body mass, and body composition, but not food intake. *Cancer Res.* **67,** 417–424 (2007).

277. Holloszy, J. O., Smith, E. K., Vining, M. & Adams, S. Effect of voluntary exercise on longevity of rats. *J. Appl. Physiol. Bethesda Md 1985* **59,** 826–831 (1985).

278. Busch, R., Neese, R. A., Awada, M., Hayes, G. M. & Hellerstein, M. K. Measurement of cell proliferation by heavy water labeling. *Nat. Protoc.* **2,** 3045–3057 (2007).

279. Fata, J. E. *et al.* The MAPK(ERK-1,2) pathway integrates distinct and antagonistic signals from TGFalpha and FGF7 in morphogenesis of mouse mammary epithelium. *Dev. Biol.* **306,** 193–207 (2007).

280. Bell, G. E. & Stern, J. S. Evaluation of body composition of young obese and lean Zucker rats. *Growth* **41,** 63–80 (1977).

281. Varady, K. A. *et al.* Modified alternate-day fasting regimens reduce cell proliferation rates to a similar extent as daily calorie restriction in mice. *FASEB J. Off. Publ. Fed. Am. Soc. Exp. Biol.* **22,** 2090–2096 (2008).

282. Masoro, E. J. *Caloric Restriction: A Key to Understanding and Modulating Aging: A Key to Understanding and Modulating Aging*. (Elsevier, 2002).

283. McCarter, R. J. & Palmer, J. Energy metabolism and aging: a lifelong study of Fischer 344 rats. *Am. J. Physiol.* **263,** E448–452 (1992).

284. Masoro, E. J., Yu, B. P. & Bertrand, H. A. Action of food restriction in delaying the aging process. *Proc. Natl. Acad. Sci. U. S. A.* **79,** 4239–4241 (1982).

285. Bertrand, H. A., Lynd, F. T., Masoro, E. J. & Yu, B. P. Changes in adipose mass and cellularity through the adult life of rats fed ad libitum or a life-prolonging restricted diet. *J. Gerontol.* **35,** 827–835 (1980).

286. Holloszy, J. O. Exercise and food restriction in rats. *J. Nutr.* **122,** 774–777 (1992).

287. Zhu, Z., Jiang, W., McGinley, J. N. & Thompson, H. J. Energetics and mammary carcinogenesis: effects of moderate-intensity running and energy intake on cellular processes and molecular mechanisms in rats. *J. Appl. Physiol. Bethesda Md 1985* **106,** 911–918 (2009).

288. Zhu, Z. *et al.* Effect of nonmotorized wheel running on mammary carcinogenesis: circulating biomarkers, cellular processes, and molecular mechanisms in rats. *Cancer Epidemiol. Biomark. Prev. Publ. Am. Assoc. Cancer Res. Cosponsored Am. Soc. Prev. Oncol.* **17,** 1920–1929 (2008).

289. Fontana, L. & Klein, S. Aging, adiposity, and calorie restriction. *JAMA J. Am. Med. Assoc.* **297,** 986–994 (2007).

290. Bartke, A. & Brown-Borg, H. Life extension in the dwarf mouse. *Curr. Top. Dev. Biol.* **63,** 189–225 (2004).

291. Coschigano, K. T., Clemmons, D., Bellush, L. L. & Kopchick, J. J. Assessment of growth parameters and life span of GHR/BP gene-disrupted mice. *Endocrinology* **141,** 2608–2613 (2000).

292. Coschigano, K. T. *et al.* Deletion, but not antagonism, of the mouse growth hormone receptor results in severely decreased body weights, insulin, and insulin-like growth factor I levels and increased life span. *Endocrinology* **144,** 3799–3810 (2003).

293. Holzenberger, M. *et al.* IGF-1 receptor regulates lifespan and resistance to oxidative stress in mice. *Nature* **421,** 182–187 (2003).

294. Masuda, H., Chikuda, H., Suga, T., Kawaguchi, H. & Kuro-o, M. Regulation of multiple ageing-like phenotypes by inducible klotho gene expression in klotho mutant mice. *Mech. Ageing Dev.* **126,** 1274–1283 (2005).

295. Bruss, M. D., Khambatta, C. F., Ruby, M. A., Aggarwal, I. & Hellerstein, M. K. Calorie restriction increases fatty acid synthesis and whole body fat oxidation rates. *Am. J. Physiol. Endocrinol. Metab.* **298,** E108–116 (2010).

296. Goodrick, C. L., Ingram, D. K., Reynolds, M. A., Freeman, J. R. & Cider, N. Effects of intermittent feeding upon body weight and lifespan in inbred mice: interaction of genotype and age. *Mech. Ageing Dev.* **55,** 69–87 (1990).

297. Varady, K. A., Roohk, D. J. & Hellerstein, M. K. Dose effects of modified alternate-day fasting regimens on in vivo cell proliferation and plasma insulin-like growth factor-1 in mice. *J. Appl. Physiol. Bethesda Md 1985* **103,** 547–551 (2007).

298. Faragher, R. G. *et al.* The gene responsible for Werner syndrome may be a cell division 'counting' gene. *Proc. Natl. Acad. Sci. U. S. A.* **90,** 12030–12034 (1993).

299. Halaschek-Wiener, J. & Brooks-Wilson, A. Progeria of stem cells: stem cell exhaustion in Hutchinson-Gilford progeria syndrome. *J. Gerontol. A. Biol. Sci. Med. Sci.* **62,** 3–8 (2007).

300. Katewa, S. D. & Kapahi, P. Dietary restriction and aging, 2009. *Aging Cell* **9,** 105–112 (2010).

301. Kemnitz, J. W. Calorie restriction and aging in nonhuman primates. *ILAR J. Natl. Res. Counc. Inst. Lab. Anim. Resour.* **52,** 66–77 (2011).

302. Bielschowsky, F. & Bielschowsky, M. Carcinogenesis in the Pituitary Dwarf Mouse. The Response to Dimethylbenzanthracene Applied to the Skin. *Br. J. Cancer* **15,** 257–262 (1961).

303. Ikeno, Y., Bronson, R. T., Hubbard, G. B., Lee, S. & Bartke, A. Delayed occurrence of fatal neoplastic diseases in ames dwarf mice: correlation to extended longevity. *J. Gerontol. A. Biol. Sci. Med. Sci.* **58,** 291–296 (2003).

304. Alderman, J. M. *et al.* Neuroendocrine inhibition of glucose production and resistance to cancer in dwarf mice. *Exp. Gerontol.* **44,** 26–33 (2009).

305. Ikeno, Y. *et al.* Reduced incidence and delayed occurrence of fatal neoplastic diseases in growth hormone receptor/binding protein knockout mice. *J. Gerontol. A. Biol. Sci. Med. Sci.* **64,** 522–529 (2009).

306. Herrington, J., Smit, L. S., Schwartz, J. & Carter-Su, C. The role of STAT proteins in growth hormone signaling. *Oncogene* **19,** 2585–2597 (2000).

307. Inagaki, T. *et al.* Endocrine regulation of the fasting response by PPARalpha-mediated induction of fibroblast growth factor 21. *Cell Metab.* **5,** 415–425 (2007).

308. Badman, M. K. *et al.* Hepatic fibroblast growth factor 21 is regulated by PPARalpha and is a key mediator of hepatic lipid metabolism in ketotic states. *Cell Metab.* **5,** 426–437 (2007).

309. Hotta, Y. *et al.* Fibroblast growth factor 21 regulates lipolysis in white adipose tissue but is not required for ketogenesis and triglyceride clearance in liver. *Endocrinology* **150,** 4625–4633 (2009).

310. Badman, M. K., Koester, A., Flier, J. S., Kharitonenkov, A. & Maratos-Flier, E. Fibroblast growth factor 21-deficient mice demonstrate impaired adaptation to ketosis. *Endocrinology* **150,** 4931–4940 (2009).

311. Fisher, F. M. *et al.* Obesity is a fibroblast growth factor 21 (FGF21)-resistant state. *Diabetes* **59,** 2781–2789 (2010).

312. Ferry, R. J., Jr, Cerri, R. W. & Cohen, P. Insulin-like growth factor binding proteins: new proteins, new functions. *Horm. Res.* **51,** 53–67 (1999).

313. McCarty, M. F. Up-regulation of IGF binding protein-1 as an anticarcinogenic strategy: relevance to caloric restriction, exercise, and insulin sensitivity. *Med. Hypotheses* **48,** 297–308 (1997).

314. Sandhu, M. S., Dunger, D. B. & Giovannucci, E. L. Insulin, insulin-like growth factor-I (IGF-I), IGF binding proteins, their biologic interactions, and colorectal cancer. *J. Natl. Cancer Inst.* **94,** 972–980 (2002).

315. Hursting, S. D., Lavigne, J. A., Berrigan, D., Perkins, S. N. & Barrett, J. C. Calorie restriction, aging, and cancer prevention: mechanisms of action and applicability to humans. *Annu. Rev. Med.* **54,** 131–152 (2003).

316. Spindler, S. R. Caloric restriction: from soup to nuts. *Ageing Res. Rev.* **9,** 324–353 (2010).

317. Iizuka, K., Takeda, J. & Horikawa, Y. Glucose induces FGF21 mRNA expression through ChREBP activation in rat hepatocytes. *FEBS Lett.* **583,** 2882–2886 (2009).

318. Sánchez, J., Palou, A. & Picó, C. Response to carbohydrate and fat refeeding in the expression of genes involved in nutrient partitioning and metabolism: striking effects on fibroblast growth factor-21 induction. *Endocrinology* **150,** 5341–5350 (2009).

319. Estall, J. L. *et al.* PGC-1alpha negatively regulates hepatic FGF21 expression by modulating the heme/Rev-Erb(alpha) axis. *Proc. Natl. Acad. Sci. U. S. A.* **106,** 22510–22515 (2009).

320. Coskun, T. *et al.* Fibroblast growth factor 21 corrects obesity in mice. *Endocrinology* **149,** 6018–6027 (2008).

321. Sarruf, D. A. *et al.* Fibroblast growth factor 21 action in the brain increases energy expenditure and insulin sensitivity in obese rats. *Diabetes* **59,** 1817–1824 (2010).

322. Xu, J. *et al.* Fibroblast growth factor 21 reverses hepatic steatosis, increases energy expenditure, and improves insulin sensitivity in diet-induced obese mice. *Diabetes* **58,** 250–259 (2009).

323. Berglund, E. D. *et al.* Fibroblast growth factor 21 controls glycemia via regulation of hepatic glucose flux and insulin sensitivity. *Endocrinology* **150,** 4084–4093 (2009).

324. McKee Alderman, J. *et al.* Calorie restriction and dwarf mice in gerontological research. *Gerontology* **56,** 404–409 (2010).

325. Heilbronn, L. K. & Ravussin, E. Calorie restriction and aging: review of the literature and implications for studies in humans. *Am. J. Clin. Nutr.* **78,** 361–369 (2003).

326. Miller, R. A. Extending life: scientific prospects and political obstacles. *Milbank Q.* **80,** 155–174 (2002).

327. Harrison, D. E. *et al.* Acarbose, 17-α-estradiol, and nordihydroguaiaretic acid extend mouse lifespan preferentially in males. *Aging Cell* **13,** 273–282 (2014).

328. Balfour, J. A. & McTavish, D. Acarbose. An update of its pharmacology and therapeutic use in diabetes mellitus. *Drugs* **46,** 1025–1054 (1993).

329. Strong, R. *et al.* Evaluation of resveratrol, green tea extract, curcumin, oxaloacetic acid, and medium-chain triglyceride oil on life span of genetically heterogeneous mice. *J. Gerontol. A. Biol. Sci. Med. Sci.* **68,** 6–16 (2013).

330. Lipman, R. D., Dallal, G. E. & Bronson, R. T. Effects of genotype and diet on age-related lesions in ad libitum fed and calorie-restricted F344, BN, and BNF3F1 rats. *J. Gerontol. A. Biol. Sci. Med. Sci.* **54,** B478–491 (1999).

331. Chen, B., Retzlaff, M., Roos, T. & Frydman, J. Cellular strategies of protein quality control. *Cold Spring Harb. Perspect. Biol.* **3,** a004374 (2011).

332. Hipkiss, A. R. On why decreasing protein synthesis can increase lifespan. *Mech. Ageing Dev.* **128,** 412–414 (2007).

333. Kapahi, P. *et al.* With TOR, less is more: a key role for the conserved nutrient-sensing TOR pathway in aging. *Cell Metab.* **11,** 453–465 (2010).

334. Conn, C. S. & Qian, S.-B. Nutrient signaling in protein homeostasis: an increase in quantity at the expense of quality. *Sci. Signal.* **6,** ra24 (2013).

335. Meriin, A. B. *et al.* A novel approach to recovery of function of mutant proteins by slowing down translation. *J. Biol. Chem.* **287,** 34264–34272 (2012).

336. Sherman, M. Y. & Qian, S.-B. Less is more: improving proteostasis by translation slow down. *Trends Biochem. Sci.* **38,** 585–591 (2013).

337. Kaeberlein, M. & Kennedy, B. K. Hot topics in aging research: protein translation and TOR signaling, 2010. *Aging Cell* **10,** 185–190 (2011).

338. Blackwell, B. N., Bucci, T. J., Hart, R. W. & Turturro, A. Longevity, body weight, and neoplasia in ad libitum-fed and diet-restricted C57BL6 mice fed NIH-31 open formula diet. *Toxicol. Pathol.* **23,** 570–582 (1995).

339. Price, J. C. *et al.* The effect of long term calorie restriction on in vivo hepatic proteostatis: a novel combination of dynamic and quantitative proteomics. *Mol. Cell. Proteomics MCP* **11,** 1801–1814 (2012).

340. Neese, R. A. *et al.* Advances in the stable isotope-mass spectrometric measurement of DNA synthesis and cell proliferation. *Anal. Biochem.* **298,** 189–195 (2001).

341. Neese, R. A. *et al.* Measurement in vivo of proliferation rates of slow turnover cells by 2H2O labeling of the deoxyribose moiety of DNA. *Proc. Natl. Acad. Sci. U. S. A.* **99,** 15345–15350 (2002).

342. Price, J. C. *et al.* Measurement of human plasma proteome dynamics with (2)H(2)O and liquid chromatography tandem mass spectrometry. *Anal. Biochem.* **420,** 73–83 (2012).

343. Kanehisa, M. & Goto, S. KEGG: kyoto encyclopedia of genes and genomes. *Nucleic Acids Res.* **28,** 27–30 (2000).

344. Kanehisa, M. *et al.* Data, information, knowledge and principle: back to metabolism in KEGG. *Nucleic Acids Res.* **42,** D199–205 (2014).

345. Drake, J. C. *et al.* Assessment of mitochondrial biogenesis and mTORC1 signaling during chronic rapamycin feeding in male and female mice. *J. Gerontol. A. Biol. Sci. Med. Sci.* **68,** 1493–1501 (2013).

346. Barger, J. L., Walford, R. L. & Weindruch, R. The retardation of aging by caloric restriction: its significance in the transgenic era. *Exp. Gerontol.* **38,** 1343–1351 (2003).

347. Garelick, M. G. *et al.* Chronic rapamycin treatment or lack of S6K1 does not reduce ribosome activity in vivo. *Cell Cycle Georget. Tex* **12,** 2493–2504 (2013).

348. Dai, D.-F. *et al.* Altered proteome turnover and remodeling by short-term caloric restriction or rapamycin rejuvenate the aging heart. *Aging Cell* (2014). doi:10.1111/acel.12203

349. Lewis, S. E., Goldspink, D. F., Phillips, J. G., Merry, B. J. & Holehan, A. M. The effects of aging and chronic dietary restriction on whole body growth and protein turnover in the rat. *Exp. Gerontol.* **20,** 253–263 (1985).

350. Lambert, A. J. & Merry, B. J. Use of primary cultures of rat hepatocytes for the study of ageing and caloric restriction. *Exp. Gerontol.* **35,** 583–594 (2000).

351. Merry, B. J. & Holehan, A. M. Effect of age and restricted feeding on polypeptide chain assembly kinetics in liver protein synthesis in vivo. *Mech. Ageing Dev.* **58,** 139–150 (1991).

352. Hsieh, C.-C. & Papaconstantinou, J. Akt/PKB and p38 MAPK signaling, translational initiation and longevity in Snell dwarf mouse livers. *Mech. Ageing Dev.* **125,** 785–798 (2004).

353. Bates, P. C. & Holder, A. T. The anabolic actions of growth hormone and thyroxine on protein metabolism in Snell dwarf and normal mice. *J. Endocrinol.* **119,** 31–41 (1988).

354. Lee, A. S. The glucose-regulated proteins: stress induction and clinical applications. *Trends Biochem. Sci.* **26,** 504–510 (2001).

355. Ullrich, S. J., Moore, S. K. & Appella, E. Transcriptional and translational analysis of the murine 84- and 86-kDa heat shock proteins. *J. Biol. Chem.* **264,** 6810–6816 (1989).

356. Pfaffenbach, K. T. *et al.* GRP78/BiP is a novel downstream target of IGF-1 receptor mediated signaling. *J. Cell. Physiol.* **227,** 3803–3811 (2012).

357. Hayes, J. D., Flanagan, J. U. & Jowsey, I. R. Glutathione transferases. *Annu. Rev. Pharmacol. Toxicol.* **45,** 51–88 (2005).

358. Boylston, W. H., DeFord, J. H. & Papaconstantinou, J. Identification of longevity-associated genes in long-lived Snell and Ames dwarf mice. *Age Dordr. Neth.* **28,** 125–144 (2006).

359. Cao, S. X., Dhahbi, J. M., Mote, P. L. & Spindler, S. R. Genomic profiling of short- and long-term caloric restriction effects in the liver of aging mice. *Proc. Natl. Acad. Sci. U. S. A.* **98,** 10630–10635 (2001).

360. Cho, C. G. *et al.* Modulation of glutathione and thioredoxin systems by calorie restriction during the aging process. *Exp. Gerontol.* **38,** 539–548 (2003).

361. Youngman, L. D., Park, J. Y. & Ames, B. N. Protein oxidation associated with aging is reduced by dietary restriction of protein or calories. *Proc. Natl. Acad. Sci. U. S. A.* **89,** 9112–9116 (1992).

362. Forster, M. J., Sohal, B. H. & Sohal, R. S. Reversible effects of long-term caloric restriction on protein oxidative damage. *J. Gerontol. A. Biol. Sci. Med. Sci.* **55,** B522–529 (2000).

363. Bhattacharya, A. *et al.* Attenuation of liver insoluble protein carbonyls: indicator of a longevity determinant? *Aging Cell* **10,** 720–723 (2011).

364. Fok, W. C. *et al.* Short-term treatment with rapamycin and dietary restriction have overlapping and distinctive effects in young mice. *J. Gerontol. A. Biol. Sci. Med. Sci.* **68,** 108–116 (2013).

365. Wang, M. & Miller, R. A. Augmented autophagy pathways and MTOR modulation in fibroblasts from long-lived mutant mice. *Autophagy* **8,** 1273–1274 (2012).

366. Eskelinen, E.-L. New insights into the mechanisms of macroautophagy in mammalian cells. *Int. Rev. Cell Mol. Biol.* **266,** 207–247 (2008).

367. Klionsky, D. J. & Emr, S. D. Autophagy as a regulated pathway of cellular degradation. *Science* **290,** 1717–1721 (2000).

368. Klionsky, D. J. *et al.* Guidelines for the use and interpretation of assays for monitoring autophagy. *Autophagy* **8,** 445–544 (2012).

369. Goldberg, A. L. Protein degradation and protection against misfolded or damaged proteins. *Nature* **426,** 895–899 (2003).

370. Chondrogianni, N. & Gonos, E. S. Proteasome dysfunction in mammalian aging: steps and factors involved. *Exp. Gerontol.* **40,** 931–938 (2005).

371. Judge, S., Judge, A., Grune, T. & Leeuwenburgh, C. Short-term CR decreases cardiac mitochondrial oxidant production but increases carbonyl content. *Am. J. Physiol. Regul. Integr. Comp. Physiol.* **286,** R254–259 (2004).

372. Gredilla, R. & Barja, G. Minireview: the role of oxidative stress in relation to caloric restriction and longevity. *Endocrinology* **146,** 3713–3717 (2005).

373. Koizumi, A., Weindruch, R. & Walford, R. L. Influences of dietary restriction and age on liver enzyme activities and lipid peroxidation in mice. *J. Nutr.* **117,** 361–367 (1987).

374. Busch, R. *et al.* Measurement of protein turnover rates by heavy water labeling of nonessential amino acids. *Biochim. Biophys. Acta* **1760,** 730–744 (2006).